About gradients and oscillations : the role of the Wnt-signaling pathway in somite formation during embryonic development

Alexander Aulehla

UNIVERSITE PIERRE & MARIE CURIE
LA SCIENCE A PARIS

THESE DE DOCTORAT DE
L'UNIVERSITE PIERRE ET MARIE CURIE

Spécialité

Biologie du Développement--La logique du vivant

Présentée par

M. Alexander AULEHLA

Pour obtenir le grade de

DOCTEUR de l'UNIVERSITE PIERRE ET MARIE CURIE

A propos de gradients et d'oscillations: le rôle de la voie de signalisation Wnt dans la formation des somites au cours du développement embryonnaire

Soutenue le 18 septembre 2008

devant le jury composé de:

M. le Pr. Olivier POURQUIE	Directeur de thèse
Mme le Pr. Muriel UMBHAUER	Examinateur
M. le Pr. Albert GOLDBETER	Rapporteur
M. le Pr. Julian LEWIS	Rapporteur

dedicata a Mirabel

Acknowledgments

I'm deeply grateful to Olivier Pourquié for the opportunity to prepare this thesis. The positive experience in his laboratory and his enthusiasm for research definitively contributed to my decision in favor of a career in basic research and I'm very thankful for this.

I would like to thank Prof. Albert Goldbeter and Prof. Julian Lewis for their time and effort in evaluating my thesis as rapporteurs and for being part of the jury.

I would like to thank Prof. Muriel Umbhauer for being in the jury of my thesis.

I'm very much indebted to Prof. Bernhard Herrmann for his guidance during the time in his laboratory in Freiburg. His view of research clearly was an important influence for my future approach to science.

I thank the Swiss Foundation for Medical-Biological Grants/ Swiss National Science Foundation for their financial support.

I thank my colleagues in the laboratory in Kansas City. Only through the scientific discussion with them could my research progress and the ideas mature.

I would like to thank the managers and technicians, both in our lab as well as in the core facilities at the Stowers Institute. Their great help is highly appreciated.

I thank Bertrand Bénazeraf for this critical reading of my thesis.

The help of Joanne Chatfield in writing, editing and finalizing this thesis can not be appreciated high enough.

I'm very appreciative for the constant support by our families - grazie.

I'm thankful to my children Nina and Dante for the joy and meaning they bring to our lives.

Most of all, I wish to thank Mirabel for her loving support. I feel very fortunate to have her by my side; she has everything I am dreaming of.

Dans l'échange entre la théorie et l'expérience, c'est toujours la première qui engage le dialogue. C'est elle qui détermine la forme de la question, donc les limites de la réponse.

François Jacob,
La logique du vivant

TABLE OF CONTENTS

Résume

Une caractéristique fondamentale des vertébrés est leur organisation métamerique, visible au niveau de la colonne vertébrale. Cette organisation se met en place au cours du développement embryonnaire et l'émergence des précurseurs des vertèbres, les somites, formés à partir du mésoderm paraxial présomitique (PSM). Depuis la découverte d'une activité transcriptionelle oscillatoire de la voie de signalisation Notch dans le PSM, on propose que cette activité oscillatoire représente l'action d'une horloge embryonnaire, l'horloge de segmentation, responsable de contrôler la formation des somites de façon périodique.

Dans cette étude, je présente la découverte d'une nouvelle association de la voie Wnt avec l'horloge de segmentation en décrivant l'activité oscillatoire de *Axin2*, une cible de la voie Wnt, dans le PSM. Ensuite, j'ai mise en place un system d'imagerie bi-photon qui nous permet d'observer l'action de l'horloge de segmentation en temps réel et *in vivo* dans les embryons de souris. Ce système permet de mesurer directement les paramètres des oscillations. Ultérieurement je décris la découverte d'un gradient d'expression de la protéine β-caténine dans le PSM. A l'aide d'expériences de recombinaisons homologues conditionnelles nous avons déterminé que ce gradient de β-caténine contrôle la maturation et différentiation des cellules dans le PSM. De plus, ce gradient constitue un signal essentiel et permissif pour les oscillations de l'horloge de segmentation. En conclusion, je propose un nouveau modèle de mise en place des somites incorporant les résultats présentés.

Mots cles: Developpement embryonnaire, somitogenèse, oscillationes transcriptionelles, voie des signalisation Wnt/β-caténine

About gradients and oscillations: the role of the Wnt-signaling pathway in somite formation during embryonic development

Summary

A fundamental characteristic of all vertebrates is the metameric organization of their body plan, best exemplified by the vertebral column. This organization originates during embryonic development and the emergence of the vertebrae precursor, the somites, which form from the paraxial presomitic mesoderm (PSM). The discovery of oscillatory transcriptional activity of the Notch-signaling pathway within the PSM supports the existence of an embryological clock, the segmentation clock, which is responsible in controlling the periodic formation of somites.

Here, I present the discovery of oscillatory mRNA expression of *Axin2*, a target of the Wnt-signaling pathway, in the PSM. This establishes a novel link between Wnt signaling and the segmentation clock. I then describe the generation of a two-photon, real-time imaging technology that allows visualizing segmentation clock activity in real-time in living mouse embryos. This enables us to directly measure oscillation parameters in the PSM. Finally, I describe the discovery of a β-catenin protein gradient in the PSM. Using conditional gene targeting experiments, we establish that this gradient controls PSM maturation and differentiation. Moreover, this gradient represents a permissive signal that allows segmentation clock activity to occur. Based on the results presented, I propose a novel model for somite formation.

Key words: embryonic development, somitogenesis, transcriptional oscillations, Wnt/β-catenin signaling

Résumé substantiel

Une caractéristique fondamentale des vertébrés est leur organisation métamérique, visible au niveau de la colonne vertébrale, du système nerveux périphérique et du système vasculaire. Cette organisation se met en place au cours du développement embryonnaire par l'émergence des précurseurs des vertèbres, les somites, formés à partir du mésoderme paraxial présomitique (PSM). Les somites sont des structures essentielles du développement embryonnaire, la compréhension des mécanismes qui contrôlent leur mise en place constitue donc un enjeu majeur de la biologie du développement. Leur formation intervient de façon séquentielle est directionnelle: les premiers somites se forment d'abord dans la partie antérieure de l'embryon, et périodiquement les somites suivants sont ajoutés postérieurement. Depuis la découverte d'une activité transcriptionelle oscillatoire de la voie de signalisation Notch dans le PSM, on propose que cette activité oscillatoire représente l'action d'une horloge embryonnaire, l'horloge de segmentation, responsable de contrôler la formation des somites de façon périodique.

Dans cette étude, je présente la découverte d'une nouvelle association de la voie Wnt avec l'horloge de segmentation en décrivant l'activité oscillatoire de *Axin2*, une cible de la voie Wnt, dans le PSM. De manière intéressante, la voie Wnt oscille en anti-phase avec la voie Notch et est nécessaire pour obtenir des oscillations de la voie Notch.

Par la suite j'ai mis en place un system d'imagerie bi-photon qui nous permet d'observer l'action de l'horloge de segmentation en temps réel et *in vivo* dans les embryons de souris. Pour réaliser ce système, on a d'abord généré un nouveau système de gène rapporteur fluorescent. Ce système exprime la protéine fluorescente Venus avec deux

moyens de déstabilisation au niveau de l 'ARNm et au niveau de la protéine. Ce rapporteur répond à l'activation du promoteur du gène *Lfng* d'une façon dynamique et oscillatoire. Nous avons généré des souris transgéniques ayant intégrées le rapporteur. Ce système permet de mesurer directement les paramètres des oscillations. En mesurant directement la période des oscillations en relation avec la position dans le PSM, on montre que les oscillations ralentissent progressivement vers la partie antérieure du PSM. Par conséquent, la période des oscillations ne correspond pas à la période de la formation des somites.

Ultérieurement je décris la découverte d'un gradient d'expression de la protéine β-caténine dans le PSM. A l'aide d'expériences de recombinaisons homologues conditionnelles nous avons déterminé que ce gradient de β-caténine contrôle la maturation et différenciation des cellules dans le PSM. L'accumulation de β-caténine dans le PSM d'embryon de souris maintient les cellules du PSM indifférenciées, incapable de former des somites. De plus, ce gradient constitue un signal essentiel et permissif pour les oscillations de l'horloge de segmentation. En utilisant le système d'imagerie avec les embryons de souris mutantes, on trouve que les cellules du PSM peuvent continuer à montrer des oscillations transcriptionelles. Sous l'influence de l'expression d'une protéine β–caténine stabilisée, les cellules du PSM montrent des oscillations synchronisées ectopiques à un niveau antérieur où ces oscillations sont arrêtées dans les embryons témoins. Ces résultas suggèrent donc que l'horloge de segmentation ne requière pas une boucle d'autorégulation intégrant la β-caténine. De ce fait, l'origine des oscillations reste à être découverte.

En conclusion, je propose un nouveau modèle de mise en place des somites incorporant les résultats présentés. Ce modèle, nommé « L'Appendix model », essaye d'assigner une nouvelle fonction aux oscillations observées. Comme élément central ce modèle propose que le changement de caractéristique oscillatoire le long du PSM soit une conséquence directe des oscillations mêmes. En plus, les cellules du PSM antérieur sont groupées selon une certaine caractéristique de leur oscillation, leur phase. Selon ce modèle, la périodicité de la formation des somites n'est pas contrôlée par la fréquence des oscillations de la transcription. La périodicité et la définition de l'unité qui va former un somite résultent du rassemblement des cellules selon leur phase, le nombre d'oscillations qu'elles ont effectuées et l'interaction avec le gradient permissif de β-caténine.

Adresse:

Stowers Institute for Medical Research

Pourquié Laboratory

1000 East 50th Street

Kansas City, Missouri, 64110, USA

1. Introduction

Among the mysteries of life, the development of a living organism during the course of embryogenesis is, without doubt, one of the most fascinating. How does a single cell, the fertilized oocyte, develop into such a complex and beautiful living being – for example, a vertebrate embryo? How does this embryo then develop into an adult organism, prepared to leave the protection of the mother and engage in life? Studying this wonderful development from a single cell to a complex organism allows us to glimpse into the beauty of nature.

To approach the phenomenon of embryonic development, an analytical approach is widely used. As a whole, embryonic development is artificially separated into various sub-processes, which then become targets of our investigation. While following this kind of approach, I always believe that it is essential not to forget that this separation is artificial, since all processes are interconnected and are only meaningful if considered in the context of the whole organism.

The phenomenon addressed in this work is the establishment of a segmented body plan in vertebrate embryos.

1.1 Body segmentation in vertebrates

In vertebrates, the segmentation of the body can first be seen during embryogenesis at the level of the formation of somites, the precursors of the vertebrae. Somites were first described by Marcello Malpighi in 1686 in his *opera omnia*. With the help of the recently developed microscope, Marcello Malpighi described “vesiculas vertebrarum” which formed symmetrically on each side of the neural tube and first

appeared anteriorly, close to the head region (Figure 1). As he observed the development of the chicken embryo in the egg over time (*de ovo incubato)*, he noticed that more and more pairs of somites were becoming visible along the body axis, indicating that their formation does occur in a sequential manner. His observations and impressive drawings uncovered the basic features of somite formation.

- Somites form symmetrically on each side of the neural tube.
- Somites form sequentially.
- Somites form in an anterior-to-posterior progression.

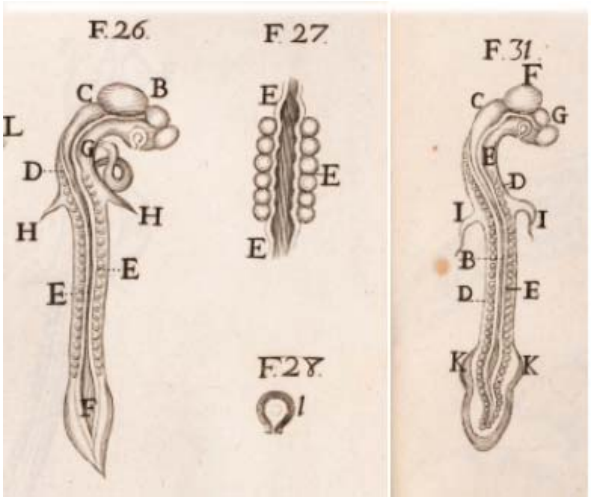

Figure 1. *de ovo incubato* in *opera omnia* by Marcello Malpighi, 1686. This is considered the first description of somites, termed "vesiculas vertebrarum" (E in F26; enlarged in F27). Note that with progression of time, more and more somites become visible along the axis within the paraxial mesoderm (F31).

Despite the early recognition of these basic features more than 300 years ago, the underlying mechanism(s) still remains, to a large extent, enigmatic. The work presented here addresses the phenomena of periodicity and directionality of somite formation.

To introduce into the topic of this work, the basic nomenclature, anatomy and function of somites shall be described first.

1.1.1 Somite nomenclature

Somites are enumerated in a cranio-caudal direction using Arabic numbers. In addition, in order to identify the intrinsic developmental stage of each somite, a Roman numbering system, running in a caudal-to-cranial direction, was included (Ordahl, 1993). For instance, the somite that just formed is somite I, while the somite that formed just before somite I is somite II and so on. By combining both labeling strategies, each somite can be identified and at the same time its developmental age at the time point of observations is known. For instance, somite III/9 is somite 7 in a 9-somite embryo (Figure 2). This nomenclature system was adopted for the still unsegmented paraxial mesoderm, or presomitic mesoderm (PSM), that contains the somite precursors. Thus, the region forming the next somite is somite 0, while the adjacent, more posterior region is somite -I and so on (Pourquie and Tam, 2001).

Figure 2. Somite nomenclature exemplified on a scanning electron microscopy image of a mouse embryo at the nine-somite stage. While Arabic numbers are used to label successive somites in an anterior-to-posterior direction (for example, S7, S8, S9), Roman numbers are used to indicate the intrinsic developmental age of each somite. Thus, the most recently formed somite is labeled SI, and this labeling is continued to the developmentally older somite, located anteriorly, SII, and so on. For somites yet to form, this labeling system has been extended to the PSM (e.g., S-I, S-II) to indicate prospective somite formation ordering.

1.1.2 The epithelial somite and its derivatives

Somites are epithelial spheres that form on each side of the neural tube within the paraxial mesoderm (Christ and Ordahl, 1995). Shortly after their formation, a maturation process is initiated under the influence of adjacent tissue: 1) the ectoderm dorsally, 2) the notochord ventrally, 3) the neural tube medially and 4) the lateral plate mesoderm laterally – all are instructive for this maturation process (reviewed in (Christ et al.,

2007)). As a consequence of these inductive events, somites become compartmentalized into the sclerotome ventrally and dermomyotome dorsally (Brand-Saberi et al., 1993; Pourquie et al., 1995; Pourquie et al., 1993; Pourquie et al., 1996). The sclerotome will give rise to the axial skeleton (including vertebrae), the associated tendons and the ribs. The dermomyotome will subdivide further into the myotome and the dermatome. The myotome will give rise to all striated muscles with the exception of head muscles, which are derived from the cephalic mesoderm. The dermatome will give rise to the dermis of the back, while the dermis of the ventro-lateral body originates from the somatopleura. In addition, somites contribute to many other tissues such as: the meninges, vessel endothelium, smooth muscle cells of the dorsal aorta and lymphatic endothelial cells. Thus, somites carry enormous developmental potential and are critical anatomical components of the vertebrate embryo.

As mentioned above, with the emergence of somites, the first morphological sign of segmentation of the body plan becomes visible in vertebrate embryos. This initial, primary segmentation involves the paraxial mesoderm. Importantly, the primary segmentation of the paraxial mesoderm has, in turn, critical implications for overall body patterning. For instance, the segmented arrangement of the peripheral nervous system and of the blood vessels is a direct consequence of and imposed by the arrangement of somites. In this respect, an important property of somites is their polarization into an anterior and posterior half.

1.1.3 Somite polarity

Each somite is subdivided into an anterior and posterior half based on anatomical, functional and molecular properties. Anatomically, only the sclerotome is subdivided into anterior and posterior halves by von Ebner's fissure (Remak, 1850; Von Ebner, 1888). The dermomyotome does not show any evidence of subdivision on an anatomical level. Functionally, it has long been known that only the anterior sclerotome half of each somite is permissive for invading neural crest cells and motor neurons, while the posterior half has repulsive properties in respect to the migration of neural crest cells (Bronner-Fraser, 1986; Keynes and Stern, 1984; Rickmann et al., 1985). Thus, migrating neural crest cells are governed through predefined paths and, therefore, the polarity of somites is essential for the proper alignment of the peripheral nervous system.

The antero-posterior (AP) polarization of somites is established in the anterior PSM before somites are actually formed. Molecularly, this process is tightly linked to the Notch/Delta-signaling pathway and its interaction with the transcription factor mesoderm posterior 2 (Mesp2) (Morimoto et al., 2005; Saga and Takeda, 2001). Mesp2, which is expressed in the prospective anterior half of the somite, initiates a complex cascade of signaling events. Ultimately, Mesp2 has been shown to suppress Notch-signaling activity which, therefore, is restricted to the posterior half of the somite (Takahashi et al., 2003; Takahashi et al., 2007). The mechanism of how Mesp2 itself is regulated is not entirely clear, but it has been suggested that it is under the combinatorial control of T-box 6 (Tbx6) and Notch signaling (Yasuhiko et al., 2006). Thus, while Notch signaling activates Mesp2; in turn, Mesp2 inhibits Notch signaling, thus constituting a negative feedback loop.

1.1.4 Resegmentation

One vertebra is formed by the halves of two adjacent somites. Thus, the posterior half of one somite combines with the anterior half of the adjacent somite to form a vertebra. Therefore, initial somite boundaries do not correspond to the final vertebrae boundaries due to this resegmentation process (Remak, 1850). For this reason, somites have been originally termed protovertebrae. Importantly, resegmentation also involves the vertebral processes, such as neural arches and ribs ((Huang et al., 1996) and reviewed in (Christ et al., 1998)). Since the myotome and its derivatives are excluded from the resegmentation process, it follows that segmental muscles that are derived from one somite are connected to two adjacent vertebral processes and ribs, constituting the basis for spine motility. Thus, resegmentation is the basis for the formation of the vertebrae motion segment.

1.1.5 Axial identity of vertebrae

Somites differ along the AP axis in respect to their developmental potential, resulting in the formation of vertebrae with distinct cervical, thoracic, lumbar and sacral anatomical features. In addition, only thoracic somites possess the ability to form ribs. This axial identity is under tight control of Hox transcription factors (Kmita and Duboule, 2003). For instance, the genetic ablation of the entire Hox 9 or Hox 10 paralogous clusters results in a dramatic expansion of thoracic vertebral identity. As a consequence, supernummary ribs are formed in the lumbar region, reflecting a reprogramming of axial identity (McIntyre et al., 2007; Wellik and Capecchi, 2003). Interestingly, it was known

long before identification of the molecular identity of the instructive signal that the determination of the axial identity takes place in mesodermal cells before these cells are actually incorporated into a somite. Thus, the heterotopic transplantation of unsegmented paraxial mesoderm from the prospective thoracic region into the cervical or lumbosacral region of a host embryo results in the formation of ectopic ribs (Jacob et al., 1975; Kieny et al., 1972). This was an early indication that instructive mechanisms are active long before somites actually form.

1.1.6 Changing perspective − the presomitic mesoderm as the site of action

While initial research mainly focused on the actual event of somite formation and the differentiation into various organs, a new perspective emerged as a result of the findings of experimental embryology studies. The results indicated that somite formation merely represents the realization of a competence that is acquired by paraxial mesoderm cells much earlier during development. These intriguing findings, some of which will be outlined below, shifted the attention to the yet-to-be segmented paraxial mesoderm – the PSM.

The PSM is generated during the gastrulation process and later is formed from a posterior growth zone termed the tail bud (Tam and Tan, 1992). While somites bud off from the anterior end of the PSM, new cells enter the PSM from the posteriorly located tail bud, ensuring that enough cells are available to form all somites (e.g., 65 somite pairs in mouse embryos) (Tam, 1981). Interestingly once the PSM is formed, it is not immediately segmented into somites. Rather, newly formed PSM maintains this

unsegmented state for many hours, approximately 12-15 hours in chick and mouse embryos.

Quite strikingly, classical experimental embryology research elaborated that the PSM is already endowed with all the information required to form somites. Thus, periodicity and directionality are intrinsic properties of the cells in the PSM. For instance, when the PSM was bisected transversely, somite formation proceeded seemingly undisturbed in the two embryo fragments, and somites formed at the right time and in the right place (Packard, 1978). In addition, when the PSM was inverted cranio-caudally, somites formed in the opposite, posterior-to-anterior direction (Christ et al., 1974; Menkes et al., 1968). This was also true for very nascent PSM that was just formed through gastrulation and even within this cell population, the information for somite formation – directionality and periodicity – was already present.

Thus, both directionality and periodicity are already encoded in and intrinsic to the PSM. To date, there are no known experimental circumstances that could change the period or direction of somite formation.

1.1.7 Segmentation and epithelialization are distinct processes

Somite formation involves a mesenchymal-to-epithelial transition of cells in the anterior PSM, combined with the separation of these epithelial units. However, it is possible to functionally disconnect the processes of epithelialization and segmentation. For instance, mouse mutants lacking the gene *Paraxis* do not undergo epithelialization in the anterior PSM and, therefore, do not form somites; however, they do show segmentation of the mesoderm into metameric units and eventually, vertebrae are formed

(Burgess et al., 1996). Likewise, when the PSM of chick embryos is isolated from all surrounding tissues, epithelial somites will not form, while the segmentation of mesoderm, mainly at molecular levels, clearly occurs (Palmeirim et al., 1998). This not only indicates that epithelialization and segmentation can be functionally separated, but also emphasizes that while the epithelialization process requires surrounding signals, the segmentation of the mesoderm appears as a truly intrinsic property of this tissue. Important external signals emanate from the neural tube and ectoderm overlying the PSM (Borycki et al., 2000; Borycki et al., 1998; Correia and Conlon, 2000; Palmeirim et al., 1998). Moleculary, it has been shown that Wnt signaling originating from the ectoderm is required in order to allow somite epithelialization to occur (Schmidt et al., 2004). Recently, it has been shown that an important external signal required for epithelialization is encoded by fibronectin, an extracellular matrix component that is produced by the ectoderm and which surrounds the PSM (Rifes et al., 2007). Thus, if fibronectin surrounds the isolated PSM, then this tissue not only segments but also forms epithelial somites in isolation from all surrounding tissues.

1.1.8 Somite number control—an example of regulative development

An intriguing further observation is that within any given vertebrate species, the number of formed somites is kept rather constant. Even when the size of the embryo is experimentally reduced, the embryo responds by forming a normal number of smaller sized somites.. The two classical examples stem from studies in mouse and Xenopus *laevis* embryos. The mouse mutant *amputated* has a reduced body length, but the number of somites remains normal (Tam, 1981). At the same time smaller somites that contain

fewer cells than in control embryos are formed. Likewise, when Xenopus embryos were experimentally reduced in size, the somite size was adjusted, while the total somite number was normal (Cooke, 1975). Thus, a species-specific value for total somite number, rather than somite size exists. This has to be discussed in view of the high regulative potential of vertebrate embryos in general − if cell material is removed during the early stages of embryogenesis, the resulting embryos will exhibit a normally ordered and proportioned whole-body pattern. Since, in turn, the metameric organization of somites is tightly linked to the whole-body pattern, it appears beneficial to regulate the spacing and total number of somites in relation to the available cell material. Conceptually, this remarkable regulation of somite numbers, by adjustment of somite size, implies a globally acting mechanism, one capable of integrating axis extension into the actual size of the metameric unit.

One should also note that the universality of such a mechanism that controls somite numbers has been challenged. Depending on the experimental perturbation performed, a lack in the regulation of somite numbers was observed. For instance, a large body of literature indicates that a change in incubation temperature causes a change in the total vertebrae number in several vertebrate species, such as fish, amphibians, reptiles, birds and mice (reviewed in (Keynes and Stern, 1988). The discrepancy of these results could also be due to a different regulative potential of early versus late somitogenesis. In agreement with this proposal, J.Cooke found that in Xenopus embryos, only the first 15-20 somites (of a total of 30 somites formed) showed regulation of their size; whereas, more posterior somites lacked this regulative potential and their size was independent of available cell material (Cooke, 1981). Hence, while in experimentally, size-reduced

embryos the first 15 somites formed at a smaller size to allow for control of the number of somites, the subsequent somites formed at the same size as in control embryos. Thus, the time of observation, e.g., early versus late somitogenesis, might be essential in order to uncover somite number control mechanisms.

In any case, demonstration that somite numbers can be regulated under certain experimental settings highly influenced early models that aimed at proposing mechanisms for somitogenesis that took this potential into account.

1.2 Early theoretical models

Stimulated by the intrinsic nature of periodicity and directionality, and by the somite number control phenomenon, several theoretical models were put forth. Two of them: the "clock and wavefront model' (Cooke and Zeeman, 1976) and the model by Hans Meinhardt (Meinhardt, 1986) will be introduced here in some detail because of their direct relevance to the presented work.

1.2.1 The clock and wavefront model

Jonathan Cooke's findings about somite number control in Xenopus embryos led him, together with the mathematician E. Zeeman, to propose the ingenious "clock and wavefront model." The model has two interacting elements.

1. The Clock. To account for the periodic process of somite formation, this model proposes the existence of a cell-intrinsic oscillator, the clock, that is shared by all cells in the PSM and to which these cells are "a closely phase-organized population, because of intercellular communication" (Cooke and Zeeman, 1976). The clock switches

periodically between two states: refractory to somite formation and permissive to somite formation. The clock period is species-specific.

2. The Wavefront. A slow wavefront of developmental change, which traverses the embryo in an anterior-to-posterior manner, is put forward, reflecting the observation of progressive embryonic development along the AP axis. The nature of this wavefront is initially not specified by the authors: "it might partake of the character both of a true wave, involving propagative interactions between cells, and of a purely kinematic "wave" controlled, without ongoing cellular interaction, by a much earlier established timing gradient" ((Cooke and Zeeman, 1976) page 466). Importantly, the transit time from anterior to posterior is assumed to be species-specific. However, this assumption made sense only if one proposes a kinematic wave and accordingly, Cooke added the following refinement in a subsequent publication (Cooke, 1981): "In other words, the "wave" is not a wave at all in the sense that physical scientists would reserve for them, but rather a kinematic wavefront (Zeeman 1974), having been set up by prior arrangement rather than being propagated by present intercellular communication. Any true propagating wave of cellular activity would have a particular rate of passage per cell . . . It would therefore pass down the body in developmental times proportional to the length of tissue available within individuals." ((Cooke, 1981), page 90/91).

It is proposed that while the wavefront traverses the embryo, cells that are reached by this wavefront become competent to undergo a developmental change e.g., to form a somite. However, whether this competence is executed depends on signals from the clock. Only as the clock switches to the permissive phase do all cells traversed by the wavefront synchronously realize the developmental competence and can form a somite.

Hereby, the smooth progression of the wavefront is transformed into the periodic formation of somites. One key feature of this model is that the total transit time required for the wavefront to traverse the embryo is constant, irrespective of the actual body length. This is directly based on the observation that in Xenopus embryos which were experimentally sized reduced, the segmentation process covered the same period of time compared with unoperated, larger embryos. In other words, the larger the embryo, the faster the wavefront progression, in terms of cells traversed per time. Since the somite size, here called the wavelength, depends on the number of cells traversed during one clock oscillation, it becomes clear that control of somite size could be explained by a change in the wavefront progression speed. Smaller embryos will show a constant clock period, but their wavefront progression is slower, resulting in smaller sized somites.

1.2.2 Meinhardt's reaction-diffusion model

Hans Meinhardt's model (Meinhardt, 1982, 1986) is based on the classical reaction – diffusion models introduced by Allan Turing (Turing, 1952). It contains two elements: a gradient and an oscillator.

1. The Gradient. This model postulates the existence of a morphogen gradient within the PSM, with the peak concentration being located posteriorly in the embryo. According to Meindhardt, such a morphogen gradient could result from a reaction-diffusion mechanism (Meinhardt, 1986). Importantly, he proposed that the peak concentration of this gradient is a constant in any given species. As a consequence, the gradient profile will vary with axis length – the slope will be steeper in shorter embryos and

will be shallower in longer embryos. This feature is the basis for the somite number control mechanism (see below).

2. The Oscillator. Meinhardt proposed that cells in the PSM oscillate between two states, namely an anterior and posterior identity. The relation between these two states is of the classical reaction-diffusion mechanism. While a local inhibition exists, the two states show a reciprocal long-range activation. Thus, any given cell can only be in one state, the A (anterior) or P (posterior) state, and by being in the A state, this cell will promote the neighboring cells to be in the P state, and so on. On its own, this element would lead to a (irregular) subdivision of the embryonic field into an A-P-A pattern. Only through interaction of the oscillator with the gradient element does a regular pattern emerge that, in addition, exhibits somite number control capabilities. This model differs substantially from the clock and wavefront model by putting the two elements in direct functional interdependence. It is under the influence of the gradient, here a morphogen gradient, that oscillations occur. "Under the influence of this gradient, cells start to oscillate between (at least) two cell states: A and P. The number of oscillations is controlled by the local morphogen concentration" ((Meinhardt, 1986), page 181). On the other hand, each round of oscillations leads to a stepwise increase of a "threshold." As long as cells show a morphogen concentration above this threshold, the gradient will support oscillations. Thus, with an increasing number of oscillations and therefore, increasing threshold, the morphogen gradient will no longer meet this threshold. Because of the posterior-to-anterior distribution of the morphogen gradient, this first will occur in more anterior cells. Once cells fall below this threshold (or better, once the threshold rises above a

cell's morphogen concentration), oscillations are arrested and cells acquire a definitive A or P state, which finally will lead to boundary formation.

Thus, it is the stepwise increase of the threshold, under the influence of the oscillator, which translates the smooth morphogen gradient into the periodic formation of somites. Control of somite numbers is achieved by assuming that the gradient profile changes according to the overall axis length. The steeper slope in shorter embryos will result in the recruitment of fewer cells into a somite per stepwise increase in threshold, therefore, allowing production of a species-specific somite number. Implicit in such a scenario, the increase in threshold is also set to be species specific, analogous to a species-specific oscillation period in the clock and wavefront model.

Again, while in the clock and wavefront model both elements are essentially independent but interact, in the Meinhardt model, these two elements can actually result from one and the same mechanism (reaction-diffusion) and, more importantly, the gradient is set to be directly responsible in allowing oscillations to occur. In other words, the gradient carries a permissive function, allowing the oscillations to occur. Meinhardt puts forth the following requirement for any candidate molecules underlying these hypothetical elements: "This model would obtain strong support if the postulated oscillations in the mesoderm before somite formation could be detected. One full cycle of this oscillation should take precisely the same time as that required for the formation of one somite . . ." ((Meinhardt, 1986); page 188).

1.3 Molecular mechanisms in somitogenesis

The discovery of molecular oscillations within the PSM had to wait another 10 years until 1997. In their landmark paper, Palmeirim and colleagues described the oscillating mRNA expression of *c-hairy 1* in chick embryos (Palmeirim et al., 1997). Strikingly, these transcriptional oscillations showed a period that matched somite formation, thus providing the long-awaited experimental support for the existence of a segmentation oscillator or segmentation clock. This finding ignited numerous studies and led to the identification of oscillating mRNA expression of so called cyclic genes in mice, chick, reptiles, amphibians and fish embryos (Aulehla and Johnson, 1999; Bessho et al., 2003; Bessho et al., 2001; Dequeant et al., 2006; Forsberg et al., 1998; Gajewski et al., 2003; Gomez et al., 2008; Holley et al., 2000; Holley et al., 2002; Jouve et al., 2000; Julich et al., 2005; Li et al., 2003; McGrew et al., 1998; Oates and Ho, 2002; Sieger et al., 2004). In addition, molecular data supporting the existence of a gradient, or better gradients, within the PSM have likewise emerged (Diez del Corral et al., 2003; Dubrulle and Pourquie, 2004; Sawada et al., 2001).

In the following review article, I summarized the current state of knowledge about the molecular identity of the clock and the gradient.

1.4 On periodicity and directionality of somitogenesis

Anat Embryol (2006)
DOI 10.1007/s00429-006-0124-y

REVIEW

Alexander Aulehla · Olivier Pourquié

On periodicity and directionality of somitogenesis

Accepted: 17 August 2006

Abstract It is currently thought that the mechanism underlying somitogenesis is linked to a molecular oscillator, the segmentation clock, and to gradients of signaling molecules within the paraxial mesoderm. Here, we review the current picture of this segmentation clock and gradients, and use this knowledge to critically ask: What is the basis for periodicity and directionality of somitogenesis?

Keywords Embryology · Axial patterning · Somites · Biological models · Biological clock

Introduction

The process of somitogenesis is characterized both by its periodicity and its directionality. For instance, in the chicken embryo one pair of somites is formed every 90 min in a strict anterior-to-posterior sequence until all pairs (55 in the chicken embryo) are formed. What makes these features so intriguing is their intrinsic nature. This is reflected by the finding that both periodicity and directionality are very resistant to experimental manipulation. If paraxial mesoderm is bisected transversely, segmentation will occur normally in the anterior and later in the posterior half and segments will form at the right time and at the right place (Packard 1978). Moreover, when paraxial mesoderm is isolated from all surrounding tissues, a periodic segmentation of the paraxial mesoderm on a molecular level can be observed, indicating that the underlying mechanism is an intrinsic property of these cells (Palmeirim et al. 1998). Regarding directionality, it is utterly impossible to reverse the endogenous somitogenesis direction experimentally through microsurgical manipulations. One reason for these findings might be that paraxial mesoderm cells are endowed with the information for periodicity and directionality very early, at least as soon as they emerge as a result of the gastrulation process. Evidence for this comes from a classical study by Christ et al. (1974). This study was set up to address a controversy in the field: while several authors previously found evidence for a regulative capacity in amphibian and chicken embryos in respect to the direction of segmentation, others found that directionality was intrinsic to paraxial mesoderm (Menkes et al. 1968; Deuchar and Burgess 1967).

Bodo Christ performed microsurgical anterior-to-posterior inversions of unsegmented paraxial mesoderm in chicken embryos [segmental plate (SP), in mouse embryos the unsegmented paraxial mesoderm is termed presomitic mesoderm (PSM), which will be used throughout this review] and tested the effect on the direction of somite formation (Christ et al. 1974). Clearly, he found no sign of regulative capacity. The sequence of somite formation was unchanged in the inverted PSM, corresponding to the original orientation (Fig. 1a). This was also the case, when PSM was inverted and implanted in a host embryo at the site of the extirpated neural tube (Fig. 1b). Most intriguingly, even when paraxial mesoderm, which was still located posterior to Hensen's node representing nascent mesoderm just after the ingression through the anterior primitive streak, was inverted in a 24–30 h old embryo (and thus at a stage before any somite had formed yet), the endogenous direction of segmentation was maintained. Segments formed from posterior to anterior matching their original orientation. Thirty years later, the question of how these fascinating properties are established remains unanswered.

The discoveries of a molecular segmentation clock (Palmeirim et al. 1997) and a gradient of signaling molecules within the paraxial mesoderm (Dubrulle et al. 2001) have provided a new conceptual framework within which these questions can be readdressed. Here, we will

A. Aulehla · O. Pourquié (✉)
Howard Hughes Medical Institute and Stowers Institute for Medical Research, 1000 E. 50th Street, Kansas City MO 64110, USA
E-mail: olp@stowers-institute.org
Tel.: +1-816-9264442
Fax: +1-816-9262095

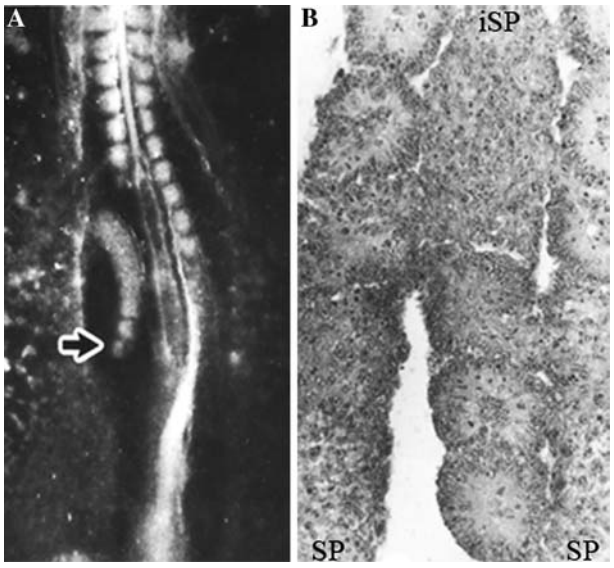

Fig. 1 The inversion of segmental plate (*SP*) does not change the original orientation of somite formation in chicken embryos. **a** Inverted *SP* (*black arrow*) shows two new somites forming now in posterior-to-anterior sequence. **b** Frontal section through an embryo, where the neural tube was replaced with an inverted *SP* (*iSP*). Note new somite formed posteriorly in inverted *SP*. Anterior is to the top. From Christ et al. (1974), with permission of the author

first review the current knowledge and models in relation to this gradient and the clock, and then discuss these models in light of the classical question: How is periodicity and directionality established?

A molecular oscillator within the paraxial mesoderm

Somites form periodically within the still unsegmented region, the PSM, of paraxial mesoderm and thus it has been proposed for many decades that a clock of whatever nature is underlying this process (for review of these early models see Aulehla and Herrmann 2004). In 1997, the discovery of a molecular oscillator, termed the segmentation clock, provided the long-awaited experimental proof (Palmeirim et al. 1997). A new class of genes, the cyclic genes, has since been defined and their number is increasing steadily. Their defining property is a highly dynamic mRNA expression pattern within the PSM. This pattern consists of a posteriorly located oscillating expression domain (the wave) and usually one stable domain (the stripe) at the anterior end of the PSM. While the wave traverses the PSM in a posterior-to-anterior direction, it will eventually replace the anterior stripe, and a new cycle starts anew with a wave of expression emerging posteriorly. It is important to point out that the impression of a moving wave is thought to be brought about by coordinated, sequential activation of expression and is not due to actual movement of cells. Thus, within one somite formation cycle, the expression of cyclic genes is switched on and off again. Strikingly, the period of these oscillations matches somite formation time and hence, it was proposed that these oscillations are part of a segmentation clock.

Cyclic genes have been identified in several vertebrate species (mouse, chicken, fish and frog). While all initially characterized genes were found to be targets or components of a single signaling pathway (Notch signaling pathway), it is now clear that at least in mouse embryos, several major signaling pathways show cyclic activation of target genes (see below).

To-date, still the largest group of cyclic genes relates to the Notch signaling pathway (for review see Bessho and Kageyama 2003; Pourquie 2003), linking this pathway to the segmentation clock. The functional importance of this pathway for the segmentation process is supported by numerous studies which showed that impairment of Notch signaling and Notch cyclic genes perturbs segmentation (del Barco Barrantes et al. 1999; Hrabe de Angelis et al. 1997; Conlon et al. 1995; Evrard et al. 1998; Zhang and Gridley 1998; Bessho et al. 2003; Huppert et al. 2005). However, although somites are clearly affected in these mouse mutants, even the most severe phenotypes (e.g., in case of the loss of RBPjK-appa; Oka et al. 1995; del Barco Barrantes et al. 1999) show that irregular segmentation and somite formation still occur.

A partial explanation for these findings was provided by the discovery of a second group of cyclic genes, which are related to another pathway, namely the Wnt signaling pathway (Aulehla et al. 2003). Interestingly, the oscillating activity of the Wnt pathway was determined to be out of phase compared to the Notch pathway: the basis for this remains unknown. A second important conclusion from this and other studies (see below) was that Wnt and Notch signaling pathways interact and influence each other in the segmentation clock. Thus, several oscillating pathways appear to be integrated within one clock, in contrast to the proposal that several molecular clocks exist and work in parallel.

Wnt signaling and the segmentation clock

Whenever multiple pathways interact, two immediate questions arise. First, where does the cross-talk happen and second, is one pathway controlling the other? These major pathways share numerous interactions in many different contexts, both during development and in disease, and consequently, there is no shortage of potential cross-talk scenarios. Experimental evidence pointing to the level of this interaction in the context of the segmentation clock is still scarce. Recently, however, experimental data from the analysis of the regulation of Delta-like1, a Notch ligand strongly expressed in the PSM, indicate that Delta-like1 in the paraxial mesoderm and tail bud of mouse embryos is regulated by Wnt signaling (in synergy with the T-box transcription factor TBX6) (Hofmann et al. 2004; Galceran et al. 2004). Interestingly, it has recently been reported that Dll1 shows cyclic mRNA expression in the PSM, adding

evidence for oscillations of Wnt signaling in the PSM (Maruhashi et al. 2005). The regulation of the Notch ligand Dll1 by Wnt signaling provides a direct link between these two signaling pathways during somitogenesis. Additionally, naked cuticle, a negative regulator of Wnt signaling, has been identified as a cyclic gene under the control of Notch signaling (Ishikawa et al. 2004). Clearly, these examples point to a tight interaction between these two pathways. The elucidation of this cross-talk will be of great interest in order to understand the segmentation clock mechanism.

Regarding a possible hierarchy between Wnt and Notch signaling, first insight was obtained by the analysis of the vestigial tail mouse mutants, which are hypomorph mutants for Wnt3a (Greco et al. 1996; Aulehla et al. 2003). In these mutants, the Wnt cyclic gene Axin2 was absent in the PSM. Interestingly, the oscillations of the Notch cyclic gene lunatic fringe (*lfng*) seemed to be arrested (Aulehla et al. 2003). Recent reports underscored this major role of Wnt signaling in the segmentation clock (Nakaya et al. 2005; Satoh et al. 2006). As was previously known, Wnt3a mutant mice show an arrest of segmentation at the level of the forelimb (Takada et al. 1994). Now Nakaya et al. (2005) extended the analysis of these mutant mice and analyzed the role of Wnt3a in left–right determination, axis elongation and somite patterning. Regarding the latter, they showed that the arrest of segmentation in these mutant embryos is accompanied by an arrest of the cyclic mRNA expression of Wnt and also of Notch cyclic genes. Another study reported the consequence of a combined loss-of-mutation of secreted Wnt antagonists SRFP1 and 2 (Satoh et al. 2006). The loss of these Wnt signaling antagonists leads to the expected over activation of Wnt signaling in the PSM, resulting in severely affected segmentation. Again, this phenotype is accompanied by an arrest of the oscillatory transcription of Notch cyclic genes *lfng* and *HES7*.

In conclusion, current data support the view that Notch signaling oscillations depend on an intact and appropriate Wnt signaling and that Wnt signaling is central to the segmentation clock mechanism.

Gradient(s) of signaling pathways within the PSM

While it is known that the PSM is polarized in an anterior-to-posterior direction very shortly after or during the gastrulation process, only recently was experimental evidence for a mechanism underlying this property provided. Dubrulle et al. (2001) first described a graded expression of FGF signaling within the PSM, with the highest level located posteriorly and decreasing activity located anteriorly. A second pathway found to establish a signaling gradient within the PSM is the Wnt-pathway (Aulehla et al. 2003). During the journey along the antero-posterior axis, a cell would experience decreasing levels of FGF and Wnt signaling until the levels drop below a critical threshold. This region has been termed the determination front, and it is believed to mark a region of developmental change. In combination with axis elongation occurring through cell recruitment at the posterior end of the embryo, this determination front becomes localized more and more posteriorly. It is thought that the interaction between the segmentation clock and these gradients at the level of the determination front defines the segment size.

In addition to FGF and Wnt signaling, a third opposing signaling gradient in the PSM has been identified (Del Corral and Storey 2004). The retinoic acid (RA) pathway is graded in opposite direction relative to FGF signaling and is counteracting the latter, thus influencing the position of the determination front.

Left–right synchronization of segment formation

Segment formation is precisely symmetric on the left and right embryo half and again, the basis for this is unknown. Recently, it was found that the RA pathway appears to play an important role in this process; when the synthesis of active RA is perturbed in mouse or chicken embryos, segmentation defects occur predominantly on the right side of the embryo (Vermot and Pourquie 2005; Vermot et al. 2005; Sirbu and Duester 2006). Similar results were found in zebrafish (Kawakami et al. 2005). Interestingly, there is a clear connection to the complex machinery establishing left–right body asymmetry since the laterality of the segmentation phenotype depends on the orientation of the situs (Vermot and Pourquie 2005; Kawakami et al. 2005). In terms of segmentation clock and gradients, both were affected in the absence of RA signaling, resulting in asymmetric mRNA expression of cyclic genes and Fgf8 between the left and right embryo half. However, these perturbed expression patterns could be secondary to another mechanism leading to the described phenotype; it is unclear how these defects are generated in the first place.

Defining segments: the gradient and the clock model

It is generally proposed that it is the interaction between the two described elements, the segmentation clock and the gradient of signaling pathways, that specifies a segment in the anterior PSM. A crucial question in this scenario, however, is how is this interaction achieved? While there is no experimental proof, the gradient and the clock model proposes the following link (Aulehla and Herrmann 2004): it is Wnt signaling in the PSM that activates oscillations of the Wnt cyclic genes (which then are linked to oscillations of Notch cyclic genes). In other words: the gradient drives the clock. Since Wnt signaling is graded in the PSM, the signal to activate the oscillations will eventually drop below a threshold and therefore, the oscillations stop in the anterior PSM. This defines the boundary between cells that are still capable

of oscillations and cells in which the oscillations have been arrested. This boundary could serve to specify the future segment size. The location of this boundary would depend on the slope of the gradient, its kinetics of regression and of the timing of the segmentation clock.

The basis for periodicity

Timing versus time

Biological clocks, best studied for the circadian clock, are usually characterized by very regular pacing as measured in astronomical time. What about a potential segmentation clock in the embryo—Does it also measure absolute time? We know, for instance, that in mouse embryos, the period of segment formation varies considerably depending on the developmental age (Tam 1981). This points to a fundamental difference between other biological clocks and embryological clocks. Embryological clocks measure developmental, not astronomical time, and are responsible for the reliable timing of a process. Timing, in the sense of deciding when it is best and most efficient to start a process, does not require regular pacing. Rather, reliable timing can require the modulation of the pacing of this clock so that the rate of segmentation is coordinated with overall development. Revealing how the modulation of this embryological clock is achieved and how this modulation is coordinated with overall development will be an exciting task for the future.

The basis for periodicity

The nature of the segmentation clock

As Pittendrigh (Pittendrigh 1954) pointed out in his seminal paper about the circadian clock in Drosophila, "If a clock is to provide information involved in controlling important functions, then clearly it must be reasonably reliable". Recently, an exciting report addressed the question of how reliability is achieved within the segmentation clock (Horikawa et al. 2006). Using cell transplantation experiments in zebrafish embryos, Horikawa et al. found experimental evidence for the precise cell-to-cell communication within the PSM postulated by Jiang et al. (2000). For instance, when a small group of PSM cells was transferred from a donor into a host PSM, the oscillations within these cells were reset so that they matched the overall oscillation behavior within the new environment (Horikawa et al. 2006). The authors conclude that the segmentation clock uses coupled-oscillators, resulting in very reliable and coordinated oscillations in the cells of the PSM.

The current molecular view of this coupled-oscillator involves negative-feedback regulation at transcriptional and translational levels, also known as the "delay-model" (Lewis 2003). While available data are in agreement with this view, it should be pointed out that no formal proof of the importance of the observed oscillations exists. This is true, since technically it has not been possible to perturb only the oscillations without interfering with the anterior, stable stripe domain characteristic for all cyclic genes. The importance of this striped expression for the final morphogenetic changes leading to somite formation cannot be overemphasized (for a review see Saga and Takeda 2001). Thus, we lack formal proof of the function of the observed mRNA and protein level oscillations in the posterior PSM. One should therefore always consider other scenarios, like post-translational modifications, as a mechanism of the segmentation clock.

In addition, we have no formal proof that the identified cyclic genes are part of the core mechanism of the segmentation clock, and neither do we know the parameters of this clock. The gold standard to definitively demonstrate the implication of a gene in a clock mechanism has been to show that altering the function of this gene alters the period of the clock oscillation. This approach has been attempted in the mouse by artificially increasing the stability of the Hes7 protein (Hirata et al. 2004). However, while this led to an alteration of the segmentation process, no clear alteration of the clock period was observed. Rather, this approach led to an arrest of the clock mechanism altogether.

It should also be noted that the deletion of Axin2, which is part of the segmentation clock mechanism, in our current models, does not result in a segmentation phenotype (Yu et al. 2005). This clearly points out that we are still far from understanding the real nature of this segmentation clock.

A crucial requirement for testing the role of the oscillations per se is the development of novel tools allowing their visualization in real-time. This has been recently reported beautifully using bioluminescence as a readout of cyclic promoter activity (Masamizu et al. 2006). We have developed a real-time imaging method allowing visualization of the oscillations with a fluorescence based reporter (A. A and O. P, unpublished). These new exiting tools will help to address the function of oscillations and will be important in understanding how global regulation is achieved within the segmentation clock.

The basis of directionality

To-date, the best candidates accounting for the directional formation of somites are gradients of signaling molecules within the PSM. It is known from classical experiments that there are very little cell movements within the PSM (Stern et al. 1988) This allows gradients formed by localized de novo production to be maintained over considerable time (cells stay approximately 18 h within the PSM of chicken embryos before being incorporated into a somite). Second, as mentioned pre-

viously, cells in the PSM gain their positional information very early during or shortly after gastrulation, indicating a potential link between gastrulation and gradient formation. The signaling pathways involved in generating gradients, namely FGF and Wnt signaling, are known to be central players within the gastrulation process (Yamaguchi et al. 1994; Takada et al. 1994; Liu et al. 1999). This could explain how cells undergoing gastrulation are endowed simultaneously with positional information in the form of a graded signaling molecule. A remaining challenge will be to formerly test this hypothesis and to understand the multiple roles of these signaling pathways in the gastrulation and segmentation processes.

Outlook

Periodicity and directionality are only part of a complex machinery underlying somitogenesis. Classical embryological data and experiments—together with molecular data, genome wide analysis, real-time imaging and mathematical modeling—will need to be integrated in order to approach the goal of a comprehensive view of this beautiful embryological process.

Acknowledgment A. A was funded by the Swiss Foundation for medical-biological grants. Current work is supported by the Stowers Institute for Medical Research and NIH grant 1R01 HD043158-01. O. P. is a Howard Hughes Medical Institute Investigator.

References

Aulehla A, Herrmann BG (2004) Segmentation in vertebrates: clock and gradient finally joined. Genes Dev 18:2060–2067

Aulehla A, Wehrle C, Brand-Saberi B, Kemler R, Gossler A, Kanzler B, Herrmann BG (2003) Wnt3a plays a major role in the segmentation clock controlling somitogenesis. Dev Cell 4:395–406

del Barco Barrantes I, Elia A, Wunnsch K, Hrabde De Angelis M, Mak T, Rossant J, Conlon R, Gossler A, Luis de la Pompa J (1999) Interaction between Notch signalling and lunatic fringe during somite boundary formation in the mouse. Curr Biol 9:470–480

Bessho Y, Kageyama R (2003) Oscillations, clocks and segmentation. Curr Opin Genet Dev 13:379–384

Bessho Y, Hirata H, Masamizu Y, Kageyama R (2003) Periodic repression by the bHLH factor Hes7 is an essential mechanism for the somite segmentation clock. Genes Dev 17:1451–1456

Christ B, Jacob HJ, Jacob M (1974) Somitogenesis in the chick embryo. Determination of the segmentation direction. Verh Anat Ges 68:573–579

Conlon RA, Reaume AG, Rossant J (1995) Notch1 is required for the coordinate segmentation of somites. Development 121:1533–1545

Del Corral RD, Storey KG (2004) Opposing FGF and retinoid pathways: a signalling switch that controls differentiation and patterning onset in the extending vertebrate body axis. Bioessays 26:857–869

Deuchar E, Burgess AMC (1967) Somite segmentation in amphibian embryos: is there a transmitted control mechanism? J Embryol Exp Morphol 17:349–358

Dubrulle J, McGrew MJ, Pourquie O (2001) FGF signaling controls somite boundary position and regulates segmentation clock control of spatiotemporal Hox gene activation. Cell 106:219–232

Evrard YA, Lun Y, Aulehla A, Gan L, Johnson RL (1998) lunatic fringe is an essential mediator of somite segmentation and patterning. Nature 394:377–381

Galceran J, Sustmann C, Hsu SC, Folberth S, Grosschedl R (2004) LEF1-mediated regulation of delta-like1 links Wnt and Notch signaling in somitogenesis. Genes Dev 18:2718–2723

Greco TL, Takada S, Newhouse MM, McMahon JA, McMahon AP, Camper SA (1996) Analysis of the vestigial tail mutation demonstrates that Wnt-3a gene dosage regulates mouse axial development. Genes Dev 10:313–324

Hirata H, Bessho Y, Kokubu H, Masamizu Y, Yamada S, Lewis J, Kageyama R (2004) Instability of Hes7 protein is crucial for the somite segmentation clock. Nat Genet 36:750–754

Hofmann M, Schuster-Gossler K, Watabe-Rudolph M, Aulehla A, Herrmann BG, Gossler A (2004) WNT signaling, in synergy with T/TBX6, controls Notch signaling by regulating Dll1 expression in the presomitic mesoderm of mouse embryos. Genes Dev 18:2712–2717

Horikawa K, Ishimatsu K, Yoshimoto E, Kondo S, Takeda H (2006) Noise-resistant and synchronized oscillation of the segmentation clock. Nature 441:719–723

Hrabe de Angelis M, McIntyre J, Gossler A (1997) Maintenance of somite borders in mice requires the delta homologue DII1. Nature 386:717–721

Huppert SS, Ilagan MX, De Strooper B, Kopan R (2005) Analysis of Notch function in presomitic mesoderm suggests a gamma-secretase-independent role for presenilins in somite differentiation. Dev Cell 8:677–688

Ishikawa A, Kitajima S, Takahashi Y, Kokubo H, Kanno J, Inoue T, Saga Y (2004) Mouse Nkd1, a Wnt antagonist, exhibits oscillatory gene expression in the PSM under the control of Notch signaling. Mech Dev 121:1443–1453

Jiang YJ, Aerne BL, Smithers L, Haddon C, Ish-Horowicz D, Lewis J (2000) Notch signalling and the synchronization of the somite segmentation clock. Nature 408:475–479

Kawakami Y, Raya Y, Marina Raya Y, Rodríguez-Esteban C, Izpisúa Belmonte J (2005) Retinoic acid signalling links left-right asymmetric patterning and bilaterally symmetric somitogenesis in the zebrafish embryo. Nature (in press)

Lewis J (2003) Autoinhibition with transcriptional delay: a simple mechanism for the zebrafish somitogenesis oscillator. Curr Biol 13(16):1398–1408

Liu P, Wakamiya M, Shea MJ, Albrecht U, Behringer RR, Bradley A (1999) Requirement for Wnt3 in vertebrate axis formation. Nat Genet 22:361–365

Maruhashi M, Van De Putte T, Huylebroeck D, Kondoh H, Higashi Y (2005) Involvement of SIP1 in positioning of somite boundaries in the mouse embryo. Dev Dyn 234:332–338

Masamizu Y, Ohtsuka T, Takashima Y, Nagahara H, Takenaka Y, Yoshikawa K, Okamura H, Kageyama R (2006) Real-time imaging of the somite segmentation clock: revelation of unstable oscillators in the individual presomitic mesoderm cells. Proc Natl Acad Sci USA 103:1313–1318

Menkes B, Sandor S, Elias S (1968) Researches on the formation of axial organs of the chick embryo. IV. Rev Roum Embryol Cytol 5:131–137

Nakaya MA, Biris K, Tsukiyama T, Jaime S, Rawls JA, Yamaguchi TP (2005) Wnt3alinks left-right determination with segmentation and anteroposterior axis elongation. Development 132:5425–5436

Oka C, Nakano T, Wakeham A, de la Pompa JL, Mori C, Sakai T, Okazaki S, Kawaichi M, Shiota K, Mak TW, Honjo T (1995) Disruption of the mouse RBP-J kappa gene results in early embryonic death. Development 121:3291–3301

Packard DSJ (1978) Chick somite determination: the role of factors in young somites and the segmental plate. J Exp Zool 203:295–306

Palmeirim I, Henrique D, Ish-Horowicz D, Pourquié O (1997) Avian hairy gene expression identifies a molecular clock linked to vertebrate segmentation and somitogenesiss. Cell 91:639–648
Palmeirim I, Dubrulle J, Henrique D, Ish-Horowicz D, Pourquié O (1998) Uncoupling segmentation and somitogenesis in the chick presomitic mesoderm. Dev Genet 23:77–85
Pittendrigh CS (1954) On temperature independence in the clock system controlling emergence time in drosophila. Proc Natl Acad Sci USA 40:1018–1029
Pourquie O (2003) Vertebrate somitogenesis: a novel paradigm for animal segmentation? Int J Dev Biol 47:597–603
Saga Y, Takeda H (2001) The making of the somite: molecular events in vertebrate segmentation. Nat Rev Genet 2:835–845
Satoh W, Gotoh T, Tsunematsu Y, Aizawa S, Shimono A (2006) Sfrp1 and Sfrp2 regulate anteroposterior axis elongation and somite segmentation during mouse embryogenesis. Development 133:989–999
Sirbu IO, Duester G (2006) Retinoic-acid signalling in node ectoderm and posterior neural plate directs left-right patterning of somitic mesoderm. Nat Cell Biol 8:271–277
Stern CD, Fraser SE, Keynes RJ, Primmett DR (1988) A cell lineage analysis of segmentation in the chick embryo. Development 104:231–244
Takada S, Stark KL, Shea MJ, Vassileva G, McMahon JA, McMahon AP (1994) Wnt-3a regulates somite and tailbud formation in the mouse embryo. Genes Dev 8:174–189
Tam PP (1981) The control of somitogenesis in mouse embryos. J.Embryol.Exp Morphol 65(Suppl):103–128
Vermot J, Pourquie O (2005) Retinoic acid coordinates somitogenesis and left-right patterning in vertebrate embryos. Nature 435:215–220
Vermot J, Gallego Llamas J, Fraulob V, Niederreither K, Chambon P, Dolle P (2005) Retinoic acid controls the bilateral symmetry of somite formation in the mouse embryo. Science 308(5721):563–566
Yamaguchi TP, Harpal K, Henkemeyer M, Rossant J (1994) fgfr-1 is required for embryonic growth and mesodermal patterning during mouse gastrulation. Genes Dev 8:3032–3044
Yu HM, Jerchow B, Sheu TJ, Liu B, Costantini F, Puzas JE, Birchmeier W, Hsu W (2005) The role of Axin2 in calvarial morphogenesis and craniosynostosis. Development 132:1995–2005
Zhang N, Gridley T (1998) Defects in somite formation in lunatic fringe-deficient mice.Nature 394:374–377

As pointed out in the review, a formal proof for the importance of the oscillations as a time-measuring mechanism is still missing. A main reason is the technical challenge to address the functional significance of the oscillations *per se*. An elegant recent publication from Susan Cole addressed this issue. In a sophisticated knock-out experiment, her group tested the significance of the mRNA oscillations of *lunatic fringe* (*Lfng*) (Shifley et al., 2008). *Lfng* was the second cyclic gene to be identified and showes a striking oscillatory expression behavior in the PSM of mouse and chick embryos (Aulehla and Johnson, 1999; Forsberg et al., 1998; McGrew et al., 1998). The functional analysis indicated that this gene is essential for proper somite formation (Evrard et al., 1998; Zhang and Gridley, 1998). Importantly, the *Lfng* expression pattern consists of a posterior oscillatory expression domain and a more anterior, stable- and striped-expression domain. These two expression domains are driven by distinct regulatory sequences as the enhancer/promoter analysis in transgenic mice indicated (Cole et al., 2002; Morales et al., 2002). By genetically deleting the enhancer element responsible for driving the oscillatory expression of *Lfng*, a situation was created in which only the oscillatory expression was lost while preserving the anterior stable-expression domain. In sharp contrast to the conventional deletion of the entire *Lfng* function, which results in a severe disruption of somite formation, the selective deletion of only the oscillatory expression domain has a very mild, if any, somite formation defect. The formation of somites, as indicated by the expression of the somite marker *Uncx4.1* (Leitges et al., 2000) appears almost normal (Shifley et al., 2008). While this obviously does not allow one to conclude about the function of oscillations in general (since only one cyclic gene

has been removed and the segmentation clock remained active), it is a strong reminder that a more differentiated approach to test the significance of the oscillatory component of cyclic genes is indicated.

In summary, while compelling data exist supporting the view of a molecular oscillator in the PSM across vertebrates, it remains a challenge to find an experimental handle to affect the pace of these oscillations and, thereby, to functionally link oscillations to clock function.

2. Goal of this work

The presented work has four goals:

1. We aimed to identify novel components related to the oscillation phenomenon in the PSM.
2. A major goal was to visualize the transcriptional oscillations in real-time imaging in live mouse embryos.
3. We functionally tested the role of the Wnt-signaling gradient in the somite formation process and especially its connection to the oscillation phenomenon in the PSM.
4. Finally, based on the results of this work, we put forward a new model – the Appendix model.

3. Results

3.1 Wnt3a plays a major role in the segmentation clock controlling somitogenesis

Developmental Cell, Vol. 4, 395–406, March, 2003, Copyright ©2003 by Cell Press

Wnt3a Plays a Major Role in the Segmentation Clock Controlling Somitogenesis

Alexander Aulehla,[1] Christian Wehrle,[2] Beate Brand-Saberi,[3] Rolf Kemler,[2] Achim Gossler,[4] Benoit Kanzler,[1] and Bernhard G. Herrmann[1,*]
[1]Abteilung Entwicklungsbiologie and
[2]Abteilung Molekulare Embryologie
Max-Planck-Institut für Immunbiologie
Stübeweg 51
D-79108 Freiburg
Germany
[3]Anatomisches Institut II
Albert-Ludwigs-Universität
Albertstr. 17
D-79104 Freiburg
Germany
[4]Institut für Molekularbiologie
OE5250
Medizinische Hochschule Hannover
Carl-Neuberg-Str. 1
D-30625 Hannover
Germany

Summary

The vertebral column derives from somites generated by segmentation of presomitic mesoderm (PSM). Somitogenesis involves a molecular oscillator, the segmentation clock, controlling periodic Notch signaling in the PSM. Here, we establish a novel link between Wnt/β-catenin signaling and the segmentation clock. *Axin2*, a negative regulator of the Wnt pathway, is directly controlled by Wnt/β-catenin and shows oscillating expression in the PSM, even when Notch signaling is impaired, alternating with *Lfng* expression. Moreover, *Wnt3a* is required for oscillating Notch signaling activity in the PSM. We propose that the segmentation clock is established by Wnt/β-catenin signaling via a negative-feedback mechanism and that *Wnt3a* controls the segmentation process in vertebrates.

Introduction

In 1686 Malpighi reported, in *Opera Omnia*, the existence of a segmentation process in vertebrate embryos, indicated by the formation of somites, the precursors of the vertebrae, all striated muscles, and the dermis of the back (Christ and Ordahl, 1995). While considerable progress has been made in understanding the maturation and function of somites, the answer to the question of how somites form still remains largely elusive. Somites bud off from the presomitic mesoderm (PSM) as pairs of epithelial spheres in an anterior to posterior sequence (Gossler and Hrabe de Angelis, 1998). Their formation is a periodic process, repeated approximately every 90 min in chick embryos and every 90–120 min in mouse embryos (Tam, 1981). While somites form at the anterior PSM, new cells emerging from a growth zone, the primitive streak or tail bud, are added to the posterior end of the PSM. These new PSM cells are already endowed with an intrinsic program leading to segmentation (Keynes and Stern, 1988).

In order to account for this intrinsic segmentation program and periodicity, several models, comprising the "clock and wavefront" model, Meinhardt's model, the "cell cycle" model, and the "clock and trail" model, proposing an oscillator as a principal component, have been put forward (Cooke and Zeeman, 1976; Kerszberg and Wolpert, 2000; Meinhardt, 1986; Stern et al., 1988). The discovery of oscillating expression of *c-hairy1* in the PSM of chick embryos provided the first molecular evidence for the existence of a segmentation clock (Palmeirim et al., 1997). Meanwhile, several other cycling genes, such as *lunatic fringe* (*Lfng*), *her1*, *c-hairy2*, *Hes1*, and *Hey2* have been identified in different species (Pourquie, 2001). They all behave in a similar manner with respect to the dynamics of their expression pattern in the PSM and all depend on Notch signaling (Barrantes et al., 1999; Jouve et al., 2000; Leimeister et al., 2000). These data linked Notch signaling to the segmentation clock. However, though impairment of Notch signaling affects intrasegmental polarization and the formation of regular boundaries, it does not prevent segmentation (Conlon et al., 1995; Evrard et al., 1998; Hrabe de Angelis et al., 1997; Oka et al., 1995; Zhang and Gridley, 1998). Thus, the role of Notch-dependent periodic gene expression in the segmentation process remains unresolved.

Recently, a graded distribution of Fgf8 along the PSM and a role of *Fgf8* in setting the segment boundary position have been reported (Dubrulle et al., 2001). These data provided molecular evidence for a gradient, predicted in several models to play an essential role in the segmentation process (Cooke and Zeeman, 1976; Meinhardt, 1986).

Thus, there is now molecular evidence for the functional importance of a gradient and a segmentation clock in the PSM. However, the mechanism by which the segmentation clock is established and by which it interacts with the gradient in forming a regular array of segments has not been uncovered.

Here, we provide evidence for a novel link between Wnt/β-catenin signaling and the segmentation clock and for a graded distribution of Wnt signaling along the PSM. Furthermore, we present data suggesting that the segmentation clock involves a negative-feedback loop between Wnt/β-catenin signaling and the Wnt inhibitor Axin2. Our data suggest a major role of *Wnt3a* in the clock and gradient controlling the segmentation process.

Results

Axin2 Expression in the PSM Oscillates

In the course of a large-scale screen for genes specifically transcribed in the tail bud and/or PSM, we isolated

*Correspondence: herrmann@immunbio.mpg.de

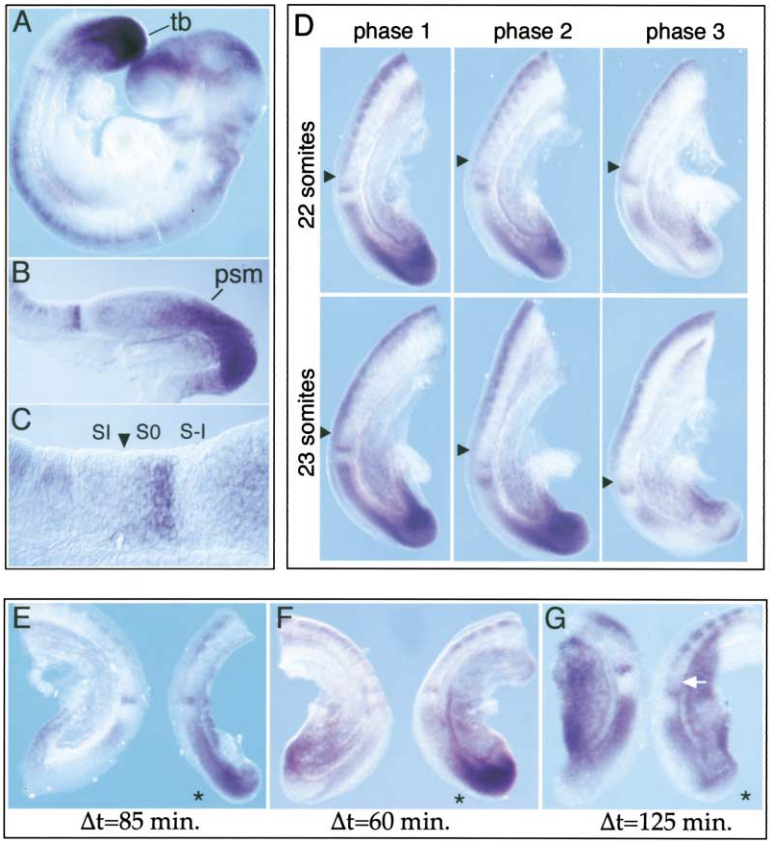

Figure 1. *Axin2* Shows Oscillating and Graded mRNA Expression in the PSM

Whole-mount in situ hybridization showing *Axin2* expression in 9.5 dpc embryos; (A) whole-mount embryo, (B) sagittal section of caudal region, and (C) enlargement of anterior PSM emphasizing the stripe of *Axin2* in the caudal half of presomite 0 (S0); note the graded distribution of *Axin2* mRNA along the PSM (A and B).

(D) Cyclic pattern of *Axin2* mRNA expression, shown for 22- and 23-somite stage embryos; note the change from strong expression in tail bud and graded distribution along PSM (phase 1, n = 71/143) to two stripes in anterior PSM (S0 and S-I, phase 2, n = 24/143) to weak expression in tail bud and posterior PSM with broad domain caudal of S-I (phase 3, n = 48/143).

(E–G) Embryo half culture experiments showing a change in the *Axin2* expression pattern during the incubation period of 85 min (E) or 60 min (F); after 125 min incubation time, similar patterns were observed, while a new somite had formed (white arrow) (G). Arrowheads, the SI/S0 boundary; asterisks, the incubated embryo half; PSM, presomitic mesoderm; tb, tail bud.

Axin2, a negative regulator of the Wnt/β-catenin signaling cascade (Behrens et al., 1998). *Axin2* is expressed in the tail bud, PSM, dorsomedial lip of the dermomyotome of mature somites, lateral plate mesoderm, limb buds, brain, spinal cord, and branchial arches I and II (Figure 1A and data not shown). *Axin2* shows strong expression in the tail bud and a graded distribution in the PSM, with a sharp anterior boundary in presomite I (S-I), separated from a stripe of expression in the caudal half of S0 (Figures 1A–1C; Figure 1D, phase 1). This PSM pattern was detectable throughout somitogenesis (data not shown).

The analysis of a larger number of 9.5 dpc embryos revealed additional patterns of *Axin2* expression in the PSM, which could be grouped into three different phases (Figure 1D). Out of 143 embryos examined, 71 showed the pattern described above, representing phase 1. In part of the embryos (n = 24/143), a second stripe has formed in the anterior PSM, followed by a gap (phase 2). In another subset of embryos (n = 48/143), *Axin2* expression is strongly downregulated in the tail bud, while a broader domain of *Axin2*-positive cells remains in the anterior PSM and is separated from the stripe in S0 (phase 3). The dynamic change of expression is repeated in each cycle of somite formation, as shown here for 22- and 23-somite stage embryos. This observation suggested that *Axin2* expression in the PSM is controlled by the segmentation clock, similarly to the *Notch1* target genes *c-hairy1* and *Lfng* (Aulehla and Johnson, 1999; Forsberg et al., 1998; McGrew et al., 1998; Palmeirim et al., 1997).

To obtain further evidence for this finding, we performed embryo half culture experiments and assayed for a change in the expression of *Axin2* after culturing one of the two halves for a defined time period. When a culture period between 30 and 90 min was chosen, most embryos (34/39) showed a difference in the expression patterns of the two PSM halves (Figures 1E–1F and data not shown). The changes were most evident in the tail bud region, where the expression changed from very strong to absent or vice versa. This demonstrated that *Axin2* expression in the PSM oscillates during a segmentation cycle period. Moreover, when a culture period of 125 ± 10 min was chosen (n = 11/14), the expression pattern was very similar in both PSM halves, and a new somite had formed on the incubated half (Figure 1G). Thus, the period of oscillations of *Axin2* expression is in concordance with the segmentation cycle. *Axin2* is the first member of the Wnt/β-catenin pathway showing oscillating expression in the PSM, and this finding links the Wnt signal cascade to the segmentation process.

Axin2 and *Lfng* Transcription Oscillate out of Phase

All previously known cycling genes are *Notch1* targets and share the same oscillation characteristics; they all cycle in phase (see introduction). To determine whether *Axin2* behaves in a similar manner, we compared the

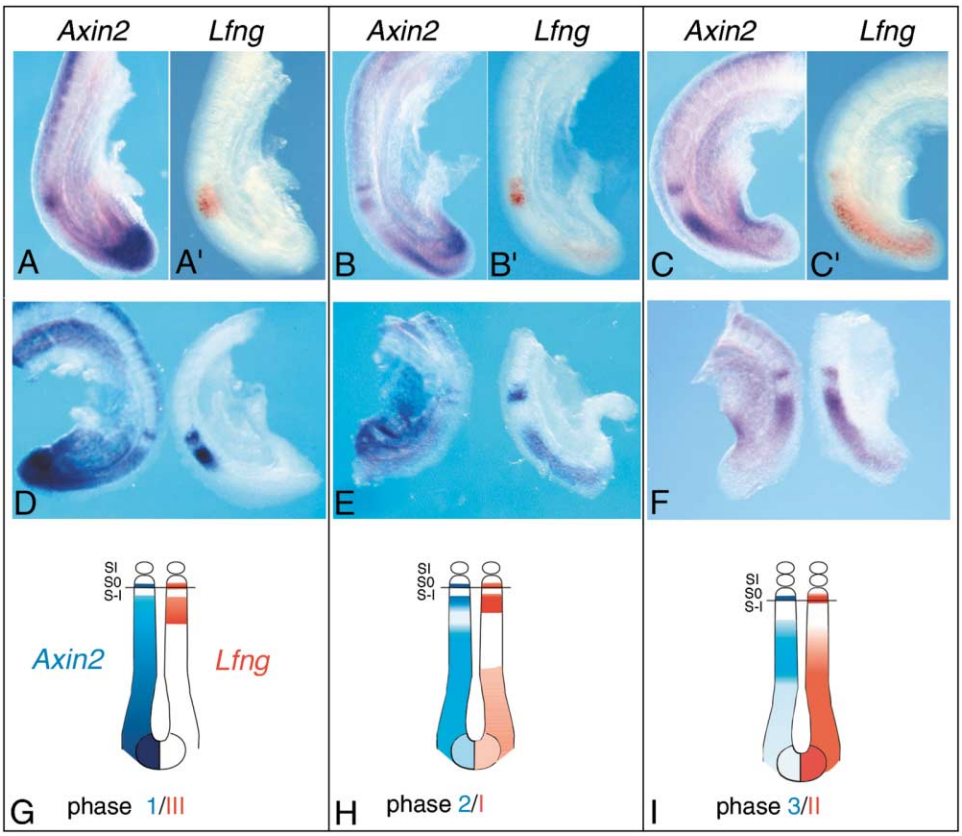

Figure 2. *Axin2* and *Lfng* Transcription Oscillate out of Phase

Whole-mount in situ hybridization of 9.5 dpc embryos (A–C′) or embryo halves (D–F), stained for *Axin2* and *Lfng*.
(A–C′) The same embryos were stained first for *Lfng* (A′–C′) and then for *Axin2* (A–C).
(D–F) Embryo halves were stained for either *Axin2* (left) or *Lfng* (right).
(G–I) Schematic representation of expression patterns shown for phase 1 (A, A′, and G), phase 2 (B, B′, and H), and phase 3 (C, C′, I) of the *Axin2* expression cycle in relation to cyclic *Lfng* (nomenclature for *Lfng* cycles according to Pourquie and Tam [2001]); note the alternating waves of *Axin2* and *Lfng* expression in the tail bud and posterior PSM, while expression of both genes overlaps and is stable in the anterior PSM.

mRNA expression of *Axin2* and *Lfng* in whole-mount embryos (n = 140) and embryo halves (n = 45). Strikingly, when *Axin2* is strongly expressed in the tail bud and posterior PSM, *Lfng* expression is weak or absent in the tail bud but shows expression in the anterior PSM, overlapping with *Axin2* in this region (Figures 2A, 2A′, and 2D). Likewise, when *Axin2* expression in the tail bud is fading, *Lfng* expression is upregulated in the tail bud and posterior PSM (Figures 2B, 2B′, and 2E). In phase 3 of the *Axin2* cycle, *Lfng* shows maximal expression in the tail bud and PSM (C, C′, and F). A comparison of the cycling expression patterns of both genes is schematically shown in Figures 2G–2I. Thus, *Axin2* and *Lfng* oscillate out of phase, apparently alternately, in the posterior PSM and tail bud, clearly distinguishing *Axin2* from all cycling genes described so far.

Axin2 Expression Still Oscillates When Notch Signaling Is Impaired

In mouse embryos lacking Dll1, the ligand of Notch1, all previously known cycling genes are strongly downregulated (Barrantes et al., 1999; Pourquie, 2001). Therefore, we asked whether *Axin2* is also dependent on Delta/Notch signaling. In *Dll1*$^{-/-}$ embryos, we observed a marked difference in the expression level of *Axin2* in the tail bud and posterior PSM of various specimens (n = 21), although the maximum expression level appeared lower and downregulation was not as strong as in wild-type (Figures 3A and 3B; see Figure 1D, phases 1 and 3, for comparison). The stripe of stable *Axin2* transcripts in S0 was never observed in *Dll1*$^{-/-}$ embryos (Figures 3A–3E), and expression sites outside the paraxial mesoderm appeared unaffected (data not shown).

A more detailed examination of *Axin2* expression was then carried out by *Dll1*$^{-/-}$ embryo half culture experiments (n = 21), whereby one embryo half was incubated for 45–90 min. In most embryos, the expression of *Axin2* in the posterior PSM and tail bud differed between the fixed and the incubated halves (n = 13/21). In a subset of embryos, a switch from strong to weak expression (n=8/13; Figure 3D) or vice versa had occurred during the incubation period (n = 5/13; Figure 3E).

These data show that the expression of *Axin2* in the PSM still oscillates when Delta/Notch signaling is impaired, though *Axin2* oscillations may be modulated by the Notch signal cascade. The expression of *Wnt3a* and

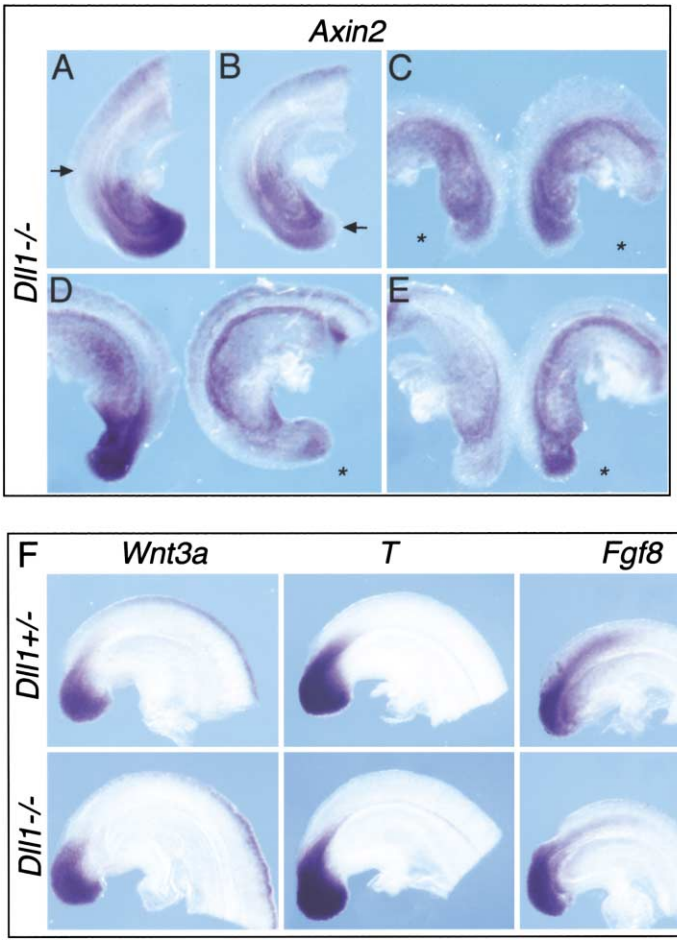

Figure 3. *Axin2* mRNA Expression Oscillates Even When Notch Signaling Is Impaired

In situ hybridizations of *Dll1*$^{-/-}$ whole-mount embryos (A and B) and embryo halves (C–E). (A and B) A marked difference in *Axin2* expression levels is observed in the PSM and, in particular, in the tail bud of *Dll1*$^{-/-}$ embryos. (A) Embryo showing graded expression peaking posteriorly; note the absence of anterior stripe of stable *Axin2* expression (arrow). (B) Expression in the tail bud is weak (arrow) and nongraded in the PSM.

In embryo half culture experiments, a strong difference in *Axin2* expression is detectable in the tail bud/PSM between the fixed and the incubated half, changing from strong to weak (D) ($\Delta t = 60$ min) or vice versa (E) ($\Delta t = 60$ min). No change was observed in control embryo halves (n = 4), both incubated for 75 min (C). *Wnt3a* and *Brachyury* (*T*) expression were not altered, and *Fgf8* expression was slightly reduced in *Dll1*$^{-/-}$ embryos (F). Asterisks, incubated embryo halves.

the *Wnt3a* target *Brachyury* was not affected, and the expression of *Fgf8* in the PSM appeared slightly reduced in *Dll1*$^{-/-}$ embryos (Figure 3F).

Axin2 Is a Direct Target of the Wnt/β-Catenin Signaling Cascade

Cyclic activation of *Axin2* in the tail bud and posterior PSM of *Dll1*$^{-/-}$ embryos suggests that Notch signaling is not essential for the segmentation clock. This raised the question, how is *Axin2* expression regulated? In a screen for genes inducible by Wnt1 in mouse embryonic stem cells, we found that *Axin2* was upregulated. This opened the possibility that *Axin2* is directly controlled by the Wnt/β-catenin signaling pathway. Indeed, the *Axin2* promoter region contains multiple Lef1/Tcf consensus binding sites. Seven such sites were identified in a 3.6 kb region comprising intron 1. This region (Ax2 P/I1) was cloned upstream of a luciferase reporter and tested in HEK293 cells for activation by a dominant active form of β-*catenin*, β-*catS33A*. A 6-fold induction of the reporter activity was achieved, which was further increased by cotransfection of *Tcf1E*. In contrast, point mutations introduced into the Lef1/Tcf binding sites strongly interfered with reporter gene induction (Figure 4A). These data provide strong evidence that *Axin2* is a direct target of the Wnt/β-catenin pathway.

In order to test whether *Axin2* expression in the embryo is also controlled by Wnt signaling, we cloned the same regulatory region upstream of the *lacZ* reporter and introduced it into mouse embryos. Embryos expressing *lacZ* from the wild-type *Axin2* promoter (n = 14/17) showed β-galactosidase activity in accordance with the mRNA expression pattern of *Axin2*, including expression in the tail bud and PSM (Figure 4B, left panel). In contrast, none of the transgenic embryos injected with the construct containing the mutant promoter (n = 0/17) showed staining in the tail bud or PSM, whereas, in most of these embryos (n = 16/17), the mid/hindbrain region (Figure 4B, right panel) and, in some (n = 8/17), a few other sites were β-gal positive (data not shown). These data demonstrate that *Axin2* expression in the tail bud and PSM directly depends on Wnt/β-catenin signaling.

Wnt3a Controls Oscillations of Notch Signaling in the Posterior PSM

The above data suggested that Wnt/β-catenin signaling in the tail bud and PSM oscillates and is controlled by the segmentation clock, as has been shown for Notch signaling (Pourquie, 2001). Since Wnt/β-catenin signaling still oscillates when Notch signaling is impaired, does Delta/Notch signaling also oscillate when Wnt signaling is impaired? To answer that question we made use of mutant embryos harboring the *Wnt3a* hypomorphic allele *vestigial tail* (*vt*). It has been shown that *Wnt3a* expression is reduced in the tail bud of *vt/vt* embryos from

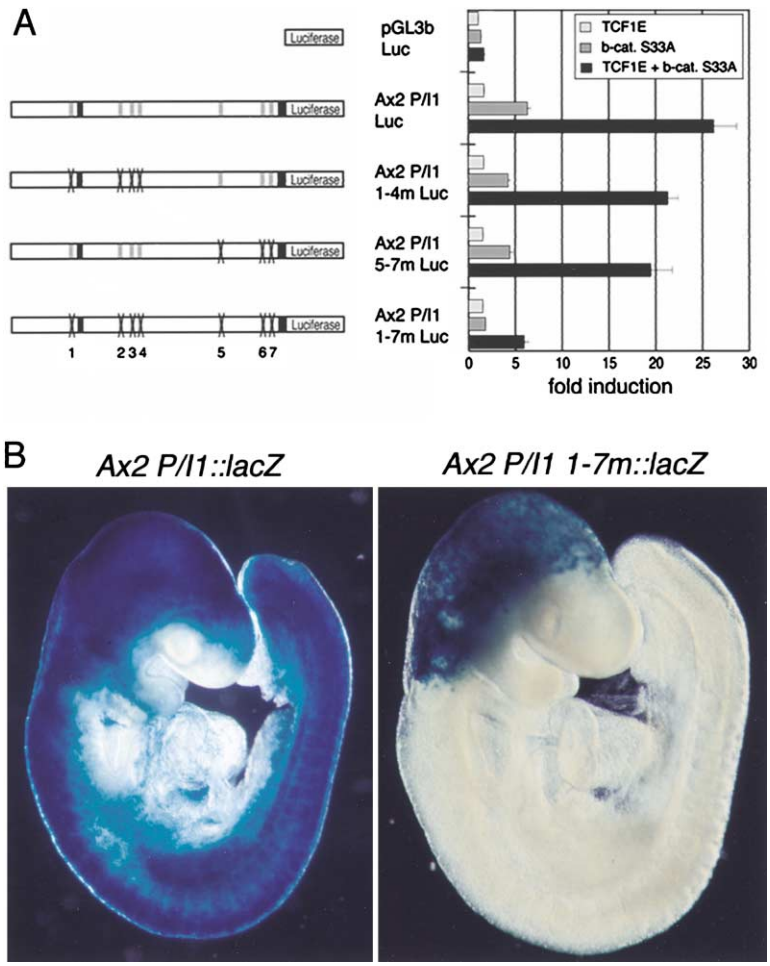

Figure 4. *Axin2* Is a Direct Target of Wnt/β-Catenin Signaling

(A) An *Axin2* promoter fragment (Ax2-P/I1) drives luciferase expression in HEK293 cells in the presence of the dominant active β-*catenin* allele *S33A*; expression is further upregulated by coexpression of *Tcf1E*. Mutation of Tcf/Lef binding sites in the *Axin2* promoter slightly (1–4 m and 5–7 m) or strongly (1–7m) reduce β-catenin/Tcf1E-mediated transcriptional activation, depending on the number of sites altered. Exons 1 and 2 of *Axin2*, black boxes; wild-type Tcf/Lef binding sites, gray boxes; mutated binding sites, crosses.

(B) Reporter assay of the wild-type (*Ax2 P/I1::lacZ*) or mutated (*Ax2 P/I1 1-7m::lacZ*) *Axin2* promoter driving *lacZ* gene expression in transgenic 9.5 dpc mouse embryos; the wild-type promoter functions in accordance with the observed mRNA expression pattern of *Axin2*, while β-gal activity is absent from all structures derived from the primitive streak/tail bud, including the PSM, of the embryos harboring the mutated promoter-reporter construct.

9.5 dpc onward, and this precedes an overt loss of somites that is first apparent at 10.5–11.0 dpc (Greco et al., 1996). We reasoned that, within this time frame, between downregulation of *Wnt3a* and onset of a morphological phenotype, one can study the effects of reduced Wnt3a signaling on the segmentation program, well before the absence of *Wnt3a* expression in the tail bud results in a complete arrest of posterior development (Takada et al., 1994).

All embryos examined were therefore analyzed at 10.25 dpc. As expected, *Wnt3a* transcripts were not detectable in *vt/vt* tails of 10.25 dpc embryos (Figure 5A). *Axin2* was strongly downregulated in the tail bud and PSM of mutant embryos, except for a faint stripe of expression in the anterior PSM (Figure 5A). This demonstrates that *Axin2* acts downstream of *Wnt3a* and that Wnt/β-catenin signaling had been arrested in the mutant PSM. *Fgf8* expression was also downregulated in the mutants, although *Brachyury* transcripts were readily detectable. In gastrulating *Xenopus* embryos, *eFGF* is involved in a positive-feedback loop with *Brachyury* (Schulte-Merker and Smith, 1995). However, our data suggest that, in the context of the PSM, *Fgf8* is controlled by *Wnt3a* and may not be downstream of *Brachyury*. It is unclear why *Brachyury,* which is also controlled by *Wnt3a*, is strongly expressed in the mutant. One possible explanation would be that *Brachyury* transcripts might be stabilized.

The expression analysis of Notch pathway genes revealed an interesting behavior. *Dll1* expression was hardly affected in the PSM of *vt/vt* embryos but was visibly downregulated in the tail bud (Figure 5A). *Notch1* expression in *vt/vt* tails was not significantly different from that in heterozygous *vt/+* controls. In sharp contrast, however, the expression pattern of *Lfng* was strongly altered in *vt/vt* embryos (n = 19/21) (Figure 5B), showing a single broad stripe of expression in the PSM, which coincided with the anterior domain of strong *Notch1* expression in most specimens. No wave and stripe pattern, typical of oscillating *Lfng* expression, was found, and expression in the posterior PSM and tail bud was downregulated.

These data strongly suggest that oscillating *Lfng* expression in the posterior PSM and tail bud depends on *Wnt3a*. Since *Lfng* is a direct target of Notch signaling (Cole et al., 2002; Morales et al., 2002), these data argue that the oscillations of Notch signaling in the posterior PSM are controlled by Wnt/β-catenin signaling. In contrast, the stable *Lfng* expression in the anterior PSM is differently controlled, as shown previously (Cole et al., 2002; Morales et al., 2002). The combined data strongly suggest that Wnt/β-catenin signaling acts upstream of Delta/Notch signaling in the segmentation clock.

Since neither Wnt/β-catenin nor Delta/Notch signaling oscillates anymore in the PSM of *vt/vt* embryos, we asked what effect the lack of these processes would

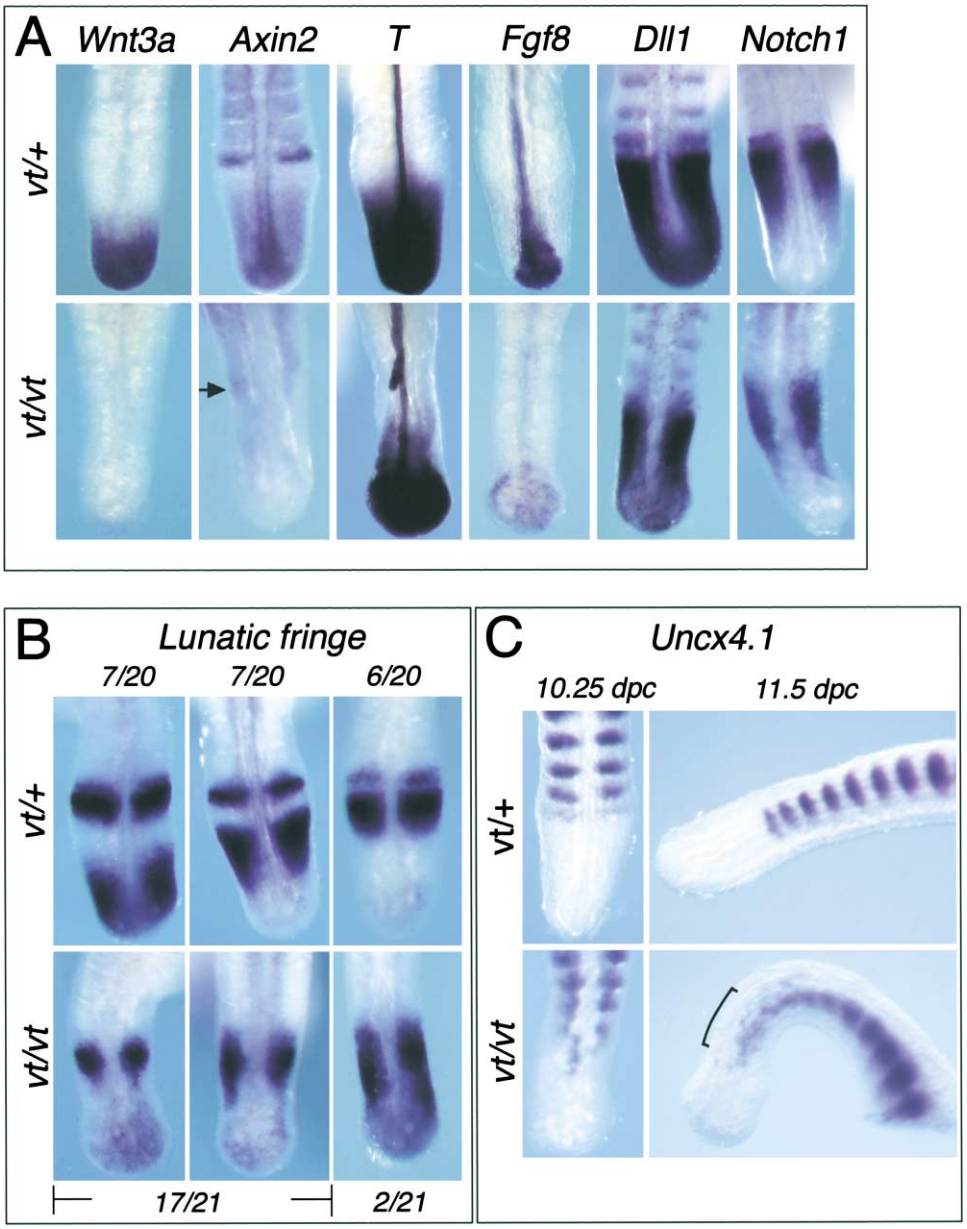

Figure 5. The Clock and the Segmentation Process Are Impaired in the *Wnt3a* Mutant *vestigial tail*

In situ hybridizations of whole-mount 10.25 dpc *vt*/+ or *vt/vt* embryo tails, analyzed for marker gene expression. Note downregulation of *Axin2* and *Fgf8* in the absence of *Wnt3a* (A), the noncyclic expression pattern of *Lfng* (B), and the expansion (anterior tail) or "salt and pepper" pattern (bracket) of *Uncx4.1* expression in *vt/vt* embryos (C).

(A) The arrow indicates a faint anterior *Axin2* stripe.

have on somite formation in the mutant. To answer this question we analyzed *vt/vt* tails at 10.25 and 11.5 dpc for *Uncx4.1* expression. *Uncx4.1* is a marker for the caudal halves of segmented somites and acts downstream of *Dll1* (Barrantes et al., 1999). Mutant *vt/vt* embryos showed a broadening of the *Uncx4.1* domain in the anterior tail region. The posterior tail region showed a "salt and pepper"-like pattern of *Uncx4.1* expression and no morphologically visible signs of segmentation (Figure 5C), confirming previous observations (Takada et al., 1994).

These data show that *Wnt3a* plays a crucial role in the control of Notch signaling and in the segmentation process, in addition to its function in axial elongation (Takada et al., 1994).

Wnt/β-Catenin Signaling Controls the Segmentation Process

The vertebral malformations observed in *vt/vt* embryos in combination with the molecular data described above provided strong hints that Wnt/β-catenin signaling plays an important role in the segmentation process. To gain

further molecular evidence to substantiate this idea we set out to manipulate the Wnt/β-catenin signaling cascade in vivo. In one set of experiments, the *Axin2* gene was misexpressed in the PSM of transgenic mouse embryos under control of the PSM-specific "msd" promoter of *Dll1* (Beckers et al., 2000; *msd::Axin2*). This promoter is supposed to provide constitutive, nonoscillating expression in the posterior and anterior PSM, but not in the tail bud. In another set of experiments, the tissue-specific msd promoter was combined with a Tet operator, providing additional temporal control of *Axin2* expression (*msd-TetO::Axin2*; see Experimental Procedures).

Our data show that misexpression of *Axin2* affects the segmentation process. The phenotype varied between specimens, ranging from moderate to strong impairment of somitogenesis (n = 16). Somites were irregular in size and were not aligned on either side of the neural tube (Figures 6A–6I). In addition, marker gene expression analysis revealed expanded caudal halves of somites and fuzzy boundaries (Figures 6B, 6G, and 6H). In two extreme cases, somite boundaries were not detectable in the posterior region with *Uncx4.1* as marker (Figure 6C and data not shown). Interestingly, embryos examined for *Lfng* expression showed an altered pattern, asymmetry between left and right (Figures 6D, 6E, and 6I), ectopic upregulation in the PSM (Figures 6D, 6E, and 6I) and a disruption of the characteristic wave and stripe pattern (Figure 6I). The marker *Uncx4.1* also revealed a striking increase of the somite size toward the caudal ends of the embryos (Figures 6F and 6H), suggesting that the size of somites is controlled by Wnt/β-catenin signaling.

Since an increase of the Wnt inhibitor Axin2, expressed from the transgene, resulted in larger somites, a higher dosage of Wnt3a should have the opposite effect. To test this prediction, we implanted microcarrier beads covered with NIH3T3 cells expressing Wnt3a into the posterior PSM of chick embryos, between paraxial and lateral mesoderm. Embryos were harvested after the paraxial mesoderm next to the beads had undergone segmentation. Indeed, NIH3T3-Wnt3a cells induced smaller somites and an anterior shift of segment boundaries, compared with the contralateral side (Figures 6K–6M) (n = 17/26 operations). The reduction of the somite size was confirmed by cell counting (Figure 6O). The effect was local and short range and appeared to be triggered only by a subset of the implanted beads. Beads covered with NIH-3T3 cells expressing *lacZ* were implanted into control embryos (n = 12), all of which showed normal somite development (Figure 6N).

The combined data show that Wnt/β-catenin signaling plays a direct role in the patterning and segmentation of paraxial mesoderm and suggest that *Wnt3a* and *Axin2* are key players in this process.

Discussion

Previously, a link between the Delta/Notch signaling cascade and the segmentation clock has been established (Holley et al., 2002; Pourquie, 2001). Here, we demonstrate that the Wnt/β-catenin signaling cascade plays a major role in the clock and in the control of segmentation. We discovered that *Axin2*, a negative regulator of Wnt signaling, shows oscillating mRNA transcription in the presomitic mesoderm (PSM) and tail bud. Cyclic *Axin2* expression alternates with *Lfng* expression, a Notch pathway cycling gene, and occurs even when Notch signaling is impaired. In contrast, *Lfng* was downregulated in the posterior PSM when Wnt3a activity was lacking and did not show a cyclic expression behavior anymore. This implies that Notch signaling is (indirectly) controlled by *Wnt3a*. Moreover, misexpression of *Axin2* in the PSM resulted in ectopic upregulation of *Lfng*, disrupting its cyclic expression pattern, and impaired the segmentation process. Therefore, Notch signaling appears to act downstream of *Axin2*. In addition, we show that *Axin2* is a direct target of Wnt/β-catenin signaling in the PSM and acts downstream of *Wnt3a*, strongly suggesting that Wnt3a controls Notch signaling via Axin2. Furthermore, misexpression of *Axin2* in the PSM resulted in enlarged somites, while expression of *Wnt3a* from NIH3T3 cells transplanted on beads into the PSM of chick embryos had the opposite effect, the formation of smaller somites. We also provide indirect evidence for a graded distribution of Wnt3a activity in the PSM. We propose that Wnt3a plays a major role in the segmentation process.

Periodic Wnt/β-Catenin Signaling May Be Generated via a Negative-Feedback Mechanism Involving Axin2

We have shown that *Axin2* is a direct target of Wnt/β-catenin signaling in the tail bud and PSM. *Axin2* transcripts in these sites accumulate and disappear in a periodic manner. This oscillating behavior can be explained in at least two ways. One possibility is that *Axin2* transcription is constant and mRNA degradation occurs periodically; another possibility is that degradation is constant and transcription is initiated periodically. *Lfng* expression behaves in a similar manner to *Axin2*, and, recently, strong evidence in favor of the latter explanation has been presented (Morales et al., 2002). We think that this explanation is very likely true for *Axin2*, also.

Since Axin2 has been shown to act as negative regulator of Wnt/β-catenin signaling, upregulation of Axin2 would inhibit Wnt/β-catenin signaling and shut off Axin2 transcription. Such a negative-feedback mechanism involving Axin2 has been proposed previously (Jho et al., 2002; Lustig et al., 2002). In order to generate oscillating Wnt/β-catenin signaling, rather than completely switching off this pathway, an additional component needs to be introduced, the degradation of Axin2 transcripts and protein. The former is actually observed in the PSM, and evidence for the latter comes from a recent report. It has been observed that Axin protein is hypophosphorylated and destabilized by Wnt signaling (reviewed in Seidensticker and Behrens, 2000), and, since Axin2 acts in a similar way to Axin, it may also be destabilized by Wnt signaling.

Though other mechanisms cannot be ruled out, we think that a negative-feedback control of Wnt/β-catenin signaling is the simplest and most likely explanation for

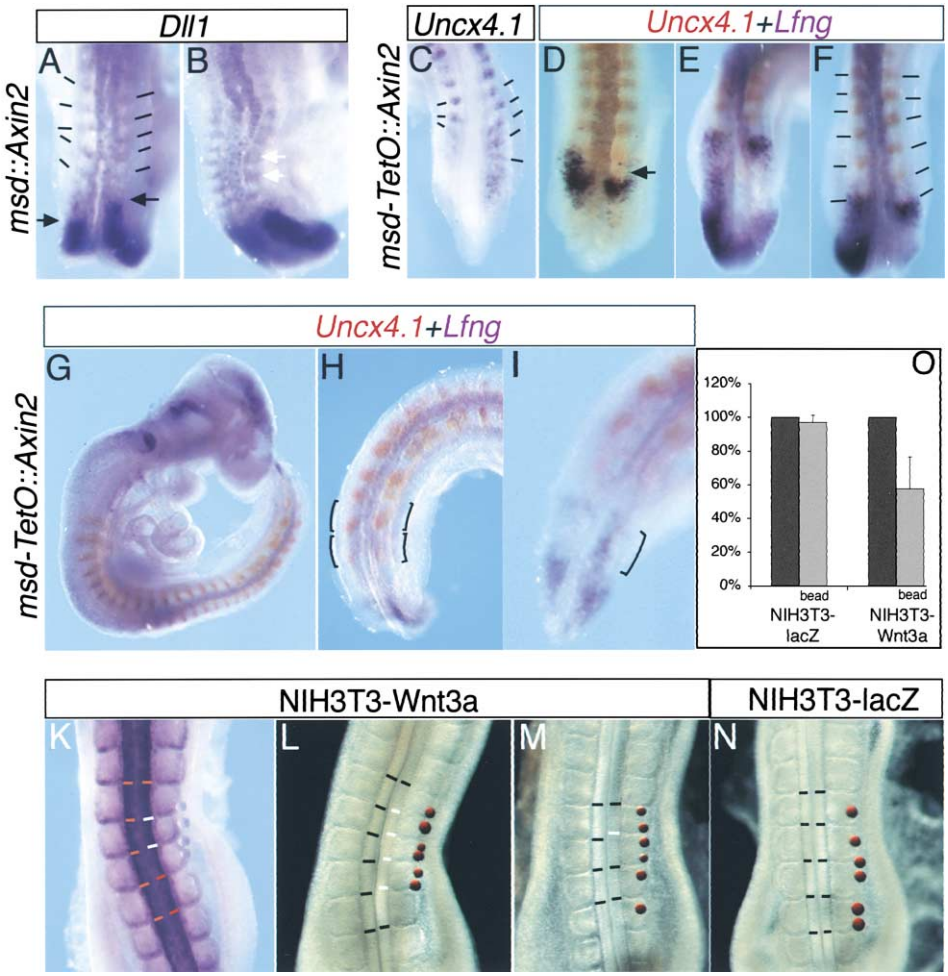

Figure 6. Wnt/β-Catenin Signaling Controls the Segmentation Process

Whole-mount in situ hybridization of 9.5–10.25 dpc embryos misexpressing *Axin2* in the PSM, (A and B) under spatially restricted control of the *Dll1* msd promoter and (C–I) under spatial and temporal control of the msd-TetO promoter.

(A and B) Analysis of *Dll1* expression reveals irregular size and spacing of somites; left and right PSM expression is not aligned anteriorly ([A], black arrows). In addition, several caudal somite halves are expanded ([B], white arrows).

(C) Severe impairment of segmentation and skewed boundaries, as indicated by *Uncx4.1* expression, are observed 48 hr after doxycyclin induction; note the scattered *Uncx4.1*-positive cells in the caudal region.

(D–F) Analysis of *Lfng* reveals asymmetrical expression in the PSM 36 hr after induction, combined with irregular segmentation indicated by *Uncx4.1*.

(D) The additional segment on the right half is indicated by the black arrow.

(E and F) The same embryo shown at a different angle.

(G–I) Embryo harvested 48 hr after induction, showing normal anterior development (G) before segmentation is severely impaired (H); note the expansion of caudal somite halves, increase of somite size, and ectopic upregulation of *Lfng* in one side of the PSM ([I], bracket), where *Lfng* expression is uniform in the entire PSM (I).

(K–N) Chick embryos carrying microcarrier beads, covered with cells expressing *Wnt3a* (K–M) or *LacZ* (N), 20–24 hr after implantation into the posterior PSM. Smaller somites are visible on the operated side compared with the contralateral side.

(K) Embryo stained for *c-delta1* expression (the smaller somite indicated by white lines).

(L) Multiple smaller somites.

(M) A segment boundary is shifted anteriorly (white line) on the operated side.

(N) Control embryo showing normal somite development.

(O) Cell count of somites on the implantation side (light gray; bead NIH3T3-lacZ or NIH3T3-Wnt3a cells) compared with somites on the contralateral side (set to 100%).

the observed cyclic expression pattern of Axin2 in the PSM and tail bud.

Wnt May Control Notch Signaling via Axin2

We have shown that *Axin2* mRNA expression oscillates alternately with *Lfng* expression, raising the question, how are the cyclic signaling activities of Wnt and Notch intercalated? Our data show that Notch signaling in the posterior PSM is downregulated when Wnt3a activity and Axin2 are lacking but is ectopically upregulated when Axin2 is overexpressed. These observations suggest that Notch signaling acts downstream of Axin2 and,

thus, downstream of Wnt3a. How could this tight link between Wnt and Notch signaling be achieved?

A direct link between both signaling cascades has been suggested previously. In *Drosophila*, the intracellular domain of Notch, N_{ICD}, has been shown to bind to the PDZ domain of dishevelled (dsh). Dsh interacts antagonistically with Notch, and, therefore, it has been suggested that dsh blocks Notch signaling directly through binding of N_{ICD} (Axelrod et al., 1996). Axin also binds to the PDZ domain of Dvl, the vertebrate homolog of dsh, and the Axin homolog Axin2 is likely to act in a similar manner (Seidensticker and Behrens, 2000). Therefore, in the PSM, Dvl might inhibit Notch signaling through binding of N_{ICD}, whereas Axin2 binding to the PDZ domain of Dvl might release N_{ICD} and thus trigger Notch target gene activation.

In summary, negative-feedback inhibition of Wnt/β-catenin signaling via Axin2 might trigger Notch target gene activation and link both pathways. Destabilization of Axin2 would then reestablish Wnt signaling and lead to inhibition of Notch. Such a mechanism would explain the alternating waves of Wnt/β-catenin and Notch target activation observed in the PSM. However, the Notch signaling cascade also appears to have a modulating effect on the oscillations of Wnt signaling, as indicated by our data on *Axin2* expression in *Dll1*$^{-/-}$ embryos.

The Graded Distribution of *Axin2* Transcripts Indicates a Gradient of Wnt Activity in the PSM

Our data have demonstrated that *Axin2* expression in the posterior PSM and tail bud depends on *Wnt3a*. This conclusion is based on two arguments. First, *Axin2* transcription is not detectable in the PSM and tail bud of 10.25 dpc *vt/vt* embryos, well before axial development is arrested. Second, transgenic embryos expressing the *lacZ* reporter under control of a mutated *Axin2* promoter, deficient in Lef/Tcf binding sites, do not show reporter activity in the tail bud and PSM. In addition, we have observed that *Axin2* mRNA expression is graded along the PSM, with the highest level in the tail bud, during phase 1 of the cycle (see Figure 1) and can be detected up to S-I.

The combined data suggest that Wnt/β-catenin signaling reaches up to the anterior PSM and occurs in a graded manner. However, *Wnt3a* transcription is restricted to the tail bud. These observations would be easily explained by the assumption that Wnt3a protein, following translation in the tail bud, is not rapidly degraded but subjected to slow decay in the extracellular environment. A gradient of Wnt3a protein and signaling activity would thus be established along the PSM, while the embryo elongates caudally. In agreement with this interpretation is the finding that other components of the Wnt/β-catenin pathway, such as the regulatory proteins *Lef1* and *Tcf1*, are also expressed in the entire PSM (Galceran et al., 1999). This could be coincidental but makes perfect sense in the light of the data presented here. Whatever the mechanism may be, our data provide indirect evidence for a gradient of Wnt/β-catenin signaling along the PSM.

Wnt Controls Segmentation: A Model Integrating "the Gradient and the Clock"

We propose that *Wnt3a* controls intracellular oscillations of Wnt/β-catenin (Wnt) and Notch (N_{ICD}) signaling activity in the PSM. At the onset of the clock cycle, Wnt activates *Axin2* transcription through Dvl, which may inhibit Notch signaling ("Wnt on-Notch off"; Figure 7A). Axin2 protein accumulates and inhibits Wnt signaling downstream of Dvl, through a negative feedback mechanism, and may also remove the inhibition of Notch through interaction with Dvl ("Wnt off-Notch on"). Notch then upregulates *Lfng*. In parallel, *Axin2* mRNA and protein are degraded, probably triggered by constant Wnt signaling upstream of Dvl. Thus, Wnt/β-catenin signaling downstream of Dvl is reestablished, and a new cycle begins.

While the embryo elongates caudally, *Wnt3a* expression is restricted to the posterior end of the body axis. Possibly because of slow decay of Wnt3a protein in the extracellular environment, a Wnt3a gradient is established along the PSM (Figure 7B).

Cells are exposed to several waves of alternating Wnt and Notch signaling, whereby Wnt signaling activity becomes weaker with each cycle (Figure 7C). As cells come to lie in the anterior PSM, Wnt signaling activity falls below a threshold and is permanently inactivated, and the clock is arrested. At this point, *Notch1* is strongly upregulated, and *Axin2* expression is stabilized. The loss of Wnt signaling activity may permit upregulation of genes controlling somite boundary formation and intrasegmental polarity.

Because of decay of Wnt3a protein, the position along the A-P axis having a threshold value of Wnt activity shifts posteriorly with time (Figure 7B). During the "Wnt on" phase of the cycle, the segment boundary position is defined between posterior PSM cells undergoing another oscillation cycle and a block of cells in which the clock has been arrested. The somite size depends on the slope of the Wnt gradient and the duration of one cycle of the segmentation clock.

Our data provide evidence for several principal elements predicted by previous models to be required for the segmentation process (Cooke and Zeeman, 1976; Meinhardt, 1986; Stern et al., 1988). Most importantly, we provide molecular data suggesting a mechanism by which the clock and the gradient may be established and interact.

Future experiments need to address several propositions of the model. Among them, the molecular mechanism by which the Wnt and Notch signaling pathways are coupled has to be explored in more detail. Specifically, it remains to be confirmed that Notch signaling is indeed controlled by oscillations of Wnt signaling, rather than acting downstream of a general Wnt signal in the PSM. In particular, a more direct demonstration of the functional importance of the proposed negative-feedback mechanism generating oscillations of Wnt signaling for the segmentation clock is needed.

Wnt3a Acts Upstream of *Fgf8* in the PSM

In a previous publication, evidence was presented that segment boundary formation is controlled by a gradient of Fgf8 in the PSM (Dubrulle et al., 2001). It has been

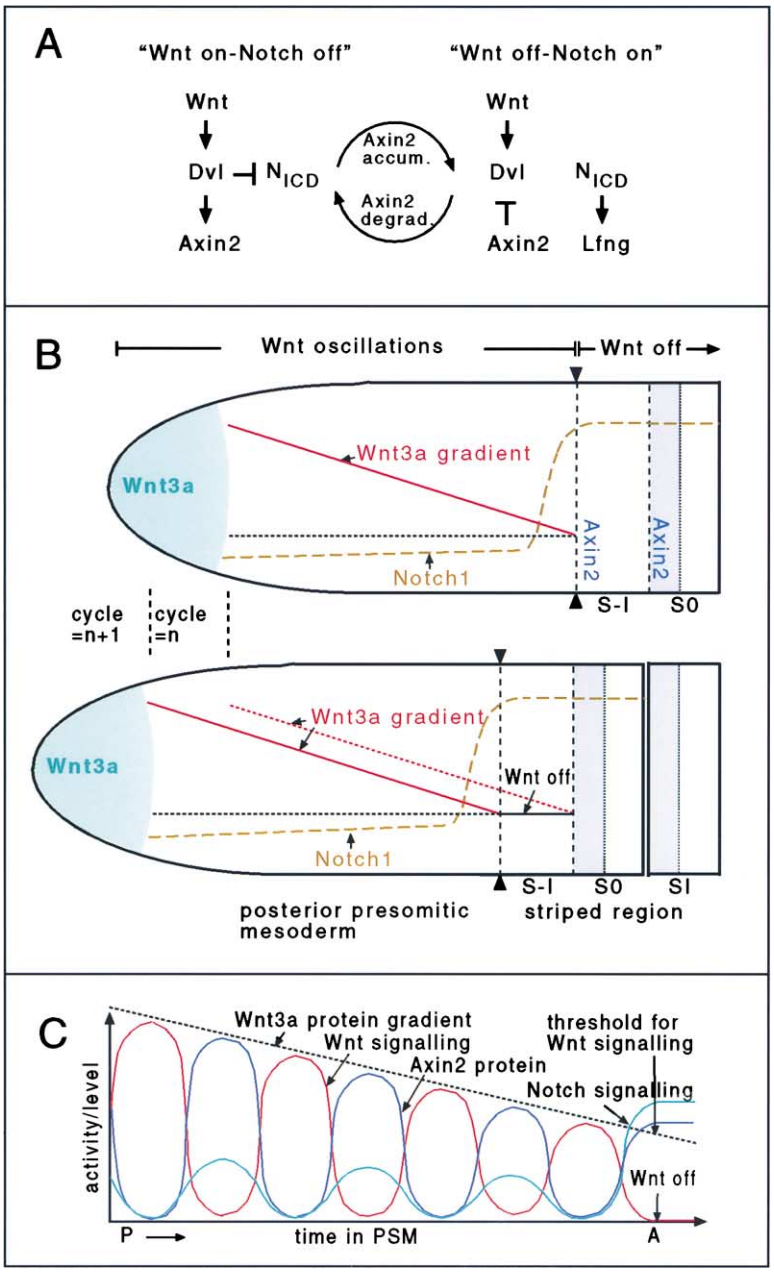

Figure 7. Model of Segmentation Process, Integrating the Gradient and the Clock

(A) The segmentation clock: PSM cells oscillate between two states, "Wnt on-Notch off" and "Wnt off-Notch on". Wnt, Wnt signaling; Dvl, vertebrate dishevelled; N_{ICD}, Notch intracellular domain; arrow: activation, bar: inhibition.

(B) The gradient and the clock: while the embryo elongates caudally, Wnt3a expression is restricted to the tail bud; Wnt3a protein/signaling forms a gradient along the PSM and suppresses differentiation; below a threshold value (black/black-dotted line), Wnt signaling becomes permanently inactivated (Wnt off). The position along the A-P axis having a threshold value of Wnt signaling activity shifts posteriorly with time because of decay of Wnt3a protein; segment boundary positions (black arrowheads) are defined during the "Wnt on" phase between (posterior) cells undergoing another oscillation cycle (Wnt on) and (anterior) cells, in which Wnt signaling is switched off (Wnt off); the latter have escaped suppression by Wnt and are free to form a segment.

(C) The gradient and clock in a single PSM cell: oscillations of Wnt signaling downstream of Dvl (red) and Axin2 protein (blue) alternate out of phase; Notch signaling (green) oscillates in phase with Axin2 protein. Notch1 is upregulated when Wnt activity has fallen below the threshold (Wnt off); *Axin2* is stabilized. P, posterior; A, anterior. For details, see text.

shown that a threshold value of Fgf8 protein is involved in determining the boundary position. In light of our data showing a similar function of Wnt3a, the questions arise, which of the two signals, Wnt3a or Fgf8, is the prime determinant, and which acts downstream? First, we show that Fgf8 is strongly downregulated in the tail bud and PSM of *vt/vt* embryos. Second, our data provide evidence that the clock and the gradient are linked via *Wnt3a*. We propose that Wnt3a acts upstream of Fgf8 in the segmentation process. Some of the effects that Wnt signaling has on somitogenesis may therefore be attributable to effects on the proposed Fgf8 gradient, and, at the moment, it cannot be ruled out that they may be independent of those on Notch signaling.

There is evidence that FGF may enhance Wnt/β-catenin signaling. Akt/PKB, a negative regulator of the β-catenin inhibitor GSK3β, can be activated by the PI3-kinase pathway. The latter is positively regulated by Ras, which, in turn, is activated by FGF (Fukumoto et al., 2001; Jun et al., 1999). Thus, in the PSM, Fgf8 might act as a relay enhancer of Wnt/β-catenin signaling.

Future experiments need to address the particular role each of the two signals plays in defining the segment boundary position and the proposed link between the signal and the clock.

Finally, the functional link between *Wnt3a* and the segmentation clock, demonstrated in this work, also recalls previous reports showing that the regulation of *Hox* genes is functionally connected to the segmentation clock (Dubrulle et al., 2001; Zakany et al., 2001) and that *Wnt3a* is involved in the control of positional information along the body axis (Ikeya and Takada,

2001). Moreover, *Wnt3a* is required for the elongation of the body axis (Greco et al., 1996; Takada et al., 1994). Thus, *Wnt3a* appears to control and integrate all three processes, body axis elongation, allocation of positional information, and segmentation.

Experimental Procedures

Isolation of *Axin2*

Axin2 (TB112) was identified in a large-scale screen for genes specifically expressed in the tail bud and PSM of 9.5 dpc mouse embryos, as described (Neidhardt et al., 2000), among 960 clones of a 9.5 dpc tail bud library prepared with the SuperScript plasmid cDNA library construction kit (Life Technologies) in vector pSV-Sport1.

Whole-Mount In Situ Hybridization

For antisense transcript preparation, clone TB112 (2800 bp) was used as template for *Axin2*. *Dll1*, *Notch1*, and *Uncx4.1* were isolated in our screens. For *Lfng*, *Fgf8*, and *Wnt3a*, the original cDNA clones described in the literature were used. Whole mount in situ hybridizations were done as described (Aulehla and Johnson, 1999; Neidhardt et al., 2000). For double labeling, NBT/BCIP (violet) or INT/BCIP (red) was used as an alkaline phosphatase substrate. *Dll1*$^{-/-}$ embryos were identified by morphological criteria. *Dll1*$^{-/-}$ embryos were as follows: *Wnt3a* (n = 4), *Brachyury* (n = 8), and *Fgf8* (n = 3); *Wnt3a vt/vt* embryos were as follows: *Wnt3a* (n = 15), *Axin2* (n = 17), *Brachyury* (n = 5), *Fgf8* (n = 17), *Notch1* (n = 14), *Dll1* (n = 9), *Uncx4.1* (n = 9), and *Lfng* (n = 21).

Embryo Half Culture Experiments

Embryo culture experiments were performed essentially as described (Correia and Conlon, 2000). Embryos were bisected in the midline with fine Tungsten needles, one embryo half was fixed immediately, and the other was incubated in a hanging drop for various times. Somites were counted before and after incubation.

Microcarrier Bead Implantation

NIH3T3-Wnt3a or NIH3T3-LacZ cells were grown on microcarrier beads (Hillex 38–72 μm; SoloHill) under standard conditions. Using fine tungsten needles, we implanted beads between posterior segmental plate and lateral mesoderm in chicken embryos of HH12–14 (Hamburger and Hamilton, 1992). Incubation after surgery varied between 14 hr and 26 hr.

Quantitative Analysis

Cell nuclei were stained with DAPI. Embryos were flat mounted in 50% formamide/PBT and optically sectioned with a laser scanning microscope; cells comprising the dorsal surface of the somites (NIH3T3-Wnt3a, n = 3; NIH3T3-lacZ, n = 2) were counted, and contralateral somites were analyzed accordingly as control. Cell numbers are represented as mean percentages ±SD relative to contralateral control somites, set to 100%.

Axin2 Promoter Analysis

Axin2 was found among several genes, upregulated in ES cells after coculture with NIH3T3 cells expressing *Wnt1*, as described (Arnold et al., 2000). A 3.6 kb genomic fragment (Ax2 P/I1) comprising exon 1, intron 1, part of exon 2, and upstream sequences, including the transcription start of the Axin2 gene, was amplified by PCR and cloned in front of the *luciferase* gene of the vector pGL3 (Promega). This construct was called *Ax2 P/I1-Luc*. Point mutations were introduced into the Lef/Tcf binding sites T1-T7 with the QuickChange Multi Site-Directed Mutagenesis Kit (Stratagene). Transfections were carried out in HEK 293 cells according to standard techniques by the calcium phosphate precipitation method. One microgram of each construct, together with 0.2 μg of *pCMV-β-galactosidase* as standard for normalizing transfection efficiency, 50 ng of *pCS2*$^{+}$*TCF1E*, and 0.5 μg *pCS2*$^{+}$*S33A*, alone or in combination, was transfected. The total amount of DNA used was brought to 1.75 μg with *pCS2*$^{+}$. The cells were lysed 48 hr after transfection, and luciferase and β-galactosidase activities were measured on a Luminoskan Ascent luminometer (Thermo Labsystems). Normalized luciferase activities were compared with a *pCS2*$^{+}$ control to calculate the fold induction. For assaying *Axin2* promoter activity in transgenic embryos, we cloned the *lacZ* gene downstream of the wild-type or the mutated (1–7 m) *Axin2* promoter. Constructs were injected into pronuclei, and embryos were assayed in situ for β-galactosidase activity in 8.75–9.5 dpc mouse embryos.

Transgene Constructs

For misexpression of *Axin2* in the PSM, two constructs were used. For msd*::Ax2*, the ORF of the *lacZ* gene contained in the reporter construct *Dll1*$^{tg'msd'/lacZ}$ (Beckers et al., 2000) was replaced by the mouse *Axin2* ORF (Behrens et al., 1998). For msd-*TetO::Ax2*, the *Tet* operator was isolated from the plasmid pUHD10-3 and cloned between the msd promoter fragment and minimal promoter in the construct *Dll-Ax2*. In misexpression experiments, this construct was injected in combination with construct *pActTsIns*, expressing the transcriptional silencer *Tet-tTS* (Clontech) under control of the human β-*actin* promoter, flanked by tandem copies of the chicken β-*globin* insulator (courtesy of Moises Mallo). *Axin2* expression from this construct is silenced in the absence of doxycycline by binding of Tet-tTS to the Tet operator sequence. *Msd::Ax2* or *msd-TetO::Ax2/ActTsIns* was injected into pronuclei of fertilized eggs according to standard procedures. Embryos were taken at 9.5 dpc. Three embryos showing severe impairment of segmentation were obtained after *Dll::Ax2* injection, and 13 were obtained after *Dll-TetO-Ax2/ActTsIns* injection. *Axin2* expression was induced by a single intraperitoneal injection of 1 mg doxycycline-HCl (Sigma) into pregnant females at 8.25 dpc, followed by repeated (six times at 4 hr intervals) intragastric administration of 1.6 mg doxycycline, which is supposed to trigger dissociation of the silencer from the Tet operator. In addition, 4 mg/ml doxycycline and 5% sucrose were added to the drinking water. Embryos were harvested 36–48 hr after the first administration of doxycycline.

Acknowledgments

We thank Moises Mallo for construct *pActTsIns*, Stephan Kuppig for help with the LSM, Andreas Kispert for NIH3T3-Wnt3a cells, Walter Birchmeier for the full-length cDNA of mouse *Axin2*, Andreas Hecht for construct pCS2+TCF1E, Andy McMahon, Gail Martin, and Randy Johnson for generous gifts of cDNA clones, Elsa Huber, Laurent Morawiec, and Hans Garbers for pronuclear DNA injections, Anton J. Gamel for help with chick operations, Nicoletta Bobola, Hermann Bauer, Stephan Gasca, Lorenz Neidhardt, Michael Hofmann, and Thomas Mayr for support and discussions, Birgit Koschorz, Volker Köchlin, Manuela Scholze, Tina Engist, Mahela Konrath, and Anton Grubisic for technical assistance, and Davor Solter and Randy Cassada for support and comments on the manuscript. A.A. was supported, in part, by the German National Merit Foundation Scholarship and by the Max-Planck Society. This work was supported in SFB592 to B.G.H. and SFB271 to A.G. by the Deutsche Forschungsgemeinschaft.

Received: May 2, 2002
Revised: November 20, 2002

References

Arnold, S.J., Stappert, J., Bauer, A., Kispert, A., Herrmann, B.G., and Kemler, R. (2000). Brachyury is a target gene of the Wnt/beta-catenin signaling pathway. Mech. Dev. *91*, 249–258.

Aulehla, A., and Johnson, R.L. (1999). Dynamic expression of lunatic fringe suggests a link between notch signaling and an autonomous cellular oscillator driving somite segmentation. Dev. Biol. *207*, 49–61.

Axelrod, J.D., Matsuno, K., Artavanis-Tsakonas, S., and Perrimon, N. (1996). Interaction between Wingless and Notch signaling pathways mediated by dishevelled. Science *271*, 1826–1832.

Barrantes, I.B., Elia, A.J., Wunsch, K., De Angelis, M.H., Mak, T.W., Rossant, J., Conlon, R.A., Gossler, A., and de la Pompa, J.L. (1999). Interaction between notch signalling and lunatic fringe during somite boundary formation in the mouse. Curr. Biol. *9*, 470–480.

Beckers, J., Caron, A., Hrabe de Angelis, M., Hans, S., Campos-Ortega, J.A., and Gossler, A. (2000). Distinct regulatory elements direct delta1 expression in the nervous system and paraxial mesoderm of transgenic mice. Mech. Dev. *95*, 23–34.

Behrens, J., Jerchow, B.A., Wurtele, M., Grimm, J., Asbrand, C., Wirtz, R., Kuhl, M., Wedlich, D., and Birchmeier, W. (1998). Functional interaction of an axin homolog, conductin, with beta-catenin, APC, and GSK3beta. Science *280*, 596–599.

Christ, B., and Ordahl, C.P. (1995). Early stages of chick somite development. Anat. Embryol. (Berl.) *191*, 381–396.

Cole, S.E., Levorse, J.M., Tilghman, S.M., and Vogt, T.F. (2002). Clock regulatory elements control cyclic expression of Lunatic fringe during somitogenesis. Dev. Cell *3*, 75–84.

Conlon, R.A., Reaume, A.G., and Rossant, J. (1995). Notch1 is required for the coordinate segmentation of somites. Development *121*, 1533–1545.

Cooke, J., and Zeeman, E.C. (1976). A clock and wavefront model for control of the number of repeated structures during animal morphogenesis. J. Theor. Biol. *58*, 455–476.

Correia, K.M., and Conlon, R.A. (2000). Surface ectoderm is necessary for the morphogenesis of somites. Mech. Dev. *91*, 19–30.

Dubrulle, J., McGrew, M.J., and Pourquie, O. (2001). FGF signaling controls somite boundary position and regulates segmentation clock control of spatiotemporal *Hox* gene activation. Cell *106*, 219–232.

Evrard, Y.A., Lun, Y., Aulehla, A., Gan, L., and Johnson, R.L. (1998). lunatic fringe is an essential mediator of somite segmentation and patterning. Nature *394*, 377–381.

Forsberg, H., Crozet, F., and Brown, N.A. (1998). Waves of mouse Lunatic fringe expression, in four-hour cycles at two-hour intervals, precede somite boundary formation. Curr. Biol. *8*, 1027–1030.

Fukumoto, S., Hsieh, C.M., Maemura, K., Layne, M.D., Yet, S.F., Lee, K.H., Matsui, T., Rosenzweig, A., Taylor, W.G., Rubin, J.S., et al. (2001). Akt participation in the Wnt signaling pathway through Dishevelled. J. Biol. Chem. *276*, 17479–17483.

Galceran, J., Farinas, I., Depew, M.J., Clevers, H., and Grosschedl, R. (1999). Wnt3a−/−-like phenotype and limb deficiency in Lef1(−/−)Tcf1(−/−) mice. Genes Dev. *13*, 709–717.

Gossler, A., and Hrabe de Angelis, M. (1998). Somitogenesis. Curr. Top. Dev. Biol. *38*, 225–287.

Greco, T.L., Takada, S., Newhouse, M.M., McMahon, J.A., McMahon, A.P., and Camper, S.A. (1996). Analysis of the vestigial tail mutation demonstrates that Wnt-3a gene dosage regulates mouse axial development. Genes Dev. *10*, 313–324.

Hamburger, V., and Hamilton, H.L. (1992). A series of normal stages in the development of the chick embryo. 1951. Dev. Dyn. *195*, 231–272.

Holley, S.A., Julich, D., Rauch, G.J., Geisler, R., and Nusslein-Volhard, C. (2002). her1 and the notch pathway function within the oscillator mechanism that regulates zebrafish somitogenesis. Development *129*, 1175–1183.

Hrabe de Angelis, M., McIntyre, J., II, and Gossler, A. (1997). Maintenance of somite borders in mice requires the Delta homologue DII1. Nature *386*, 717–721.

Ikeya, M., and Takada, S. (2001). Wnt3a is required for somite specification along the anteroposterior axis of the mouse embryo and for regulation of *cdx-1* expression. Mech. Dev. *103*, 27–33.

Jho, E.H., Zhang, T., Domon, C., Joo, C.K., Freund, J.N., and Costantini, F. (2002). Wnt/beta-catenin/Tcf signaling induces the transcription of Axin2, a negative regulator of the signaling pathway. Mol. Cell. Biol. *22*, 1172–1183.

Jouve, C., Palmeirim, I., Henrique, D., Beckers, J., Gossler, A., Ish-Horowicz, D., and Pourquie, O. (2000). Notch signalling is required for cyclic expression of the hairy-like gene HES1 in the presomitic mesoderm. Development *127*, 1421–1429.

Jun, T., Gjoerup, O., and Roberts, T.M. (1999). Tangled webs: evidence of cross-talk between c-Raf-1 and Akt. Sci STKE *1999*, PE1.

Kerszberg, M., and Wolpert, L. (2000). A clock and trail model for somite formation, specialization and polarization. J. Theor. Biol. *205*, 505–510.

Keynes, R.J., and Stern, C.D. (1988). Mechanisms of vertebrate segmentation. Development *103*, 413–429.

Leimeister, C., Dale, K., Fischer, A., Klamt, B., Hrabe de Angelis, M., Radtke, F., McGrew, M.J., Pourquie, O., and Gessler, M. (2000). Oscillating expression of c-Hey2 in the presomitic mesoderm suggests that the segmentation clock may use combinatorial signaling through multiple interacting bHLH factors. Dev. Biol. *227*, 91–103.

Lustig, B., Jerchow, B., Sachs, M., Weiler, S., Pietsch, T., Karsten, U., van de Wetering, M., Clevers, H., Schlag, P.M., Birchmeier, W., and Behrens, J. (2002). Negative feedback loop of Wnt signaling through upregulation of conductin/axin2 in colorectal and liver tumors. Mol. Cell. Biol. *22*, 1184–1193.

McGrew, M.J., Dale, J.K., Fraboulet, S., and Pourquie, O. (1998). The lunatic fringe gene is a target of the molecular clock linked to somite segmentation in avian embryos. Curr. Biol. *8*, 979–982.

Meinhardt, H. (1986). Models of segmentation. In Somites in Developing Embryos, R.E. Bellairs, D.A. Edie, and J.W. Lash, eds. (New York: Plenum Press), pp. 179–189.

Morales, A.V., Yasuda, Y., and Ish-Horowicz, D. (2002). Periodic Lunatic fringe expression is controlled during segmentation by a cyclic transcriptional enhancer responsive to notch signaling. Dev. Cell *3*, 63–74.

Neidhardt, L., Gasca, S., Wertz, K., Obermayr, F., Worpenberg, S., Lehrach, H., and Herrmann, B.G. (2000). Large-scale screen for genes controlling mammalian embryogenesis, using high-throughput gene expression analysis in mouse embryos. Mech. Dev. *98*, 77–94.

Oka, C., Nakano, T., Wakeham, A., de la Pompa, J.L., Mori, C., Sakai, T., Okazaki, S., Kawaichi, M., Shiota, K., Mak, T.W., and Honjo, T. (1995). Disruption of the mouse RBP-J kappa gene results in early embryonic death. Development *121*, 3291–3301.

Palmeirim, I., Henrique, D., Ish-Horowicz, D., and Pourquie, O. (1997). Avian hairy gene expression identifies a molecular clock linked to vertebrate segmentation and somitogenesis. Cell *91*, 639–648.

Pourquie, O. (2001). Vertebrate somitogenesis. Annu. Rev. Cell Dev. Biol. *17*, 311–350.

Pourquie, O., and Tam, P.P. (2001). A nomenclature for prospective somites and phases of cyclic gene expression in the presomitic mesoderm. Dev. Cell *1*, 619–620.

Schulte-Merker, S., and Smith, J.C. (1995). Mesoderm formation in response to Brachyury requires FGF signalling. Curr. Biol. *5*, 62–67.

Seidensticker, M.J., and Behrens, J. (2000). Biochemical interactions in the wnt pathway. Biochim. Biophys. Acta *1495*, 168–182.

Stern, C.D., Fraser, S.E., Keynes, R.J., and Primmett, D.R. (1988). A cell lineage analysis of segmentation in the chick embryo. Development *104*, 231–244.

Takada, S., Stark, K.L., Shea, M.J., Vassileva, G., McMahon, J.A., and McMahon, A.P. (1994). Wnt-3a regulates somite and tailbud formation in the mouse embryo. Genes Dev. *8*, 174–189.

Tam, P.P. (1981). The control of somitogenesis in mouse embryos. J. Embryol. Exp. Morphol. Suppl. *65*, 103–128.

Zakany, J., Kmita, M., Alarcon, P., de la Pompa, J.L., and Duboule, D. (2001). Localized and transient transcription of Hox genes suggests a link between patterning and the segmentation clock. Cell *106*, 207–217.

Zhang, N., and Gridley, T. (1998). Defects in somite formation in lunatic fringe-deficient mice. Nature *394*, 374–377.

3.2. Real-time imaging of the somite segmentation clock

The accumulated findings since the discovery of the first cyclic gene provided the long awaited experimental support for the existence of a molecular clock within the PSM. However, as outlined in the introduction, no experimental condition is known which can affect the period of these oscillations. An important reason, I believe, is the technical limitation in visualizing these oscillations appropriately. The methodology relied on static, mRNA-expression analysis by *in situ* hybridization, in combination with the culture of half embryos. While extremely successful, this approach has inherent limitations. Most notably, only two time points can be analyzed per sample. This lack of temporal resolution could be compensated for by analyzing many samples. For instance, the analysis of *Axin2* expression as presented in section 3.1 of this work involved more than 140 embryos and ~50 bisected embryos. While this allows a prediction of the full oscillation cycle, the fact that only two time points per sample are available still precludes a clear picture of the precise period, due to the uncertainty as to whether a peak or trough is reached. An elegant approach to retrieve temporal information even from the snapshot mRNA-expression pattern analysis made use of the fact that in zebrafish embryos, several consecutive waves of mRNA expression are present at any given time point in the PSM (Giudicelli et al., 2007). Thus, the distance between two consecutive waves corresponding to the wavelength was measured. Together with mathematical modeling, the period along the AP axis was modeled and, thus far, this represents the most advanced methodology to approach the oscillation characteristics. Still, it appears that our methodology is lacking behind the conceptual progress in the field; while an increasing number of sophisticated models have been based on a molecular oscillator,

this oscillator was practically still invisible. For this and other reasons, it was an important challenge to establish a methodology that allowed the real-time imaging of the segmentation clock activity. The goal was to achieve a high temporal and spatial resolution and for this reason, a fluorescent-based approach was chosen. A very similar approach based, however, on bioluminescence was reported in a study by Prof. Kageyama (Masamizu et al., 2006).

We have divided the experimental setup into four distinct but interconnected parts.

3.2.1. Establishment of static culture conditions

3.2.2. Generation of a dynamic, fluorescent-based reporter protein

3.2.3. Real-time imaging using two-photon microscopy

3.2.4. Data analysis

3.2.1. Establishment of static culture conditions

The *in vitro* culture of mouse embryos has become a standard methodology since the discovery by New and colleagues that the best development of rodent embryos is achieved if the culture medium is constantly agitated during the *in vitro* culture (New et al., 1976a). In addition, detailed studies on the optimal medium composition have been performed by these authors (New et al., 1976b). However, the goal of imaging the embryos during the *in vitro* culture necessitates that the embryo develops in static conditions, without any agitation. It appears that these requirements constitute a much bigger challenge to the normal development of the mouse embryo. A study by Jones *et al*. reported static culture conditions compatible with imaging of mouse development (Jones

et al., 2002). When I tested these culture conditions, it became apparent that while somites do form, their formation is irregular and unsatisfactory. Most importantly, I observed a drastic reduction in *de novo* mRNA production during the *in vitro* culture. Thus, when performing mRNA *in situ* hybridization of embryos cultured for various times, the staining intensity was greatly reduced and color revelation times had to be increased considerably. As a consequence of this, the fluorescence of transgenic mouse embryos (LuVeLu, see below) disappeared soon after initiation of culture.

The main variable affecting this disappearance in fluorescence was found to be the oxygen concentration. When the concentration in the gas phase of the incubation gas mixture was increased from 21% to 65% O_2, or better, an oxygen-partial pressure of 0.65 standard atmosphere (atm) (pO_2=0.65 atm), the fluorescent signal remained robust during the course of the imaging experiments. At the same time, endogenous mRNA production remained higher and somite formation appeared more regular, supporting the beneficial effect of higher oxygen concentration during static embryo culture. In this respect, the static culture conditions used have to be compared to the historically first system of rodent embryo culture, the watch-glass culture system. Using this system, Denis New cultured mouse embryos at day 8.5 *dpc* (days post coitum) up to the 24- to 32-somite stage, and he noted that the older, but not the younger embryos benefited from a higher oxygen concentration (60%) in the gas phase (New, 1966). Once the culture efficiency was improved through agitating the medium containing the embryo, the oxygen concentration had to be adjusted, e.g., reduced (reviewed in (Cockroft, 1997)). Thus, increasing the oxygen concentration under static culture conditions serves mainly to overcome the limited diffusion of oxygen into the medium and assures that the oxygen

needs of the embryo are met during real-time imaging. As a side note, I determined the actual oxygen saturation measured at the bottom of the dish to be lower than expected. By using a fluorescent-based, fiber optic oxygen meter placed on the bottom of the dish, the oxygen saturation was ~35% (when the gas phase contained 65% Oxygen; Figure 3).

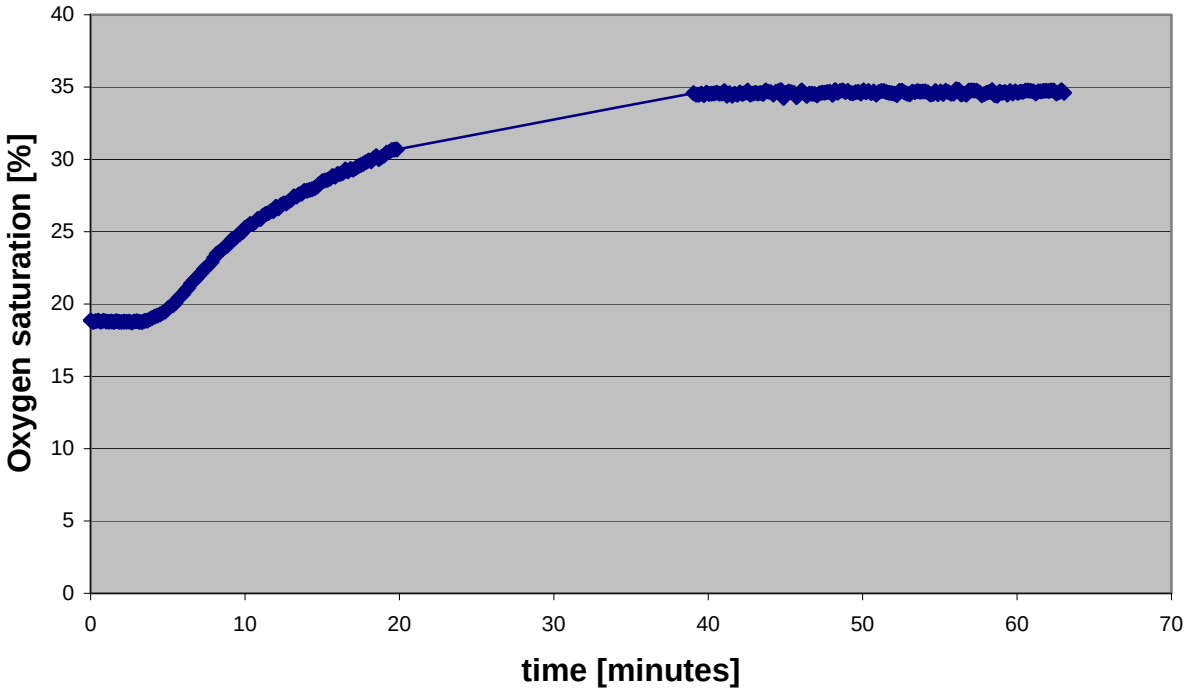

Figure 3. Oxygen saturation was measured using a fluorescent-based oxygen meter at the bottom of a 35mm Petri dish, filled with 3ml of PBS. At time 0, the gas mixture was changed to 65% O_2, 5% CO_2 and 30% Nitrogen.

Since the mesoderm is located internally, the factual oxygen concentration might be even lower at the surface of PSM cells. A second important change to the protocol of Jones *et al*. concerned the presence of HEPES in the incubation medium (Jones et al., 2002) which, when combined with CO_2 buffering turned out to invariably impair embryonic development. In addition, if CO_2 was used for buffering, HEPES was not

required in order to maintain a stable pH of ~7.4 during long-term culture of embryos. Therefore, HEPES was omitted from the culture medium.

Finally, the age of the embryos is an important variable to consider. Embryos at stage 9.0 *dpc* of development are more sensitive to *in vitro* culture, while isolated mouse embryo tails at day 10.0 to 11.0 *dpc* show a very robust *in vitro* development. These embryo tails develop routinely for 16-24 hours, elongate and form many distinct somites (Figure 4). The observation that the age of the embryo affects culture outcome might reflect the physiological changes in metabolism that occur during development. Before onset of a placental function (thus, without allantoic blood flow) the embryo develops in the hypoxic uterine environment. At this time, the main energy source is glucose (Shepard et al., 1997). After placental function is established, which is estimated to occur at around somite 17 at 9.0 *dpc* (New et al., 1976a), oxygen concentration and consumption increase, and energy metabolism shifts more toward mitochondrial respiration (Shepard et al., 1997). In light of this drastic switch, it is clear that any culture condition might need to be adjusted to the age of the embryo in order to balance culture conditions with the embryonic repertoire in metabolic function at the time of culture. I interpret the findings that embryos at 9.0 *dpc* are more difficult to accommodate to *in vitro* culture to reflect the fact that at this developmental time, the metabolism of the embryo undergoes dynamic changes, making it difficult to find one experimental setup that suits the needs of the embryo for an extended period of time. At day 10-11, when physiological changes in metabolism are less dynamic, it appears easier to adjust *in vitro* culture settings to embryo metabolism.

In summary, with these modifications, mouse embryos between 9.0 *dpc* and 11.5 *dpc* can be cultured successfully on a microscope stage, while development and transcriptional activity can be observed in real time.

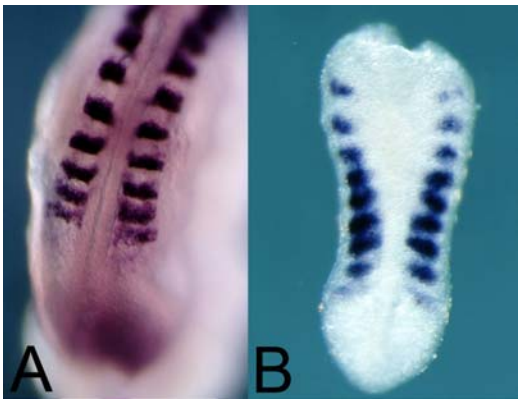

Figure 4. Whole mount *in situ* hybridization for *Uncx4.1* mRNA to indicate somites formed during the culture of mouse embryos at 9.0 *dpc* (A) or 10.5 *dpc* (B). (A) During the six-hour culture, the embryo formed two new somites. (B) Only the tail of the embryo was cultured for 18 hours, during which time six somites formed (see also time-lapse recordings presented below).

3.2.2. Generation of a dynamic, fluorescent-based reporter protein

In order to create a reporter system that is capable of visualizing oscillatory mRNA transcription, the prime requirement is a defined enhancer/promoter fragment that is responsive to the segmentation clock activity. To this end, we could make use of the enhancer/promoter fragment for the cyclic gene *Lfng*. This fragment had been identified independently by two research groups and was shown to faithfully reflect endogenous *Lfng* expression (Cole et al., 2002; Morales et al., 2002). With this 2.4-kb-long promoter fragment at hand, the second requirement was the generation of a highly dynamic reporter protein. In order to visualize dynamic changes in mRNA production, a reporter system with the capabilities of reflecting rapid changes in mRNA transcription rate is necessary. Conventional fluorescent proteins, such as GFP, are too stable to react

dynamically – once produced, these proteins have a half life of many hours and, thus, can not easily reflect dynamic changes in production rate. Therefore, the fluorescent protein of our choice, Venus, which is a yellow fluorescent protein (YFP)-variant showing an improved protein folding (Nagai et al., 2002), had to be destabilized on both protein and mRNA levels. To accelerate protein turnover, a widely used modified PEST domain was fused to the Venus protein. This sequence is derived from the mouse ornithidine decarboxylase protein and has been shown to transfer instability to heterologous proteins (Li et al., 1998). The predicted half life for a protein fused to this modified PEST domain is approximately one hour (Li et al., 1998). In addition, I fused the mRNA of *Venus* to the 3'untranslated region (UTR) of *Lfng* in order to confer fast mRNA turnover. The 3'UTR of *Lfng* contains AU-rich elements, which in turn are known to be recognized by mRNA degradation machinery (Hilgers et al., 2005; Zubiaga et al., 1995).

Indeed, the mRNA comparison supported this hypothesis. As can be observed in transgenic embryos expressing *Venus* or *GFP* under the *Lfng* promoter fragment, the exchange of simian virus 40 (SV40) UTR with the 3'UTR of *Lfng* drastically altered the mRNA expression pattern (Figure 5). When the *Lfng* 3'UTR was included, the expression pattern closely resembled endogenous *Lfng* expression, showing drastic differences among littermates (Figure 5A). However, when the same promoter fragment was used to drive GFP-SV40 mRNA (named pLEI), the mRNA expression pattern appeared diffuse throughout the PSM and no clear differences were observed among littermates (Figure 5B).

Two points are worth noting. In the original description of the *Lfng* promoter fragment used, the LacZ reporter construct contained SV40 UTR, but nevertheless, the

mRNA expression patterns of LacZ closely resembled endogenous *Lfng* patterns, with clear dynamic changes. For this reason, one group searched for common sequences between LacZ and *Lfng* RNA that could account for rapid mRNA turnover. A homology between LacZ mRNA and the 5'UTR of *Lfng* was located (Cole et al., 2002). In addition, the second group reported that the dynamic mRNA expression of LacZ was maintained even when the promoter fragment was inverted and no endogenous *Lfng* mRNA sequence remained in this construct. These results suggest that LacZ has an intrinsic short mRNA half life. In agreement with these findings, when LacZ-SV40 was exchanged with GFP-SV40 (named pLEI), diffuse GFP mRNA patterns (without obvious dynamic changes) were observed, indicating a higher stability of GFP mRNA compared to LacZ mRNA (Figure 5). Therefore, when using GFP as a reporter, the addition of the 3'UTR of *Lfng* proved to be essential to obtain mRNA patterns resembling endogenous *Lfng*. Thus, while the 3'UTR of *Lfng* is not essential when LacZ is used, it is necessary when using GFP as a reporter.

What then, is the role of the *Lfng* 3'UTR? This leads to the second point to mention, namely, the fact that there is no reason to invoke dynamic or oscillatory mRNA degradation in the generation of the oscillating expression patterns. Intronic probes for *Lfng* which reflect *de novo* transcription show very similar, dynamic expression patterns. Clearly, the observed dynamic mRNA patterns are generated via regulation of transcriptional activity. From this point of view, there is a requirement for a high mRNA turnover which, however, does not need to be oscillatory. The *Lfng* mRNA turnover rate seems to be, in part, determined by its 3'UTR. This also emphasizes that the reporter presented here, named LuVeLu, reflects transcriptional activity only. *Venus* mRNA and

Venus protein are destabilized artificially to allow this transcriptional activity to be seen. This means that only the onset of activity is meaningful and reflects transcriptional activity, likely in response to signals connected to the segmentation clock. In contrast, the off-phase is determined both by the underlying transcriptional activity and the degradation characteristics, which as stated, do not reflect the endogenous situation.

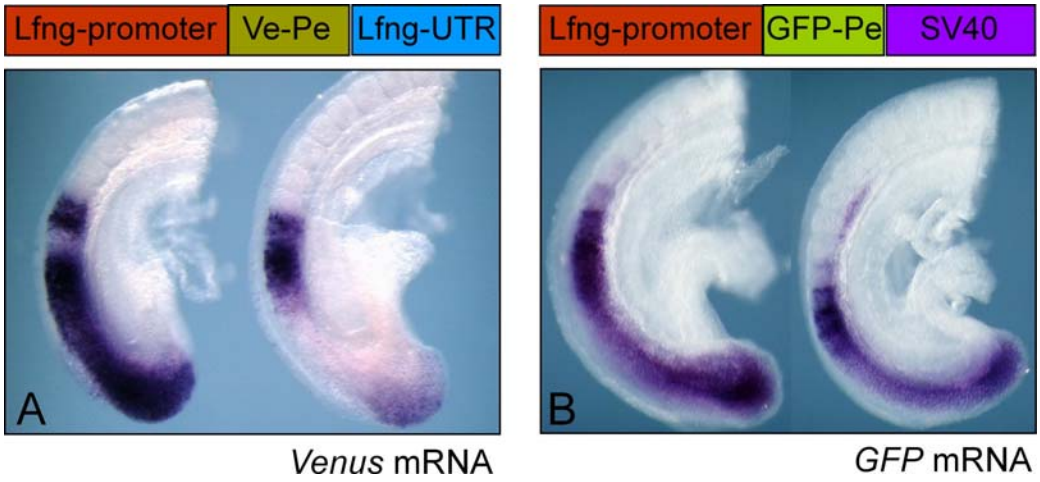

Figure 5. *In situ* hybridization of transgenic embryos, expressing *Venus* (A) or *GFP* (B) under the promoter of *Lfng*. Note the drastic differences between littermates when the mRNA contained the *Lfng* 3'UTR (A), while the expression varied only little among littermates when SV40Poly A was used (B). The basic structure of the inserted transgenic construct is shown schematically above the panels.

A transgenic mouse line (LuVeLu) expressing this dynamic reporter system under the *Lfng* promoter was generated using pronuclear injection by the animal core facility at the Stowers Institute for Medical Research. After breeding for several generations and selecting the line showing the strongest expression, the presented experiments were all performed with the same founder line (Founder 9079).

The LuVeLu mouse line shows very strong mRNA expression; however, a fluorescent signal is not visible when using a regular GFP-dissecting scope. This indicates that on one hand, the destabilization strategy was successful; however, the high mRNA and protein turnover rate causes the amount of Venus protein, and accordingly, of emitted fluorescence, to be very low. This challenge was addressed using two-photon microscopy.

3.2.3. Real-time imaging using two-photon fluorescent microscopy

For the imaging experiments described here, mouse embryo tails at day 10.5 *dpc* were dissected and placed in a 35mm Petri dish on the microscope stage, inside the incubation chamber. The excitation of Venus fluorescence was achieved with two-photon excitation (2PE). The use of 2PE has several important advantages. The two-photon technology offers the advantage that relatively low-energy light is used. Only when two low-energetic photons cooperate, a higher-energy transition occurs and the fluorescent molecule is excited. Since the likelihood of cooperation depends on the photon concentration (e.g., light intensity), it follows that this event almost exclusively occurs in the focal plane where light intensity is highest (Denk and Svoboda, 1997). Thus, while performing several scans through the embryo in order to cover the volume of the PSM, the embryo tissue outside the focal plane is exposed to low-energy light and, therefore, embryotoxicity is reduced.

In addition, since all fluorescence emanates from the focal plane, a pinhole is unnecessary in two-photon microscopy and all emitted light can be collected. Especially in strongly scattering samples such as mouse embryos, this helps to increase sensitivity.

Finally, the infrared light used for two-photon microscopy shows higher tissue penetration, which is beneficial for large samples such as mouse embryos.

Combined, two-photon microscopy has been shown to be less embryotoxic (Squirrell et al., 1999), while allowing weak signals to be detected. Using this combination of static mouse embryo culture with 2PE, mouse embryo tails were imaged for 12-18 hours. During these time-lapse recordings, several successive "waves" of fluorescence are seen to traverse the PSM in a posterior-to-anterior manner. At this point, the fluorescence stabilizes and forms a striped expression (Figure 6).

As noted several times, the impression of a moving wave is an illusion. It is the consequence of a sequential activation of Venus transcription under the influence of the *Lfng* reporter. The coordination and smoothness of this traveling but kinematic wave can now be appreciated by following the evolution of fluorescence along time with high spatial and temporal resolution. The repetitive appearance of successive waves and regular intervals indicate that we were successful in generating the first fluorescent reporter system for the segmentation clock activity.

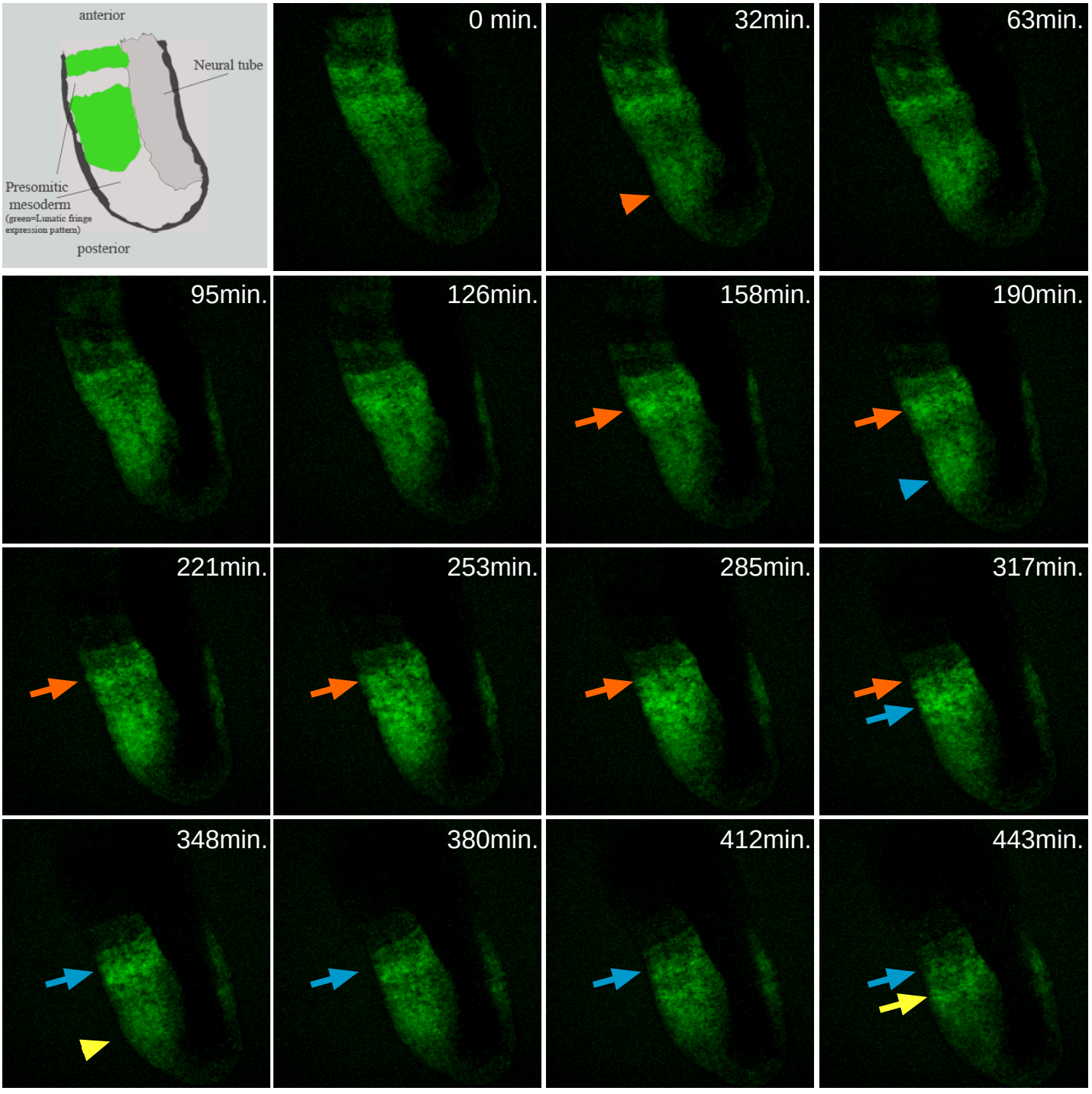
anterior
Neural tube
Presomitic
mesoderm
(green=Lunatic fringe
expression pattern)
posterior
0 min.
32min.
63min.
95min.
126min.
158min.
190min.
221min.
253min.
285min.
317min.
348min.
380min.
412min.
443min.

Figure 6

Figure 6. Real-time imaging of *lunatic fringe* oscillations in 10.5 *dpc* LuVeLu transgenic mouse embryos. The first frame shows a schematic representation of the imaged mouse embryo tail. Only the posterior part of the mouse embryo is visible; the Venus fluorescence in the PSM is in green. Note the emergence of successive waves in the posterior PSM (arrowheads). The waves appear to traverse the PSM and are then stabilized in the anterior PSM as stripes (arrows). The different colors (orange, blue and yellow) assign waves (arrowheads) and stripes (arrows) to successive cycles. The relative time difference between images is indicated.

3.2.4. Data analysis

The real-time imaging of LuVeLu embryos at 10.5 *dpc* allows visual identification of several periodic waves of Venus fluorescence to traverse the embryo in a posterior-to-anterior manner. To quantify these changes in fluorescence, the mean intensity was calculated in a defined region of interest (ROI) and then the evolution of the mean intensity in this ROI was followed over time. This allowed the determination of several basic oscillator parameters, such as period, traveling speed of the posterior wave, better kinematic wave and dependence of these parameters on the axial position in the PSM. To calculate the period, it is essential to first distinguish between the oscillator period and the cycle period.

3.2.4.1 Oscillation period vs. cycle period

The oscillation period reflects the alternating on and off expression of the reporter gene at an individual cell level. Thus, the oscillation period reflects the time required for the transcriptional activity to oscillate between on and off states in a single cell. In contrast, the cycle period is the time required to repeat a certain expression pattern, itself a result of the expression status of many cells. It reflects, for instance, how much time is required for two successive posterior waves to emerge close to the embryo tail. Therefore, the cycle period does reflect an observation at a tissue level.

The key is that identical expression patterns in successive cycles are not necessarily generated by the same cells. In other words, even if the pattern is comparable between consecutive cycles, these expression patterns are themselves generated by a constantly changing cell population. This is due to the fact that new cells enter the PSM

from the posteriorly located tail bud, while in the anterior PSM cells are incorporated into somites. Therefore, single-cell level oscillations and tissue-level mRNA pattern cycles do represent interconnected but distinct phenomena altogether.

With this logic in mind, it becomes evident that the values of oscillation periods and cycle periods are not necessarily identical. They are, in fact, quite different in most parts of the PSM. To determine the cycle period, the time point of emergence of a posterior wave was noted, and the time required for the next posterior wave to emerge was measured. Practically, the time for the emergence of many successive waves was measured and divided by the number of waves. The mean cycle period calculated in this way is 135 minutes and for age-matched mouse embryos, very little variation between embryos was found (+/- 0.4 minutes; for n=4 independent experiments, Figure 7).

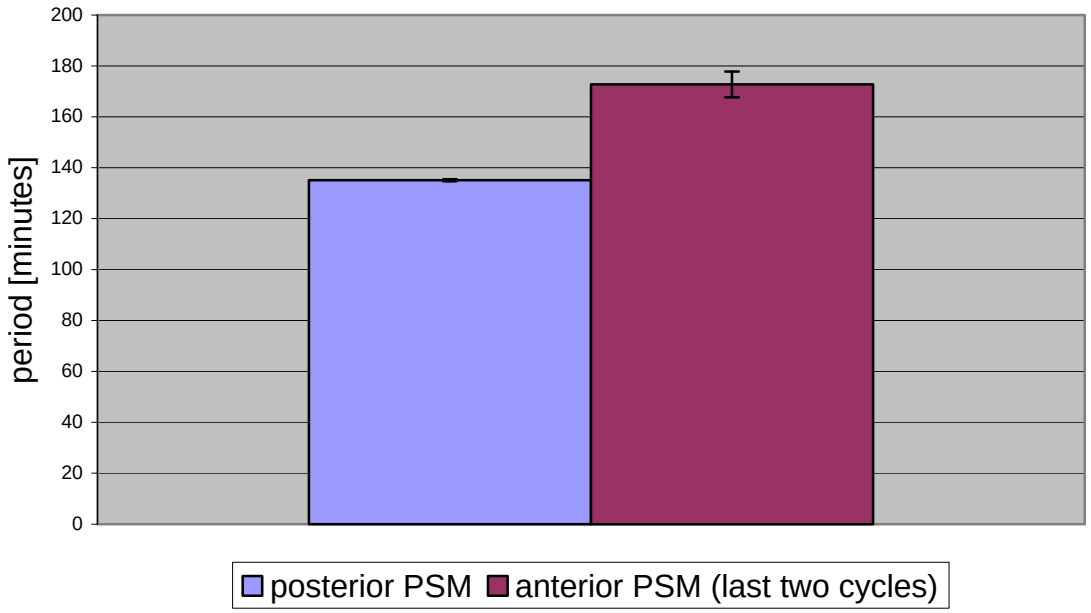

Figure 7. Oscillation period in relation to position in the PSM. The peak-to-peak distance was measured in the posterior PSM by measuring the time elapsed between the occurrences of a fluorescence peak in the most posterior PSM. This corresponds to the cycle period of 135 minutes (+/- 0.4 minutes; n=4). In the anterior PSM, the last two oscillations within a fixed region of interest (ROI) were quantified and the time from peak-to-peak fluorescence measured. This corresponds to the oscillation period in a cohort of cells just before oscillations stop and before these cells will be incorporated into a somite-forming unit. The oscillation period in this PSM region was determined to be 173 minutes (+/-5.0 minutes; n=8 waves in three independent samples). For the distinction between the cycle period and the oscillation period, see the main text.

To measure the oscillation period (e.g., the period of oscillations within a cell) ideally one should label such a single cell and follow the fluorescence evolution over time. This technical challenge has not been solved as yet in mouse embryos. Therefore, a ROI was defined within the PSM, for instance, covering somite level -III (see nomenclature description in Introduction). If the embryo itself does not move during the time-lapse recording, this ROI will cover a similar group of cells at one axial position. The relative position of this ROI will change, however, and this ROI will sequentially be

located increasingly anterior in the PSM. This is because somites will form at the anterior end of the PSM. As an example, ROI 1 is placed at Somite -III at cycle 0. In cycle n+1, one somite formed at the anterior end of the PSM and, therefore, the ROI will be located at somite level -II. At cycle n+2, the ROI will be located at somite level -I, at which time the oscillation will stop. Thus, by assuming that local cell movement can be neglected, the ROI will reflect the mean fluorescence evolution in a given set of cells. Therefore, by approximation, the period measured from these fluorescence recordings reflects the oscillation period in this set of cells at one given, absolute axial position. These measurements clearly show that the oscillation period gradually increases as the observed ROI is located more and more anteriorly in the PSM (Figure 8).

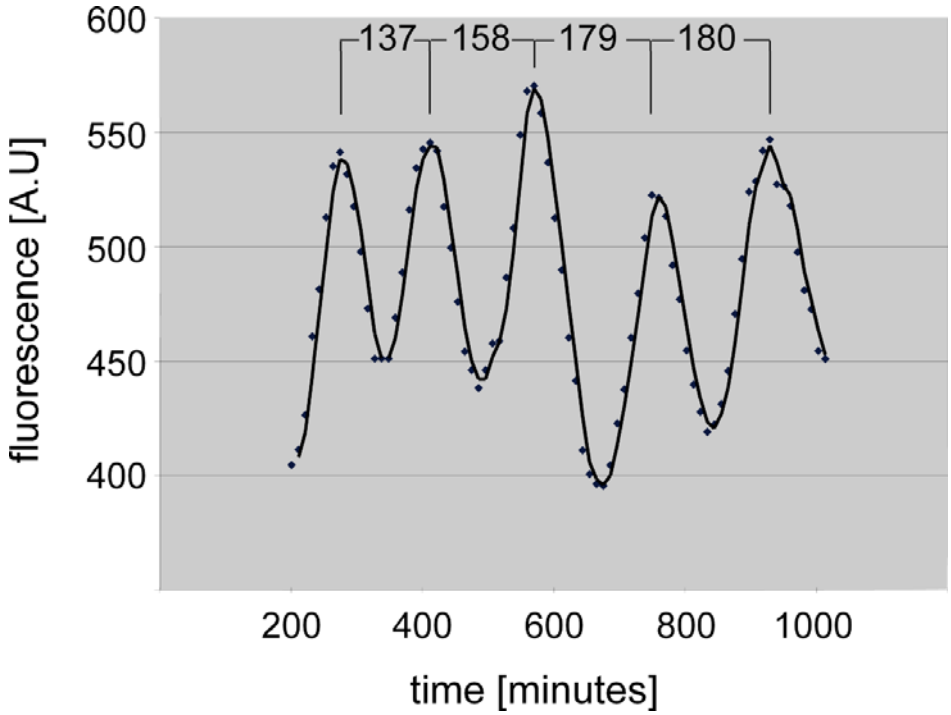

Figure 8. Quantification of fluorescence in a region of interest (ROI) within the PSM of a LuVeLu embryo during real-time imaging. The ROI was placed in the most posterior PSM and is considered to reflect the mean fluorescent intensity in a group of cells at a fixed absolute axial position within the PSM. Because of somite formation, this ROI is relatively displaced anteriorly. The trendline corresponds to the average of two points. Note the occurrence of multiple oscillations with increasing peak-to-peak distance, corresponding to a progressive increase in oscillation period. The oscillation period (in minutes) is indicated above each peak-to-peak interval.

Interestingly, the increase in the oscillation period occurs gradually throughout the entire PSM. In the example in Figure 8, the second oscillation of this group of cells still located far posteriorly in the PSM already shows an oscillation period of 158 minutes. When the period of the last two oscillations in a region in the anterior PSM was determined in several embryos (n=3), a period of 172.8 minutes was measured (Figure 7). These measurements indicate that the oscillations within PSM cells slow down considerably once cells become located increasingly anterior in the PSM. Only in the

most posterior PSM do cells oscillate with a period that matches the cycle period. In other words, in most parts of the PSM, the period of transcriptional oscillations differs from the cycle period and from the somite formation period.

Next, we measured the traveling speed of the kinematic wave of transcriptional activity within the PSM and its dependence on the relative PSM position. The impression of a moving wave, the kinematic wave, results from the phase delay between cells. Because a change in phase delay is thought to underlie the increase in the oscillation period observed in the PSM, it follows that we expect a change in traveling speed along the PSM. Indeed, this is the case. The traveling speed can now be calculated directly from the real-time imaging data. To this end, the time required for the wave to traverse a defined distance in the posterior or anterior PSM, respectively, was measured. The resulting wave traveling speed in the posterior and anterior PSM is 1.45 μm/min (+/-0.09; n=3) and 0.95 μm/min (+/-0.19; n=3), respectively (Figure 9). This slowing down of the traveling speed of the kinematic wave is due to an increase of the oscillation period once cells acquire more and more (relative) anterior PSM positions. An important conclusion to discuss is that the local oscillation period will diverge increasingly from the cycle period and, therefore, also from the somite formation period as cells are located in the anterior PSM. In addition, these data indicate that a gradual change in phase delay and oscillation period occurs along the axis, which differs from the view that a catastrophic change in oscillation behavior occurs at certain axial PSM levels.

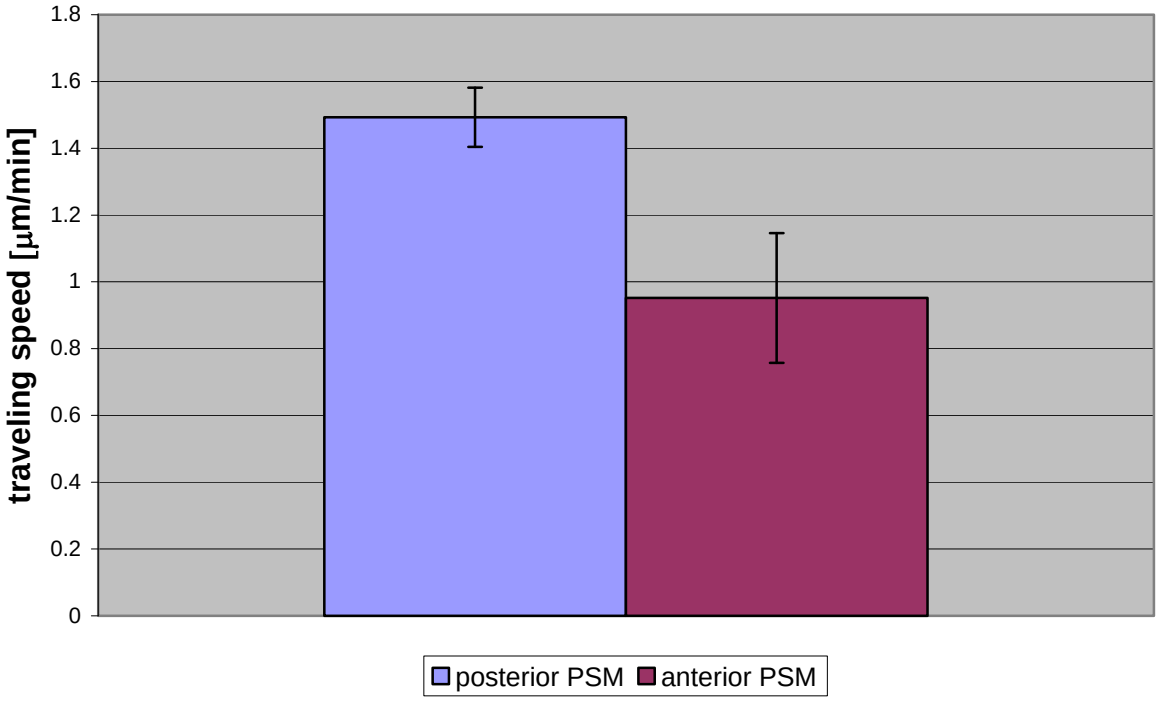

Figure 9. Determination of traveling speed of the kinematic wave of Venus in LuVeLu embryos during real-time imaging recordings. The traveling speed was calculated independently within the posterior and anterior PSM, respectively. The slowing down of the traveling speed is caused by the increase in the oscillation period observed in the anterior PSM (see Figure 8).

3.3 A β-catenin gradient links the clock and wavefront systems in mouse embryo segmentation

nature cell biology

A β-catenin gradient links the clock and wavefront systems in mouse embryo segmentation

Alexander Aulehla[1], Winfried Wiegraebe[1], Valerie Baubet[2], Matthias B. Wahl[1], Chuxia Deng[3], Makoto Taketo[4], Mark Lewandoski[5] and Olivier Pourquié[1,6,7]

Rhythmic production of vertebral precursors, the somites, causes bilateral columns of embryonic segments to form. This process involves a molecular oscillator — the segmentation clock — whose signal is translated into a spatial, periodic pattern by a complex signalling gradient system within the presomitic mesoderm (PSM). In mouse embryos, Wnt signalling has been implicated in both the clock and gradient mechanisms, but how the Wnt pathway can perform these two functions simultaneously remains unclear. Here, we use a yellow fluorescent protein (YFP)-based, real-time imaging system in mouse embryos to demonstrate that clock oscillations are independent of β-catenin protein levels. In contrast, we show that the Wnt-signalling gradient is established through a nuclear β-catenin protein gradient in the posterior PSM. This gradient of nuclear β-catenin defines the size of the oscillatory field and controls key aspects of PSM maturation and segment formation, emphasizing the central role of Wnt signalling in this process.

Somites are transient epithelial structures that give rise to the axial skeleton, and are the first overt sign of a metameric body plan in vertebrate embryos. They are produced by segmentation of the paraxial mesoderm, a periodic process that has been associated with a molecular oscillator or segmentation clock identified in studies demonstrating periodic transcription of cyclic genes in the PSM[1]. A large network of signalling genes that are involved in the Notch, Wnt and fibroblast growth factor (FGF) pathways was shown previously to be rhythmically expressed in the posterior PSM with a periodicity matching that of somite production[1–3]. Although the molecular nature of the oscillator's pacemaker remains unclear, it has been shown in mouse embryos that intact Wnt signalling is required for oscillations to occur[2,4,5]. In addition, gradients of Wnt, FGF and retinoic acid signalling translate the signalling pulse generated by the clock into the spatial periodic pattern of segments[2,6,7]. Activity of the Wnt/FGF gradient is highest in the posterior embryo; however, the antagonistic retinoic acid-signalling gradient peaks towards the anterior part of the embryo. The Wnt/FGF gradient has been shown to set up a threshold defining a PSM level — called the determination front — at which cells become responsive to the clock signal. At the determination front, mRNA oscillations cease and cells exhibit striped expression of key factors, such as *Mesoderm posterior 2* (*Mesp2*), which specify somite polarity and future segment boundaries[8,9]. Here, we examine the role of the Wnt gradient in somitogenesis and determine how it interconnects with the function of the Wnt pathway in clock oscillations of the PSM.

Using immunohistochemistry, we observed a clear posterior-to-anterior nuclear gradient of β-catenin (a key intracellular mediator of the Wnt pathway) in the PSM of mouse embryos (Fig. 1a–c). A posterior gradient for β-catenin was observed in all embryos analysed ($n = 19$), irrespective of their segmentation clock phase, as determined by the mRNA expression pattern of the cyclic Wnt target gene *Axin2* (refs 2, 10, 11; Supplementary Information, Fig. S1). To examine the role of the nuclear β-catenin gradient in somitogenesis, we used a conditional strategy to selectively delete or stabilize β-catenin in the PSM of mouse embryos. First, to selectively delete β-catenin in the PSM, mice carrying a conditional *β-catenin*^{floxed} allele[12] were crossed with the *T–Cre* mouse line in which Cre recombinase is driven by the *T* (*Brachyury*) promoter. In this transgenic mouse line, Cre is expressed in precursors of the paraxial mesoderm located in the primitive streak. In embryos homozygous for the conditional-null *β-catenin*^{floxdel} allele in primitive streak descendents, a few abnormal somites formed anteriorly and a severe axial truncation was observed (Supplementary Information, Fig. S2 and data not shown). This confirms the requirement of Wnt/β-catenin signalling in antero-posterior axis formation and gastrulation; however, further analysis of the role of β-catenin during somitogenesis was not feasible with this phenotype.

Next, we used *T–Cre* mice carrying the conditional gain-of-function allele *β-catenin*$^{lox(ex3)}$ to disrupt the β-catenin gradient by constitutively stabilizing β-catenin in the PSM. *β-catenin*$^{lox(ex3)}$ contains loxP sites flanking

[1]Stowers Institute for Medical Research, Kansas City, MO 64110 USA. [2]Molecular and Cellular Oncogenesis, The Wistar Institute, Philadelphia, PA 19104 USA. [3]Genetics of Development and Diseases Branch, National Institutes of Diabetes and Digestive and Kidney Diseases, National Institutes of Health, Bethesda, MD 20892 USA. [4]Graduate School of Medicine, Kyoto University, Kyoto, Japan. [5]Laboratory of Cancer and Developmental Biology, NCI-Frederick, National Institutes of Health, Frederick, MD 21702 USA. [6]Howard Hughes Medical Institute, Kansas City, MO 64110 USA.
[7]Correspondence should be addressed to O.P. (email: olp@stowers-institute.org)

Received 5 November 2007; accepted 10 December 2007; published online 23 December 2007; DOI: 10.1038/ncb1679

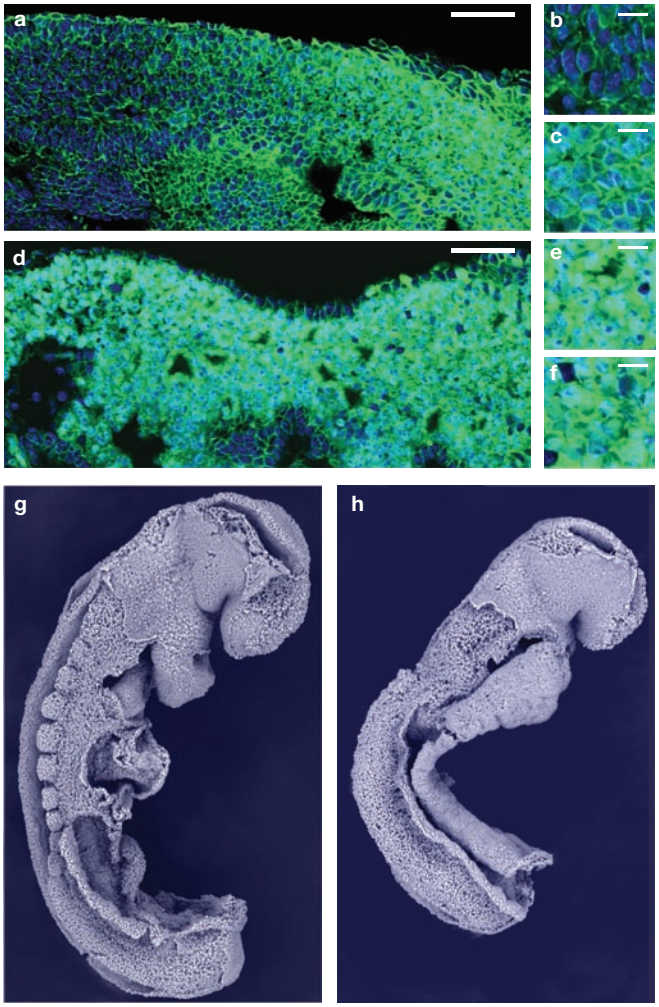

Figure 1 Conditional stabilization of β-catenin in mouse PSM disrupts somite formation. Fluorescence immunodetection of β-catenin (green) in saggital sections through the PSM of control (**a**–**c**) and mutant *β-catenin*$^{del(ex3)/+}$*–T–Cre* embryo (**d**–**f**). Nuclei were counterstained with DAPI (blue) and anterior is to the left. (**a**) A graded distribution of β-catenin protein along the antero-posterior axis showed predominant cytoplasmic localization in the anterior PSM (shown at higher magnification in **b**), and nuclear localization in the posterior PSM (shown at higher magnification in **c**). (**d**) Mutant embryo showing elevated, uniform levels of β-catenin throughout the PSM. Nuclear localization was found both in the anterior PSM (shown at higher magnification in **e**), as well as in the posterior PSM (shown at higher magnification in **f**). Scanning electron microscopy of control (**g**) and mutant *β-catenin*$^{del(ex3)/+}$*–T–Cre* embryo (**h**). The ectoderm was partially removed during embryo processing. Nine somites were formed in the control embryo (**g**); however, no somites were visible in the mutant embryo (**h**). Note expanded, unsegmented PSM in mutant embryo. Scale bars in **a** and **d** represent 50 μm; scale bars in **b**, **c**, **e** and **f** represent 10 μm.

exon 3, which codes for a crucial sequence recognized by the destruction complex that targets β-catenin for degradation[13]. This strategy resulted in accumulation of mutant β-catenin$^{del(ex3)}$ protein specifically in mesodermal lineages, including the PSM. Nuclear staining of β-catenin was elevated throughout the entire PSM of *β-catenin*$^{del(ex3)}$ mutants (Fig. 1d–f), without an appreciable posterior-to-anterior protein gradient, as seen in wild-type embryos (Fig. 1a–c). No significant difference in the proliferative state of the posterior PSM or the tail bud was observed between mutant and wild-type embryos (Supplementary Information, Fig. S1). In

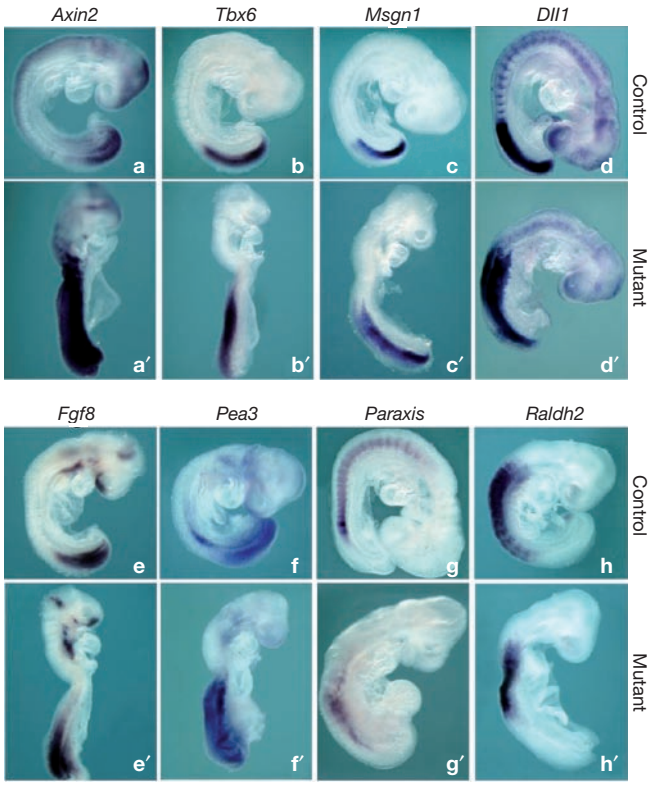

Figure 2 Expansion of posterior PSM identity in *β-catenin*$^{del(ex3)/+}$ mutant embryos. *In situ* hybridization of embryonic day 9 control ((**a**–**h**), *β-catenin*$^{del(ex3)/+}$*–T–Cre* negative) and corresponding mutant littermates ((**a′**–**h′**), *β-catenin*$^{del(ex3)/+}$*–T–Cre*). *Axin2* (**a**, **a′**), *Tbx6* (**b**, **b′**), *Msgn1* (**c**, **c′**), *Dll1* (**d**, **d′**), *Fgf8* (**e**, **e′**) and *Pea3* (**f**, **f′**) showed an expanded expression domain in mutant embryos. Note that this expansion of expression in mutants is both absolute and relative to the total axis length when compared with control littermates. (**g**, **g′**) In contrast to the control embryo (**g**), *Paraxis* was only expressed transiently in the mutant embryo (**g′**). (**h**, **h′**) A shortened *Raldh2* expression domain was found in mutant embryos (**h′**), compared with control littermates (**h**).

mutant embryos carrying the *β-catenin*$^{del(ex3)}$ allele, no sign of morphological boundary formation or somites could be seen along the body axis (Fig. 1g, h), except for up to four irregular somites seen occasionally in the most anterior aspect of mutant paraxial mesoderm. Mutant embryos could not complete the turning process during gastrulation, exhibited a rounded allantois that failed to fuse with the chorion and died at approximately day 10.5 of development. The accumulation of nuclear β-catenin throughout the PSM was accompanied by upregulation of Wnt signalling, as determined by using the Wnt-reporter mice *BAT–Gal*[14]. In *β-catenin*$^{del(ex3)}$*–BAT–Gal* embryos, significant anterior extension of *lacZ* expression was observed in the PSM (Supplementary Information, Fig. S3; $n = 8$). The Wnt-responsive gene *Axin2* (refs 10, 11) was markedly upregulated in the PSM (Fig. 2a, a′; $n = 4$), consistent with sustained activation of canonical Wnt signalling. Other direct targets of the Wnt pathway involved in PSM patterning were upregulated and shifted anteriorly in mutant *β-catenin*$^{del(ex3)/+}$ embryos, compared with control littermates. These include the genes *T-box6* (*Tbx6*; ref. 15), *mesogenin1* (*Msgn1*; ref. 16) and *Delta-like 1* (*Dll1*; refs 17, 18; Fig. 2b, b′; $n = 5$; c, c′; $n = 5$; d, d′; $n = 2$). The expression domain of *Fgf8* was slightly extended anteriorly (Fig. 2e, e′; $n = 4$). In addition, the FGF-signalling target *Pea3* (ref. 19) was clearly upregulated and shifted anteriorly in the PSM, suggesting that the strength

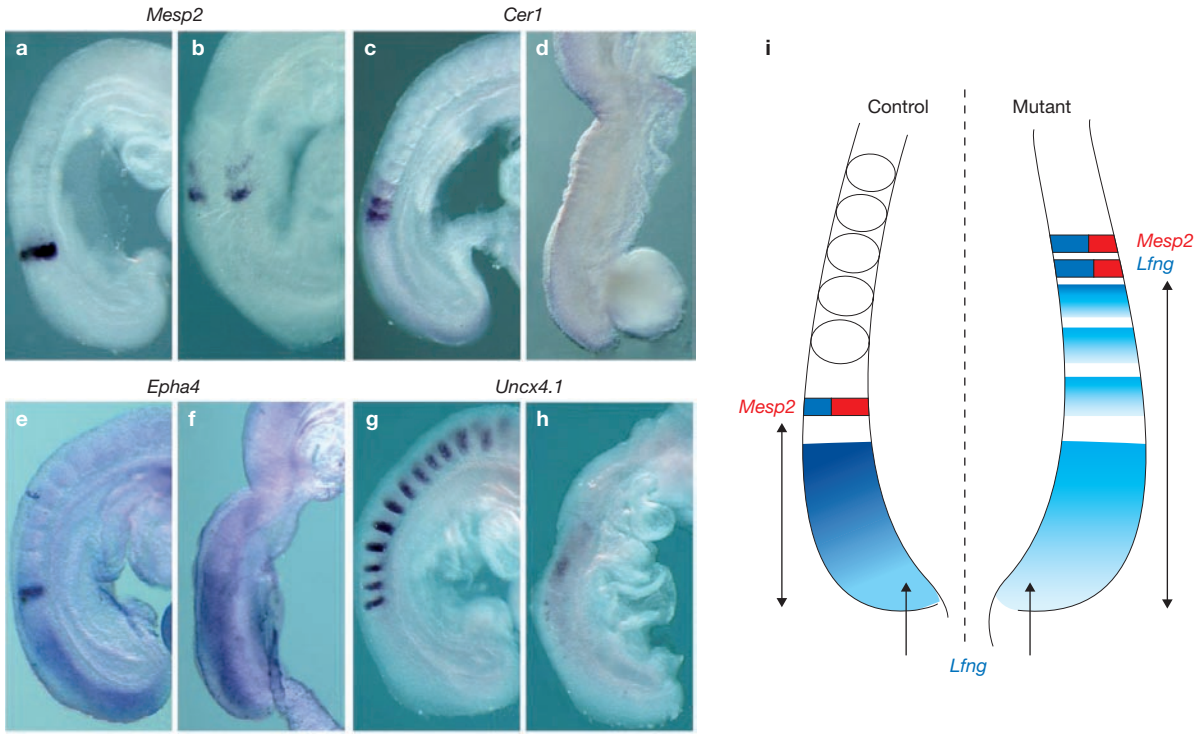

Figure 3 Anterior shift of determination front in *β-catenin*$^{del(ex3)/+}$ mutant embryos. (**a**, **b**) *Mesp2* expression in control (**a**) and mutant (**b**) embryo littermates. *Mesp2* expression was shifted anteriorly in mutants. (**c**, **d**) *Cer1* in control (**c**) and mutant (**d**) embryo littermates. (**e**, **f**) *Epha4* expression in control (**e**) and mutant (**f**) embryo littermates. *Epha4* and *Cer1* were expressed as stripes in the anterior PSM of control embryos, but this expression domain was absent in mutant embryos. (**g**, **h**) *Uncx4.1*, which marks the posterior aspect of formed somites in control embryos (**g**), was markedly downregulated in mutant embryos (**h**). (**i**) Scheme of *Mesp2* expression in control (left side) and mutant (right side) embryos. Note the anterior shift of *Mesp2* expression in mutants based on measurements (Supplementary Information, Fig. S3). *Lfng* showed up to five additional stripes in anterior mutant PSM, of which the most anterior two stripes overlap with *Mesp2* as judged from double *in situ* hybridizations (data not shown). In mutants, the posterior broad expression domain of *Lfng* was weaker but of a comparable size to control embryos.

of the FGF-signalling gradient is increased (Fig. 2f, f′; $n = 5$). The anterior PSM of *β-catenin*$^{del(ex3)/+}$ mutants, nevertheless, showed signs of maturation. Thus, markers for the anterior PSM and somites, such as *Paraxis*[20] (Fig. 2g, g′; $n = 2$), and *Raldh2* (*Aldh1a2*; ref. 21; Fig. 2h, h′; $n = 2$) were present, but their expression was only transient or reduced, respectively, compared with wild-type embryos. We found that *Mesp2* expression, which correlates with the level of the determination front in wild-type embryos (Fig. 3a), was significantly shifted anteriorly in mutant embryos (Fig. 3b, $n = 16$ and Supplementary Information, Fig. S3). Downstream targets of Mesp2 (*Epha4* and *Cer1*; ref. 22) were expressed in stripes in the anterior PSM of controls but absent from anterior PSM in mutant littermates (Fig. 3c–f; $n = 5$ for both). Furthermore, the expression of a posterior somite marker *Uncx4.1* was clearly downregulated in mutant embryos (Fig. 3g, h; $n = 3$). Thus, overexpression of β-catenin causes an anterior shift of the determination front and delays the activation of *Mesp2* expression (Fig. 3i). In wild-type embryos, the position of the *Mesp2* stripe was found to lie outside the β-catenin gradient (Supplementary Information, Fig. S1). These data indicate that downregulation of nuclear β-catenin is required for activation of Mesp2 downstream targets, and explains the absence of morphological boundary formation in mutant embryos.

Oscillations of the Wnt pathway have been postulated to rely on the function of a group of negative feedback inhibitors of the Wnt pathway, such as Axin2, dickkopf 1 (Dkk1) or Dact1 (refs 2, 3). Periodic expression of these direct Wnt targets is expected to rhythmically alter β-catenin levels in PSM cells. We did not detect visible oscillations of β-catenin protein in the PSM (Supplementary Information, Fig. S1), but fluctuations of small amplitude may, in principle, account for the oscillatory transcription of *bona fide* targets of the canonical Wnt pathway, such as *c-myc* (ref. 3) or *Axin2* (ref. 2) in the PSM. If this were the case, then oscillations of the Wnt pathway should be disrupted in *β-catenin*$^{del(ex3)/+}$ embryos in which a high level of nuclear β-catenin is constantly maintained in PSM cells. To test this hypothesis, we analysed the expression of a cyclic direct Wnt target, *Dkk1*, using an intronic probe to detect only nascent, pre-mRNA[3] (Fig.4a–d). In *β-catenin*$^{del(ex3)/+}$ mutant embryos, *Dkk1* expression levels were higher overall when compared with wild-type embryos, and expression was always detected in the posterior PSM (Fig.4c, d). When mutant littermates were compared after identical staining procedures, the intensity of *Dkk1* pre-mRNA expression varied in the posterior PSM, ranging from faint (16 out of 32 embryos) to strong (16 out of 32 embryos) (Fig. 4c, d; arrows). In addition, a clear, striped pattern of active transcription was observed in the PSM of mutant embryos (Fig. 4c, d; arrowheads). Therefore, constitutive expression of high nuclear β-catenin levels does not block dynamic expression of the Wnt cyclic gene, *Dkk1*, suggesting that Wnt-signalling oscillations still occur in *β-catenin*$^{del(ex3)/+}$ mutants.

To confirm the status of Notch oscillations in *β-catenin*$^{del(ex3)/+}$ mutants, expression of the Notch cyclic genes *lunatic fringe* (*Lfng*; Fig. 4e–h) and *Hairy and enhancer of split 7* (*Hes7*; ref. 23) was examined. Posterior expression of *Lfng* in mutant embryos varied

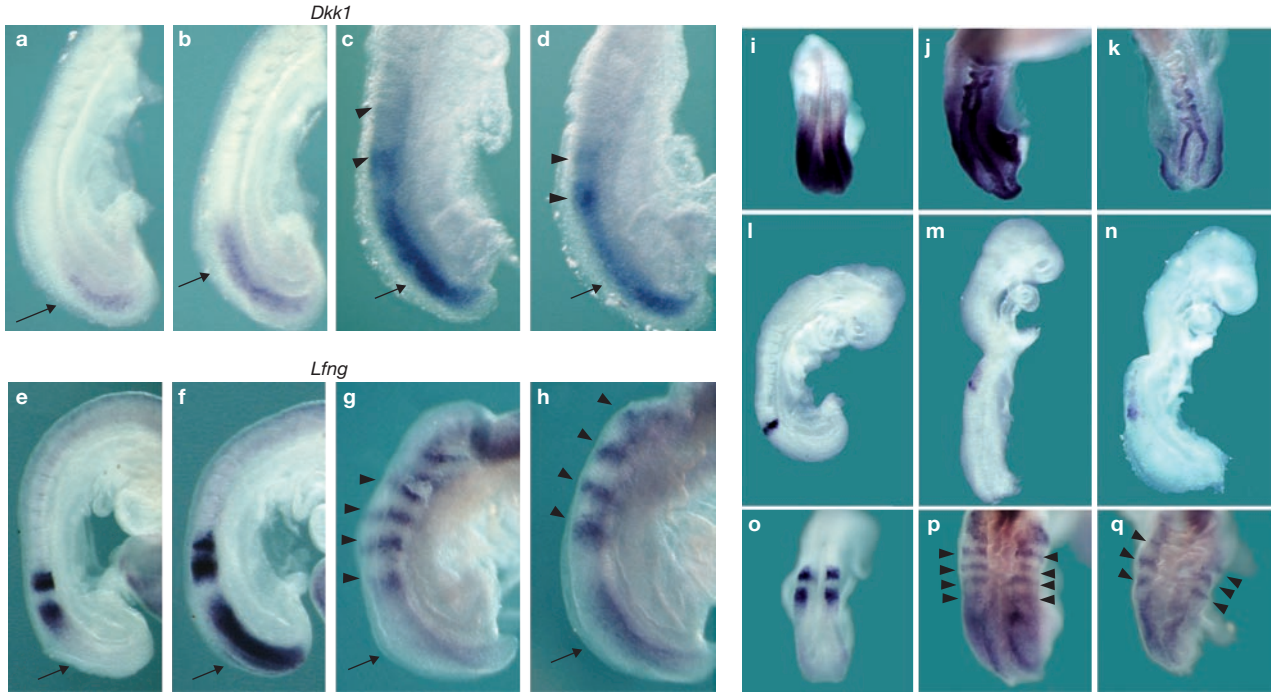

Figure 4 Dynamic expression of *Wnt* and *Notch* cyclic genes is maintained in *β-catenin*$^{del(ex3)/+}$ mutant PSM. (**a**–**d**) Intronic *Dkk1* pre-mRNA expression in control (**a**, **b**) and mutant PSM (**c**, **d**). PSM expression was highly variable in control embryos (**a**, **b**, arrows). The posterior expression domain in mutant littermates was highly variable, ranging from strong expression (**c**, arrow; 16 out of 32 embryos) to weak expression (**d**, arrow; 16 out of 32 embryos). In addition, stripes of expression in the middle PSM were observed in mutant embryos (**c**, **d**, arrowheads) but not in controls (**a, b**). (**e**–**h**) *In situ* hybridization of *Lfng* in control (**e**, **f**) and mutant (**g**, **h**) embryos. Control embryos showed a highly dynamic posterior expression domain (**e**, **f**, arrows). Supernumerary stripes of *Lfng* expression were visible in the expanded anterior PSM of mutant embryos (**g**, **h**, arrowheads). In the posterior PSM of mutant littermates, expression ranged from weak (**g**, arrow; 8 out of 22 embryos) to strong (**h**, arrow; 14 out of 22 embryos). (**i**–**q**) Analysis of compound *β-catenin*$^{lox(ex3)/+}$*–Fgfr1*$^{f/KO}$*–T–Cre* mutant embryos. Control embryos (**i**, **l**, **o**), *β-catenin*$^{lox(ex3)/+}$*–Fgfr1*$^{f/+}$ *–T–Cre* single mutant embryos (**j**, **m**, **p**) and compound *β-catenin*$^{lox(ex3)/+}$*–Fgfr1*$^{f/KO}$*–T–Cre* double mutants (**k**, **n**, **q**) were hybridized for *Dusp4* (**i**–**k**), *Mesp2* (**l**–**n**) and *Lfng* (**o**–**q**). The embryos in (**j**, **k**), (**m**, **n**), (**p**, **q**) were littermates, and were processed and stained together. Note that in compound mutants, the FGF signalling target *Dusp4* was downregulated in the PSM (**k**, $n = 8$), whereas under these conditions *Mesp2* still showed an anterior shift in the enlarged PSM (**n**, $n = 5$) compared with wild-type embryos (**l**); however, this anterior shift was less pronounced compared with the *β-catenin*$^{lox(ex3)/+}$*–Fgfr*$^{f/+}$*–T–Cre* single mutants (**m**). In the anterior PSM of compound mutants, we found several stripes of *Lfng* expression (**q**, arrowheads; $n = 5$), similar to that in the *β-catenin*$^{lox(ex3)/+}$*–Fgfr1*$^{f/+}$ *–T–Cre* single mutants (**p,** arrowheads).

considerably in intensity between littermates (Fig. 4g, h; arrows; 14/22 strong expression, 8/22 weak expression), suggesting that in the posterior PSM, Notch oscillations still occur. Up to five stripes of variable width and inter-stripe distance were found in the middle and anterior PSM, both for *Lfng* (Fig. 4g, h; arrowheads) and for *Hes7* mRNA (Supplementary Information, Fig. S4). During development, the total number of stripes increased slowly in the PSM of mutant embryos, paralleling the progressive increase in size of the PSM (Supplementary Information, Fig. S5). To rule out the possibility that the remaining wild-type allele in *β-catenin*$^{del(ex3)/+}$ mutant embryos controls the dynamic expression of *Lfng*, we generated *β-catenin*$^{del(ex3)/floxdel}$ mutants in which PSM cells express only the gain-of-function allele. The phenotype of these mutants was very similar to that of *β-catenin*$^{del(ex3)/+}$ mutants, with several stripes of *Lfng* in the PSM (Supplementary Information, Fig. S4), indicating that the remaining wild-type *β-catenin* allele does not contribute to this phenotype.

To test directly whether the multiple stripes of *Lfng* expression in the mutant PSM correspond to oscillating transcription domains, we developed a real-time imaging strategy to visualize the activity of the segmentation clock in living mouse embryos (Fig. 5 a–f). To this end, we generated transgenic animals that expressed a highly destabilized Venus reporter (a variant of yellow fluorescent protein, YFP) under the control of the cyclic *Lfng* promoter[24,25]. Real-time imaging of control reporter mouse embryos with two-photon, time-lapse microscopy revealed periodic waves of *Lfng* expression, which are initiated in the posterior PSM approximately every 2 h (Fig. 5a, c; Supplementary Information, Movie S1; $n = 3$). These waves of transcriptional activity traversed the PSM from posterior to anterior and stopped in the anterior PSM where they briefly stabilized as a striped expression domain before disappearing (Fig. 5a, arrows; Fig. 5c; Supplementary Information, Movie S1). Cells in the anterior PSM stopped oscillating once they reached a certain maturation state and due to somite formation, there was a posterior regression of the domain showing oscillations (Fig. 5c, e). To examine *Lfng* oscillations in the mutant background, mice carrying the *β-catenin*$^{del(ex3)}$ allele were crossed with the *Lfng* reporter line. Analysis of the movies generated from these mutant embryos showed that the striped expression of *Lfng* corresponds to multiple, oscillating expression domains that sweep through the expanded anterior PSM (Fig. 5b, arrows; 5d, f; Supplementary Information, Movie S2; $n = 4$). According to their axial location, these cells should have stopped oscillating, but instead they continued to do so for an extended period of time under the influence of elevated β-catenin levels (Fig. 5b, d, f). Consistently, no regression of the oscillatory domain was observed during time-lapse recordings

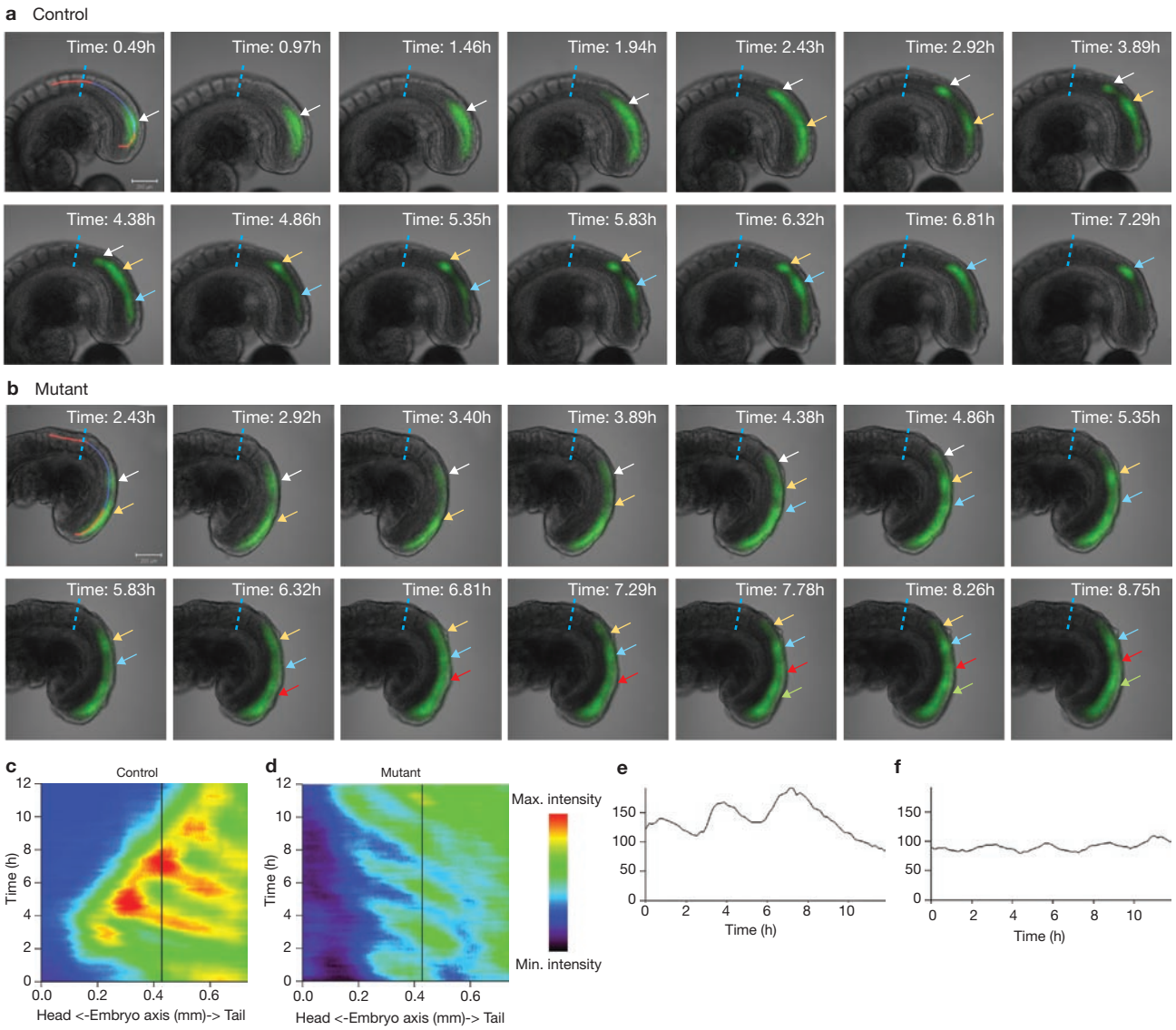

Figure 5 Real-time imaging of *Lfng* oscillations in control and *β-catenin*$^{del(ex3)/+}$ mutant embryos. (**a**, **b**) Representative time series of control (**a**) and *β-catenin*$^{del(ex3)/+}$*–T–Cre–LuVeLu* (**b**) embryos, reporting oscillations (green) of Venus–YFP fluorescence driven by the *Lfng* promoter. Only the posterior part of the embryo is shown. Arrows of different colours indicate successive Venus–YFP waves sweeping through the PSM. The corresponding time within the original time-lapse recording (Supplementary Information, Movies S1 and S2) is indicated in the upper right corner. The vertical dashed line (blue) represents a fixed point in the embryo for orientation. (**c**, **d**) Quantification of minimally processed fluorescence data. Fluorescence intensity is colour-coded (see colour code to the right of graphs) and plotted along PSM length (*x*-axis) and time (*y*-axis). The intensities were measured along the posterior line, shown in the first frame for each series in panels and centred in the PSM (**a**) and (**b**). Peaks of intensity in control (**c**) and mutant (**d**) traversed the embryos from posterior (right) to anterior (left) over time. The regression of the oscillatory field from anterior to posterior seen in control embryos was not observed in the mutant embryo during the recording time. (**e**, **f**) Fluorescence intensity (*y*-axis) at one given position within the PSM, as indicated by a vertical black line (**c**, **d**) shown over time (*x*-axis) of development. Note that at this fixed axial position, cells in the control embryo (**e**) showed three pronounced oscillations before oscillations stopped, caused by posterior regression of the oscillatory field. In contrast, cells at a similar position in the mutant embryo (**f**) continued to oscillate (five times) during the entire recording time (12 h), with lower overall intensity and lower amplitude.

(Fig. 5d). The signal intensity and the amplitude of the oscillations were, however, reduced in mutants, compared with wild-type embryos (Fig. 5). These results demonstrate that oscillations of the segmentation clock occur even in the presence of high and steady nuclear β-catenin levels. In addition, this shows that β-catenin is able to maintain clock oscillations and suggests that the arrest of oscillations under normal conditions is linked to the level of β-catenin protein in the PSM.

In this study, we have shown that by deleting β-catenin in mesoderm precursors in the primitive streak, formation of the paraxial mesoderm is blocked, causing axis truncation. In contrast, expression of a stable form of β-catenin throughout the paraxial mesoderm led to a Wnt-signalling gain of function, causing a delayed and defective maturation process and a subsequent increase in the size of the PSM along the antero-posterior axis. This suggests that the function of the Wnt-signalling gradient in the PSM is carried out by the β-catenin protein gradient.

The delay in maturation was accompanied by sustained oscillations of the Wnt and Notch pathway in PSM cells. Thus, Wnt activation in the posterior PSM provides a permissive environment for oscillations of the

segmentation clock to occur. This also suggests that the decision to stop oscillations in the anterior PSM under normal conditions is not based on a limited ability of cells to oscillate (that is, a counting mechanism) but requires the downregulation of Wnt signalling.

However, the PSM of mutant embryos retained signs of maturation and *Mesp2* became consistently activated at the level where oscillations eventually stopped in the extended anterior PSM of the *β-catenin*$^{del(ex3)}$ mutants. Thus, maintaining a high level of nuclear β-catenin was not sufficient to maintain the posterior PSM identity indefinitely, indicating that β-catenin interacts with other signalling pathways to perform this function. The Wnt/nuclear β-catenin gradient overlaps with an FGF-signalling gradient, which has also been shown to have an important role in the maintenance of posterior PSM identity[6,26,27]. *Wnt3a*/β-catenin was shown in loss-of-function experiments to function upstream of *Fgf8* (refs 2, 28). Here, we show that in a gain-of-function situation, β-catenin accumulation can increase *Fgf8* expression, and FGF signalling extends more anteriorly in the expanded PSM. Thus, some of the observed effects in *β-catenin*$^{del(ex3)}$ mutants could be mediated indirectly by the FGF gradient. To test this possibility directly, we generated compound *β-catenin*$^{lox(ex3)/+}$*–Fgfr1*$^{f/ko}$*–T–Cre* mutant embryos to block FGF signalling in the PSM (Fig. 4i–q). In the PSM of compound mutants, expression of the FGF target *Dusp4* (ref. 29) was downregulated (Fig. 4k; $n = 8$). The anterior shift of the *Mesp2* stripe was still observed in the compound mutants (Fig. 4n; $n = 5$), but was not as pronounced as that in the *β-catenin*$^{lox(ex3)/+}$*–Fgfr1*$^{f/+}$*–T–Cre* single mutants (Fig. 4m). Therefore, part of the effect of β-catenin stabilization in the PSM seems to be mediated indirectly through FGF signalling. This also suggests that the β-catenin gradient can influence PSM patterning and maturation directly, possibly through the activation of targets such as *Msgn1* (ref. 16). In addition, although no oscillations of *Lfng* were detected in the PSM of conditional homozygous *Fgfr1–T–Cre* single mutants[30], the presence of a *β-catenin*$^{del(ex3)}$ allele led to the formation of several *Lfng* stripes in the extended PSM of compound mutants (Fig. 4q; $n = 5$), indicating that *Lfng* oscillations were rescued. This is consistent with the proposed role of Wnt signalling downstream of FGF signalling in the control of *Lfng* oscillations[30]. Thus, these experiments demonstrate the lack of a simple epistatic relationship between Wnt and FGF signalling in the PSM. Rather, these pathways are tightly interconnected and seem to synergize in controlling PSM maturation, thereby defining the permissive environment for oscillations of the segmentation clock.

Although accumulation of nuclear β-catenin markedly altered PSM maturation, activity of the segmentation clock was not disrupted by these experimental conditions. We conclude that oscillations of Wnt and Notch targets are not achieved by oscillating (nuclear) β-catenin protein levels. Regulation of β-catenin protein levels has normally been regarded as essential in defining canonical Wnt-signalling activity. However, there is growing evidence that nuclear β-catenin is not the sole determinant of transcriptional activity downstream of canonical Wnt signalling, but relies also on the regulated interaction with additional (nuclear) cofactors[31]. Our data suggest that oscillations of Wnt targets in the PSM are probably caused by the cyclic activity of a β-catenin cofactor. Interestingly, cyclic recruitment of several nuclear cofactors of β-catenin to the genomic enhancer/promoter locus of Wnt targets (such as *c-myc*, a Wnt cyclic gene in mice)[3] has indeed been shown to occur[32]. This cyclic recruitment occurred even in the presence of a steady and high nuclear β-catenin level. The present study illustrates two distinct strategies of Wnt-signalling regulation that operate simultaneously in embryonic cells. Clarifying the molecular details of this versatile regulation in the developing embryo might reveal some underlying principles of signalling regulation in biological systems.

METHODS

Mice breeding and embryo production. Mice with either the conditional gain-of-function allele *β-catenin*$^{lox(ex3)}$ (see Supplementary Information), the loss-of-function allele *β-catenin*^{floxed}, described previously[12] (obtained from Jackson Laboratory, Bar Harbor, ME) or the conditional *Fgfr1*^{f} allele, described previously (see Supplementary Information), were kept on a Bl6 background. Transgenic animals for *T–Cre* (see Supplementary Information) and *BAT–Gal*[14] were described previously and kept on a Bl6 or CD1 background, respectively. To generate gain-of-function mutant embryos, *β-catenin*$^{lox(ex3)/lox(ex3)}$ animals were mated with *T–Cre* heterozygous animals (these embryos are referred to as *β-catenin*$^{del(ex3)}$ mutants). To obtain *β-catenin*$^{lox(ex3)/floxed}$ embryos, *β-catenin*$^{floxed/floxed}$ animals were first crossed with *T–Cre* animals. Double heterozygote animals were then mated with *β-catenin*$^{lox(ex3)/lox(ex3)}$ animals. To generate conditional deletion of β-catenin, we crossed *β-catenin*$^{floxed/floxed}$ with *β-catenin*$^{floxed/+}$*–T–Cre* positive animals. To generate compound *β-catenin*$^{lox(ex3)/+}$*–Fgfr1*$^{f/ko}$*–T–Cre* mutants, males heterozygous for a germline deletion of the conditional *Fgfr1* allele (see Supplementary Information) and *T–Cre* positive *(Fgfr*$^{ko/+}$*–T–Cre)* were mated with *β-catenin*$^{lox(ex3)/lox(ex3))}$*–Fgfr1*$^{f/f}$ females. For real-time imaging experiments, *LuVeLu* transgenic animals were mated with *β-catenin*$^{lox(ex3)/lox(ex3)}$ animals and double heterozygote animals were mated with *T–Cre* homozygote transgenic animals. No significant phenotypic difference was observed in this mixed genetic background.

Generation of transgenic *Lfng* reporter mice (*LuVeLu*). A reporter allowing detection of luciferase cyclic activity driven by the *Hairy and enhancer of split 1* (*Hes1*) promoter was recently described in mice[33]. To image *Lfng* oscillations *in vivo* we used a fluorescent reporter (Venus–YFP), which has the potential to achieve high cellular resolution *in vivo*. A 2-kb fragment of the cyclic *Lfng* promoter (a gift from D. Ish-Horowicz)[24,25] was used to drive the expression of Venus–YFP (a gift from A. Miyawaki)[34] and fused with a modified PEST domain (see Supplementary Information) to increase protein instability. In addition, this construct was fused with the *Lfng* 3′UTR to destabilize *Venus–YFP* mRNA. Transgenic animals were produced by pronuclear injection using standard procedures. Five out of seven transgenic lines showed correct expression and two were further bred on a CD1 outbreed background. Experiments were performed using F4 generation mice.

Genotyping. Embryos were harvested at day 9.0 of development and genotyped with PCR using the yolk sac (see Supplementary Information). For *LuVeLu*, the following primers were used: Ala 1: tgctgctgcccgacaaccact and Ala 3: tgaagaacacgactgcccagc. Detailed protocols are available in the Supplementary Information.

Culture conditions during real-time imaging. Embryos at the 7- to 12-somite stage were dissected in pre-warmed DMEM (Invitrogen), with 10% FBS, 100 mg dl^{-1} D-glucose and 20 mM HEPES. Embryos were first incubated for 1.5 h in DMEM containing 50% rat serum (produced as described previously[35]) in a rotating culture apparatus (BTC Engineering). Subsequently, embryos were transferred to a glass bottom Petri dish (MatTek) containing 1.1 ml of DMEM/50% rat serum. Embryos were then transferred to and imaged inside a microscope incubation chamber (37°C, 65% O_2 and 5% CO_2; Solent Scientific).

Two-photon microscopy. Images were acquired with a Zeiss LSM510 laser-scanning microscope (Carl Zeiss MicroImaging). Samples were excited using a Ti:Sapphire Laser (Chameleon-Ultra, Coherent) at a wavelength of 960 nm through a 20× Plan Apo Objective (numerical aperture (NA) 0.8). Emission was collected using a 500–550 nm band-pass filter. A Z-stack of 6–10 planes at 12–16 μm distance was scanned every 8.5 min. Power settings were kept constant between all experiments.

Data visualization in time-lapse movies. Carl Zeiss AIM software (Carl Zeiss MicroImaging) was used to record all data and for basic image processing. Representative *z*-planes were added and the mean fluorescence intensity for combined *z*-planes was calculated using the AIM software. For further image processing, we developed software in IDL (ITT Visual Information Solutions).

All images are recorded in 12 bit, 512 × 512 square pixels with a size of 2.5 μm × 2.5 μm. The images were scaled to 8 bit, maximum intensity was set to 255 and the minimum to zero. To smooth the fluorescent images, a boxcar filter (30 × 30 pixels) was used. We developed an algorithm based on the transmitted light image that allowed automatic definition of the embryo border within each image. Only the region covering the embryo was used to process the fluorescent signal. To emphasize small differences in intensity, the fluorescent signal was taken to the power of three. For display, the maximum number was scaled to 255 and data below 30 was clipped. We applied a boosted Laplace filter with a centre value of 19 to the raw data of the transmitted light image.

Fluorescence quantification. Data were only minimally processed for graphical representation (Fig. 5c–f), and a linear relationship of the fluorescence intensities was maintained. We developed an algorithm that automatically defined a centreline through the PSM of the embryo based on the transmitted light image (detailed Methods are available in the Supplementary Information). This included a correction for slight embryonic movement during recordings. To that end, we defined a common reference point (vertical blue dashed line in Fig. 5a, b) and then cross-correlated the bright-field intensities of the 400 most anterior pixels (red lines in PSM, Fig. 5a, b). Fluorescence intensity was sampled along the centreline (blue portion of line in PSM in Fig. 5a, b), and the mean of 30 pixels calculated by applying a boxcar filter with a kernel size of 30 (30 pixels correspond approximately to the width of the PSM). This algorithm was applied to all time-points of the experiment. These data are shown as a false-colour intensity plot, with the *x*-axis representing the position along the embryo axis and the *y*-axis representing the time during development.

***In situ* hybridization.** Single and double *in situ* hybridizations were performed as described[2] (see Supplementary Information for details of the probes). Littermates were used for comparisons and were processed identically and in parallel.

Fluorescence immunodetection. Embryos were fixed in zinc formaldehyde for 1 h at room temperature and processed for paraffin embedding and sectioning (4 μm). Immunofluorescence detection was performed according to the following protocol: antigen retrieval was carried out in citrate buffer (pH 6) placed in a microwave at 95°C for 10 min. After blocking for 10 min (Power Block Universal Blocking Reagent, Biogenex HK085–5K), slides were incubated with primary antibody (mouse monoclonal anti-β-catenin, BD Transduction Laboratories Number 610153, dilution at 1:500, anti-phospho histone 3, Upstate 06–570, 1:1000) for 1 h at room temperature, followed by an overnight incubation at 4°C. Slides were washed three times in PBS Tween (PBST) and incubated with a secondary antibody (goat anti-mouse Alexa-488 or Alexa-568, Invitrogen) for 1 h at room temperature. Slides were washed three times in PBST and nuclei were counterstained with DAPI (InnoGenex CS-2010–06) for 5 min. Slides were mounted using an anti-fade reagent (ProLong Gold, Invitrogen).

Images were acquired on a Zeiss LSM510 laser scanning microscope (Carl Zeiss MicroImaging). Alexa-488 or Alexa-568 was excited by confocal microscopy, DAPI was visualized by two-photon excitation at 720 nm and a 20× Plan Apo objective (NA 0.8) was used.

Scanning electron microscopy. After *in situ* hybridization, fixed embryos were dehydrated in an ethanol series, incubated in hexamethyldisilazane for 30 min and then dried. Samples were imaged using a Hitachi TM-1000 unit.

Measurement of anterior shift of *Mesp2* expression. Images from age-matched embryos (day 9.0 of development) were taken as lateral views and imported into ImageJ software (open source from the National Institutes of Health, USA). Using the line and measure tool, the distance from tail end to *Mesp2* expression was measured and compared with known standard scales for conversion to mm. The mean was calculated from control ($n = 11$) and $\beta\text{-catenin}^{del(ex3)/+}$ mutant embryos ($n = 10$).

ACKNOWLEDGMENTS

We thank members of the Pourquié laboratory for discussions and comments on the manuscript, S. Esteban for artwork and J. Chatfield for manuscript editing. We thank the Stowers Institute Core Facilities, especially D. Dukes and M. Durnin in the Laboratory Animal Service and S. Beckham in the Histology Facility for their excellent technical assistance. A.A was funded by the Swiss Foundation for medical-biological grants, Swiss National Science Foundation. This research was supported by Stowers Institute for Medical Research. O.P. is a Howard Hughes Medical Institute Investigator.

AUTHOR CONTRIBUTIONS

A.A. designed, performed and analysed the experiments; established the real-time imaging and wrote the manuscript. W.W. developed software to analyse the real-time imaging data. V.B. contributed in the initial phase of this project to the real-time imaging experiments. M.W., C.D., M.T. and M.L. provided genetically modified mice. O.P. supervised the project and wrote the manuscript.

1. Palmeirim, I., Henrique, D., Ish-Horowicz, D. & Pourquié, O. Avian hairy gene expression identifies a molecular clock linked to vertebrate segmentation and somitogenesis. *Cell* **91,** 639–648 (1997).
2. Aulehla, A. *et al.* Wnt3a plays a major role in the segmentation clock controlling somitogenesis. *Dev. Cell* **4,** 395–406 (2003).
3. Dequeant, M. L. *et al.* A complex oscillating network of signalling genes underlies the mouse segmentation clock. *Science* **314,** 1595–1598 (2006).
4. Nakaya, M. A. *et al.* Wnt3a links left–right determination with segmentation and anteroposterior axis elongation. *Development* **132,** 5425–5436 (2005).
5. Satoh, W., Gotoh, T., Tsunematsu, Y., Aizawa, S. & Shimono, A. Sfrp1 and Sfrp2 regulate anteroposterior axis elongation and somite segmentation during mouse embryogenesis. *Development* **133,** 989–999 (2006).
6. Dubrulle, J., McGrew, M. J. & Pourquie, O. FGF signalling controls somite boundary position and regulates segmentation clock control of spatiotemporal *Hox* gene activation. *Cell* **106,** 219–232 (2001).
7. Diez del Corral, R. *et al.* Opposing FGF and retinoid pathways control ventral neural pattern, neuronal differentiation, and segmentation during body axis extension. *Neuron* **40,** 65–79 (2003).
8. Saga, Y., Hata, N., Koseki, H. & Taketo, M. M. *Mesp2*: a novel mouse gene expressed in the presegmented mesoderm and essential for segmentation initiation. *Genes Dev.* **11,** 1827–1839 (1997).
9. Morimoto, M., Takahashi, Y., Endo, M. & Saga, Y. The Mesp2 transcription factor establishes segmental borders by suppressing Notch activity. *Nature* **435,** 354–359 (2005).
10. Lustig, B. *et al.* Negative feedback loop of Wnt signalling through upregulation of conductin/axin2 in colorectal and liver tumors. *Mol. Cell. Biol.* **22,** 1184–1193 (2002).
11. Jho, E. H. *et al.* Wnt/β-catenin/Tcf signaling induces the transcription of Axin2, a negative regulator of the signaling pathway. *Mol. Cell. Biol.* **22,** 1172–1183 (2002).
12. Brault, V. *et al.* Inactivation of the *β-catenin* gene by Wnt1-Cre-mediated deletion results in dramatic brain malformation and failure of craniofacial development. *Development* **128,** 1253–1264 (2001).
13. Gordon, M. D. & Nusse, R. Wnt signaling: multiple pathways, multiple receptors, and multiple transcription factors. *J. Biol. Chem.* **281,** 22429–22433 (2006).
14. Maretto, S. *et al.* Mapping Wnt/β-catenin signaling during mouse development and in colorectal tumors. *Proc. Natl Acad. Sci. USA* **100,** 3299–3304 (2003).
15. White, P. H., Farkas, D. R., McFadden, E. E. & Chapman, D. L. Defective somite patterning in mouse embryos with reduced levels of Tbx6. *Development* **130,** 1681–1690 (2003).
16. Wittler, L. *et al.* Expression of Msgn1 in the presomitic mesoderm is controlled by synergism of WNT signalling and Tbx6. *EMBO Rep.* **8,** 784–789 (2007).
17. Hofmann, M. *et al.* WNT signaling, in synergy with T/TBX6, controls Notch signaling by regulating Dll1 expression in the presomitic mesoderm of mouse embryos. *Genes Dev.* **18,** 2712–2717 (2004).
18. Galceran, J., Sustmann, C., Hsu, S. C., Folberth, S. & Grosschedl, R. LEF1-mediated regulation of Delta-like1 links Wnt and Notch signaling in somitogenesis. *Genes Dev.* **18,** 2718–2723 (2004).
19. Roehl, H. & Nusslein-Volhard, C. Zebrafish pea3 and erm are general targets of FGF8 signaling. *Curr. Biol.* **11,** 503–507 (2001).
20. Burgess, R., Rawls, A., Brown, D., Bradley, A. & Olson, E. N. Requirement of the *paraxis* gene for somite formation and musculoskeletal patterning. *Nature* **384,** 570–573 (1996).
21. Niederreither, K., Subbarayan, V., Dolle, P. & Chambon, P. Embryonic retinoic acid synthesis is essential for early mouse post-implantation development. *Nature Genet.* **21,** 444–448 (1999).
22. Nakajima, Y., Morimoto, M., Takahashi, Y., Koseki, H. & Saga, Y. Identification of Epha4 enhancer required for segmental expression and the regulation by Mesp2. *Development* **133,** 2517–2525 (2006).
23. Bessho, Y., Miyoshi, G., Sakata, R. & Kageyama, R. Hes7: a bHLH-type repressor gene regulated by Notch and expressed in the presomitic mesoderm. *Genes Cells* **6,** 175–185 (2001).
24. Morales, A. V., Yasuda, Y. & Ish-Horowicz, D. Periodic lunatic fringe expression is controlled during segmentation by a cyclic transcriptional enhancer responsive to notch signaling. *Dev. Cell* **3,** 63–74 (2002).
25. Cole, S. E., Levorse, J. M., Tilghman, S. M. & Vogt, T. F. Clock regulatory elements control cyclic expression of lunatic fringe during somitogenesis. *Dev. Cell* **3,** 75–84 (2002).
26. Sawada, A. *et al.* Fgf/MAPK signalling is a crucial positional cue in somite boundary formation. *Development* **128,** 4873–4880 (2001).
27. Delfini, M. C., Dubrulle, J., Malapert, P., Chal, J. & Pourquie, O. Control of the segmentation process by graded MAPK/ERK activation in the chick embryo. *Proc. Natl Acad. Sci. USA* **102,** 11343–11348 (2005).

28. Morkel, M. *et al.* β-catenin regulates Cripto- and Wnt3-dependent gene expression programs in mouse axis and mesoderm formation. *Development* **130,** 6283–6294 (2003).
29. Niwa, Y. *et al.* The initiation and propagation of Hes7 oscillation are cooperatively regulated by Fgf and notch signaling in the somite segmentation clock. *Dev. Cell* **13,** 298–304 (2007).
30. Wahl, M. B., Deng, C., Lewandoski, M. & Pourquie, O. FGF signaling acts upstream of the NOTCH and WNT signaling pathways to control segmentation clock oscillations in mouse somitogenesis. *Development* **134,** 4033–4041 (2007).
31. Hecht, A. & Kemler, R. Curbing the nuclear activities of β-catenin. Control over Wnt target gene expression. *EMBO Rep* **1,** 24–28 (2000).
32. Wang, S. & Jones, K. A. CK2 controls the recruitment of Wnt regulators to target genes in vivo. *Curr. Biol.* **16,** 2239–2244 (2006).
33. Masamizu, Y. *et al.* Real-time imaging of the somite segmentation clock: revelation of unstable oscillators in the individual presomitic mesoderm cells. *Proc. Natl Acad. Sci. USA* **103,** 1313–1318 (2006).
34. Nagai, T. *et al.* A variant of yellow fluorescent protein with fast and efficient maturation for cell-biological applications. *Nature Biotechnol.* **20,** 87–90 (2002).
35. Jones, E. A. *et al.* Dynamic *in vivo* imaging of postimplantation mammalian embryos using whole embryo culture. *Genesis* **34,** 228–235 (2002).

nature cell biology

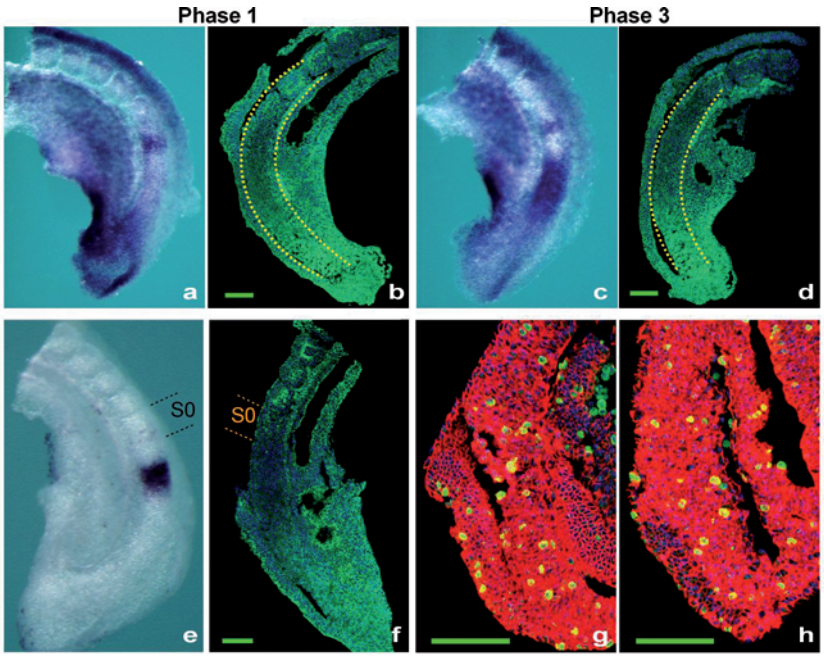

Figure S1 (**a-d**)The posterior-to-anterior gradient of β-catenin is present throughout the oscillation cycle of *Axin2* mRNA. Analysis of bisected embryos for *Axin2* mRNA (**a**,**c**, whole mount) and *β-catenin* protein of corresponding halves of same embryos (**b,d**, parasaggital sections, *β-catenin* in green). Note that while *Axin2* mRNA expression patterns changed between phase 1 (n=13, strongest expression posterior) and phase 3 (n=6, weak/absent expression in posterior PSM), the β-catenin protein distribution always showed a posterior-to-anterior gradient (n=19), irrespective of the phase of *Axin2* mRNA. Dashed lines delineate the paraxial mesoderm. (**e,f)** Comparison of the β-catenin gradient to *Mesp2* mRNA as a landmark in the anterior PSM. Bisected embryos were analyzed for *Mesp2* mRNA (**e**) and β-catenin was localized on parasaggital sections of corresponding halves (**f**, n=5). *Mesp2* striped expression is located in the presumptive somite S-II in the PSM, a region showing low β-catenin levels. The forming somite is indicated by S0. (**g**,**h**) Mitotic index analysis by Histone3-phosphorylation (H3P) immunostaining indicates no effect on cell proliferation in the posterior mesoderm upon accumulation of mutant *β-catenin*$^{del(ex3)}$. Shown are representative parasaggital sections of wild type (**g**) and mutant (**h**) *β-catenin*$^{del(ex3)/+}$ embryos stained for H3P (green) and *β-catenin* (red). Nuclei are counterstained with DAPI (blue). Note that the percentage of H3P-positive cells indicative for mitosis is unchanged between wild type (6.5%, n=7 embryos, total of 2315 cells counted) and mutant mutant *β-catenin*$^{del(ex3)/+}$ (6.5%, n=7 embryos, total of 2309 cells counted) embryos. Scale bars represent 100 μm.

Figure S2 Phenotype of conditional deletion of β-catenin in primitive streak and PSM. *In situ* hybridization of *Uncx4.1* mRNA in embryonic day 9.0 control (**a**) and mutant *β-catenin*$^{floxdel/floxdel}$;*T-Cre* (**b**) embryo. Note onset of axial truncation in mutant embryo as observed by the decreased length of mutant versus control PSM (bracket in a and b, respectively).

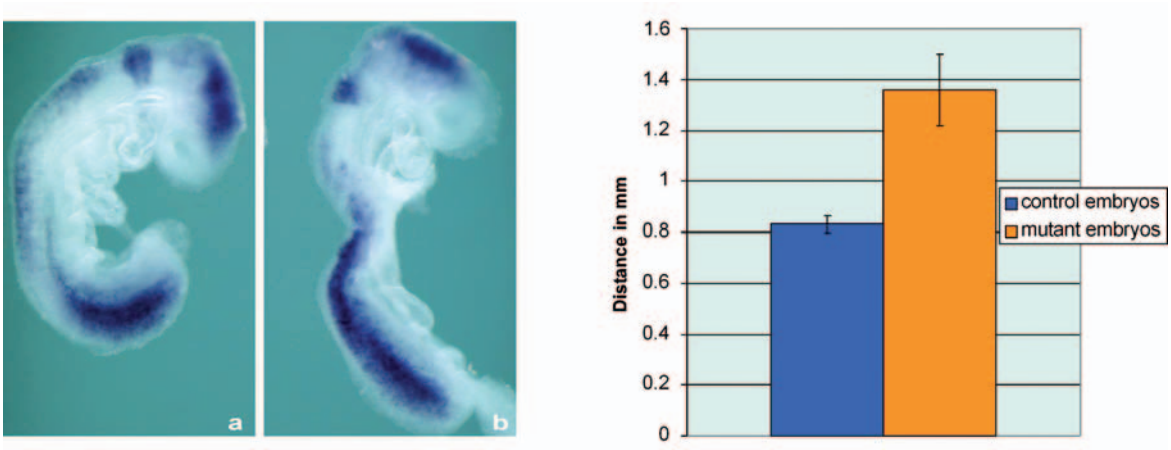

Figure S3 *BAT-Gal* Wnt-signaling reporter mice show increased activity in expanded PSM upon accumulation of β-catenin. *lacZ* mRNA *in situ* hybridization in embryonic day 9.0 control embryo (**a**) and in a *β-catenin*$^{del(ex3)/+}$; *T-Cre*; *BAT-Gal* mutant embryo (**b**). *Mesp2* expression domain is shifted anteriorly in the PSM of mutant β-catenindel(ex3)/+; T-Cre embryos. The distance from tail end to *Mesp2* expression domain in the PSM was measured in mm and compared between age-matched (9.0 dpc) control embryos (n=11) and mutant embryos (n=10). Mean distance in controls: 0.83 mm (S.D.=0.03); mean distance in mutants: 1.36 mm (S.D.= 0.14).

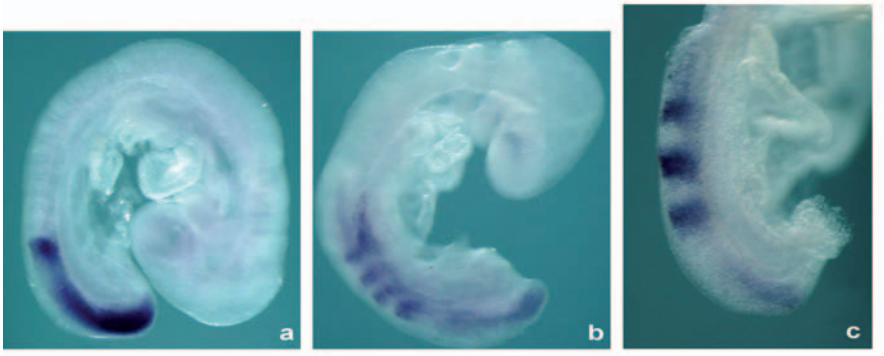

Figure S4 *Hes7* mRNA *in situ* hybridization in control (a) and mutant (b) β-catenin$^{del(ex3)/+}$; *T-Cre* positive embryo. In contrast to control embryos, multiple additional stripes of expression are observed in expanded PSM of mutant embryos. (**c**) *Lfng* mRNA *in situ* hybridization in embryo expressing exclusively the stabilized form of β-catenin in the PSM. Multiple stripes of expression are visible in the expanded PSM of mutant embryos (*β-catenin*$^{del(ex3)/floxdel}$; *T-Cre* positive).

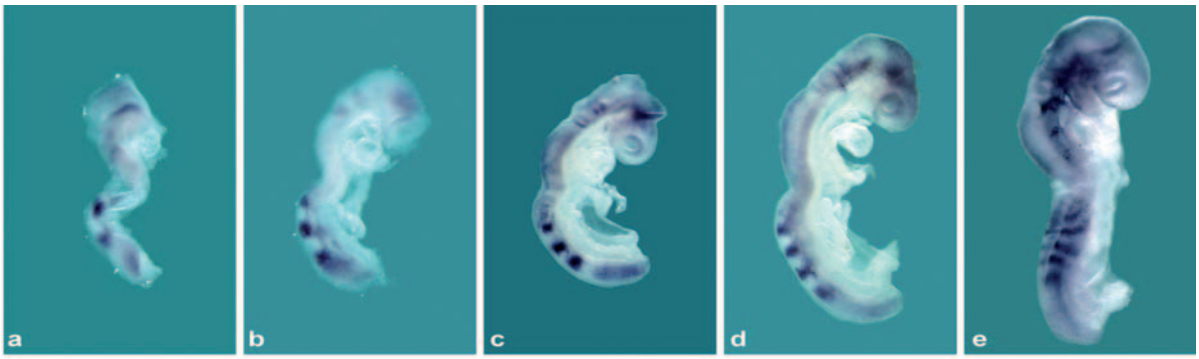

Figure S5 Time course of *lunatic fringe (Lfng)* mRNA expression in mutant *β-catenin*$^{del(ex3)/+}$embryos. Note the progressive increase in *Lfng* expression stripes in mutant embryos from day 8.5 to 9.5 of development. Approximate age of embryos (mutant embryos do not form somites) (**a**) 5-somite stage, (**b**) 8-somite stage, (**c**) 12-somite stage, (**d**)15-somite stage, (**e**) 20-somite stage. There is no further increase of *Lfng* mRNA stripes beyond the 20-somite stage and embryos deteriorate quickly thereafter.

Movie Legends

Movie S1 Real-time imaging of the segmentation clock in control embryo (day 9.0 of development, *β-catenin*$^{+/+}$*-T-Cre-LuVeLu*) (see Methods for details). Side view of merged Z-stacks. Venus-YFP fluorescence is shown in green and overlays the bright-field image. Several successive waves of YFP fluorescence traverse the PSM from posterior to anterior. Note formation of somites and posterior displacement of oscillatory field during recordings.

Movie S2 Real-time imaging of the segmentation clock in mutant embryo (day 9.0 of development, *β-catenin* $^{del(ex3)/+}$*-T-Cre-LuVeLu*). Side view of merged Z-stacks. Venus-YFP fluorescence is shown in green and overlays the bright-field image. Several waves of YFP fluorescence traverse the PSM from posterior to anterior. In contrast to control embryos, these waves show extended traveling within the expanded PSM and thus, occur partially simultaneously. No posterior displacement of the oscillatory field is observed. Note that the segmented structures visible in the center of the embryo correspond to the kinked neural tube. Note the absence of somite formation during time-lapse recording. Intensities have been scaled to allow better visualization (see graphical representation for absolute intensity values of raw data, Fig. 5 c-f).

METHODS

In situ hybridization

The probes and markers used are described in the literature: *Msgn1*[1], *Tbx6*[2], *Pea3*[3], *Fgf8*[4], *Dll1*[5], *Paraxis*[6], *Raldh2*[7], *Uncx4.1*[8], *Lfng*[9], *Dkk1*[10], *Mesp2*[11], *Cer1*[12] and *EphA4*[13]. Riken clone 2700078F24 was used to generate Dusp4 probe.

Mice breeding and genotyping

The following mice used in this study were described previously and were genotpyed according to these references: *β-catenin* $^{lox(ex3)}$ [14], *β-catenin* ^{floxed}[15], *T-Cre*[16], *BAT-Gal*[17], *Fgfr1* $^{f/f}$ [18]. Yolk sacs were lysed in a buffer containing 10 mM Tris HCl (pH 8.3), 50 mM KCl, 2 mM MgCl2, 0.1 mg/ml Gelatin, 0.45% NP-40, 0.45% Tween 20, 0.1mg/ml Proteinase K at 55°C for 2-12 h. Proteinase K was heat inactivated at 95°C for 10 min before PCR. For genotyping *LuVeLu* mice, the following primers were used: Ala1-tgctgctgcccgacaaccact and Ala3-tgaagaacacgactgcccagc. The PCR was performed with the following parameters: 94°C for 2 min, 92°C for 45 sec, 59°C for 40 sec, 72 °C for 40 sec (x 35 cycles) and 72°C for 5 min, which generated a single product of 460 bp size in transgenic animals.

Fluorescence quantification

To define a centreline through the PSM of the embryo, we first masked the whole embryo using the bright field image. Subtracting an eroded version of this mask (kernel size 50 pixels for mutant and 80 pixels for control due to the difference in size of the mutant and control embryo, respectively) resulted in an outline of the embryo. This outline was split into subregions at the edges of the image. To define the outline of somites and the PSM, we defined a second mask applied to the fluorescence signal based on a histogram-based threshold. The subregion overlapping this fluorescence-based mask outlined somites and the PSM. Using this outline, a pruned and smoothed (boxcar with kernel size of 20 pixels) skeleton was generated[19], which corresponded to the centreline through the PSM.

Generation of transgenic *Lfng* reporter mice (*LuVeLu*)

The modified PEST domain used to generate destabilized Venus fusion protein was described previously.[20]

References

1. Yoon, J.K., Moon, R.T. & Wold, B. The bHLH class protein pMesogenin1 can specify paraxial mesoderm phenotypes. *Dev Biol* **222**, 376-391 (2000).
2. Chapman, D.L., Agulnik, I., Hancock, S., Silver, L.M. & Papaioannou, V.E. Tbx6, a mouse T-Box gene implicated in paraxial mesoderm formation at gastrulation. *Dev Biol* **180**, 534-542 (1996).
3. Chotteau-Lelievre, A., Desbiens, X., Pelczar, H., Defossez, P.A. & de Launoit, Y. Differential expression patterns of the PEA3 group transcription factors through murine embryonic development. *Oncogene* **15**, 937-952 (1997).

4. Crossley, P.H. & Martin, G.R. The mouse Fgf8 gene encodes a family of polypeptides and is expressed in regions that direct outgrowth and patterning in the developing embryo. *Development* **121**, 439-451 (1995).
5. Hrabe de Angelis, M., McIntyre, J. & Gossler, A. Maintenance of somite borders in mice requires the Delta homologue DII1. *Nature* **386**, 717-721 (1997).
6. Burgess, R., Rawls, A., Brown, D., Bradley, A. & Olson, E.N. Requirement of the paraxis gene for somite formation and musculoskeletal patterning. *Nature* **384**, 570-573 (1996).
7. Niederreither, K., McCaffery, P., Drager, U.C., Chambon, P. & Dolle, P. Restricted expression and retinoic acid-induced downregulation of the retinaldehyde dehydrogenase type 2 (RALDH-2) gene during mouse development. *Mech Dev* **62**, 67-78 (1997).
8. Mansouri, A. *et al.* Paired-related murine homeobox gene expressed in the developing sclerotome, kidney, and nervous system. *Dev Dyn.* **210**, 53-65 (1997).
9. Aulehla, A. & Johnson, R.L. Dynamic expression of lunatic fringe suggests a link between notch signaling and an autonomous cellular oscillator driving somite segmentation. *Dev Biol* **207**, 49-61 (1999).
10. Dequeant, M.L. *et al.* A complex oscillating network of signaling genes underlies the mouse segmentation clock. *Science* **314**, 1595-1598 (2006).
11. Saga, Y., Hata, N., Koseki, H. & Taketo, M.M. Mesp2: a novel mouse gene expressed in the presegmented mesoderm and essential for segmentation initiation. *Genes Dev* **11**, 1827-1839 (1997).
12. Belo, J.A. *et al.* Cerberus-like is a secreted factor with neutralizing activity expressed in the anterior primitive endoderm of the mouse gastrula. *Mech.Dev* **68**, 45-57 (1997).
13. Maruhashi, M., Van De Putte, T., Huylebroeck, D., Kondoh, H. & Higashi, Y. Involvement of SIP1 in positioning of somite boundaries in the mouse embryo. *Dev Dyn* **234**, 332-338 (2005).
14. Harada, N. *et al.* Intestinal polyposis in mice with a dominant stable mutation of the beta-catenin gene. *Embo J* **18**, 5931-5942 (1999).
15. Brault, V. *et al.* Inactivation of the beta-catenin gene by Wnt1-Cre-mediated deletion results in dramatic brain malformation and failure of craniofacial development. *Development* **128**, 1253-1264 (2001).
16. Perantoni, A.O. *et al.* Inactivation of FGF8 in early mesoderm reveals an essential role in kidney development. *Development* **132**, 3859-3871 (2005).
17. Maretto, S. *et al.* Mapping Wnt/beta-catenin signaling during mouse development and in colorectal tumors. *Proc Natl Acad Sci U S A* **100**, 3299-3304 (2003).
18. Xu, X., Qiao, W., Li, C. & Deng, C.X. Generation of Fgfr1 conditional knockout mice. *Genesis* **32**, 85-86 (2002).
19. Gonzelez, R.C. & Woods, R.E. *Digital Image Processing, 3/E*. (Prentice Hall, 2007).
20. Li, X. *et al.* Generation of destabilized green fluorescent protein as a transcription reporter. *J Biol Chem* **273**, 34970-34975 (1998).

4. Discussion

4.1 Wnt-signaling oscillations indicate a complex signaling network within the segmentation clock

A main finding in this work is the discovery of Wnt-signaling oscillations in the PSM of mouse embryos. This discovery was made possible in the laboratory of Prof. Bernhard Herrmann and his design of an *in situ* hybridization mRNA expression screen. As is characteristic for most screens, it is exactly the unbiased character of a screen that allowed this unexpected result to be discovered. Previously, all data obtained from several species indicated that Notch signaling is the core of the segmentation clock (reviewed in (Pourquie, 2001)). As a result, increased evidence was presented placing Notch signaling in the center of the segmentation clock. Our findings were the first indication that a more complex system of multiple signaling pathways interact in generating the transcriptional oscillations in the PSM. Interestingly, the detailed *in situ* expression analysis clearly indicated that Wnt and Notch oscillations occur out of phase, as might be expected if, indeed, distinct signaling pathways are responsible for the activation of these cyclic genes. Thus, these findings not only revealed oscillations within the Wnt-signaling pathway, but also indicated an alternating activity of Notch and Wnt signaling – while Wnt signaling is active, Notch signaling is silenced and *vice versa*. This prompts the question about the relationship of these pathways and here, our results support the view that intact Wnt signaling is required in order for Notch-signaling oscillations to occur.

Thus, the picture that emerged from this work reveals several interconnected signaling pathways constituting the segmentation clock and, thus, changes the perspective

from viewing Notch signaling as the sole requirement to explain these oscillations. The list of Wnt-signaling-controlled cyclic genes is constantly growing (e.g., *naked cuticle 1 homolog* [*Nkd1*] (Ishikawa et al., 2004), *dickkopf homolog 1* (*Dkk1*) (Dequeant et al., 2006), *dapper homolog 1* (*Dact1*) (Suriben et al., 2006). In addition, both loss- and gain-of-function experiments have confirmed and extended the concept that adequate Wnt signaling is required in order for Notch-signaling oscillations to occur (Nakaya et al., 2005; Satoh et al., 2006; Satoh et al., 2008). Moreover, recent findings show that in addition to Notch and Wnt signaling, a third signaling pathway, namely Fgf signaling, also shows oscillatory activity in the PSM (Dale et al., 2006; Dequeant et al., 2006; Niwa et al., 2007) and the importance of Fgf signaling in allowing segmentation clock activity to occur has been functionally determined (Niwa et al., 2007; Wahl et al., 2007).

An important contribution to our picture of the segmentation clock was the genome-wide analysis of cyclic genes in the PSM of mouse embryos (Dequeant et al., 2006). This microarray analysis identified three prominent clusters of co-expressed cyclic genes related to the Wnt, Notch and Fgf pathways. Each of these clusters contained, depending on the stringency of the criteria, up to hundreds of genes, indicating the scale of the underlying genetic circuits.

Thus, the current challenge is to understand how these multiple pathways interact to generate oscillatory transcriptional activity. A key question is which of the observed oscillatory activities constitute the driving pacemaker, if at all, and this challenge is far from being mastered.

In this respect, it is interesting to note that it has been found that the absence of Notch signaling does not hinder the occurrence of Wnt-signaling oscillations. For

instance, the loss of *hairy and enhancer of split 7 (Hes7*), a target and key mediator of Notch signaling, does not hinder ongoing Wnt-signaling oscillations as judged by the cyclic expression patterns of *Axin2* (Hirata et al., 2004). In addition and in contrast to initial findings, the absence of Notch signaling does not abolish oscillations of presumed Notch target genes. Thus, in the absence of RBP-Jk, the key effector of Notch signaling, *Hes7* is proposed to still oscillate (Niwa et al., 2007). Finally, a very recent report reveals that even the constitutive activation of Notch signaling does not appear to impair segmentation clock activity in mouse embryos (Feller et al., 2008). Thus, while the constant expression of the Notch intracellular domain (Nicd), that mediates Notch-signaling activity, indeed leads to a non-cyclic, constant expression of Notch targets *Lfng* and *Hes7*, the Wnt target *Axin2* still shows dynamic expression.

It appears that Notch signaling is not the pacemaker for the mammalian segmentation clock oscillator, but rather represents a readout of the clock activity. This is similar to the situation in zebrafish embryos, where accumulating findings likewise suggest a different role for Notch signaling outside the core of the segmentation clock (Jiang et al., 2000; Ozbudak and Lewis, 2008) From Notch signaling gain- and loss-of-function experiments, these authors propose that the relevant function of this pathway is to ascertain the synchronization of oscillating PSM cells, but that Notch signaling is not the key element that generates these oscillations in the first place.

Thus, in all species under study, the question about the nature of the real oscillator that drives the periodic transcriptional activity remains a fascinating challenge.

4.2 Wnt signaling is graded as well as oscillatory in the PSM of mouse embryos

In addition to the identification of oscillations of the Wnt-signaling pathway, , its activity was also proposed to be present as a gradient in the PSM. Initial arguments were lacking the direct demonstration of a graded distribution of Wnt-signaling components. This was accomplished in the present work showing that β-catenin, a key mediator of canonical Wnt signaling, is present in a clear posterior-to-anterior gradient in the PSM of mouse embryos. Our functional analysis revealed several important roles for this protein gradient. Most strikingly, the β-catenin gradient defines the maturation status of PSM cells. Thus, elevating β-catenin protein levels maintains cells in a posterior PSM fate and somite formation does not occur. Thus, the level of β-catenin determines cell differentiation and cell behavior in the PSM. Surprisingly however, segmentation clock activity as analyzed by the use of real-time imaging technology established during the course of this work, demonstrates that Notch-signaling oscillations are ongoing. Thus, under conditions of elevated and steady β-catenin levels, oscillations of Notch signaling still occur.

Thus, we conclude that the segmentation clock activity is, to a large extent, independent of β-catenin protein levels, and consequently, clock activity does not appear to originate from a feedback that targets β-catenin. Previously, Wnt-signaling oscillations were proposed to be generated via negative feedback (see section 3.1). This was based on the finding that many of the Wnt-target cyclic genes are themselves components of the Wnt-signaling machinery and do, in fact, negatively regulate signaling activity. While acting on different levels upstream of β-catenin, the cyclic genes *Axin2*, *Dkk1*, *Dact1* are all inhibitors of Wnt signaling. Ultimately, their activation should lead to a destabilization

of β-catenin. Thus, if these inhibitors are produced periodically, then it follows that β-catenin protein levels are expected to change periodically. We did not detect evidence of oscillating β-catenin protein levels and importantly, a functional significance of oscillating β-catenin protein levels in regard to segmentation clock activity are not supported by our data. Despite stable β-catenin protein levels, segmentation clock oscillations still occur.

In addition, our findings suggest that Wnt-signaling output is not solely determined by the amount of β-catenin protein. The expression of the Wnt target *Dkk1* in mutants expressing stabilized β-catenin shows variable expression patterns between different embryos. Even within individual mutant embryos, *Dkk1* is expressed in stripes within the PSM. Thus, while all PSM cells contain high and steady levels of β-catenin, these cells do not all express the Wnt target *Dkk1*. Again, this suggests that Wnt-signaling output, as judged by the expression of its downstream targets, is not determined solely by the amount of β-catenin in the nucleus. Importantly, similar results of striped mRNA expression were found with other Wnt targets, such as *Mesogenin* and *delta-like 1 (Dll1)*, supporting the conclusion that Wnt-signaling downstream targets are not expressed uniformly but retain a dynamic expression even when β-catenin has accumulated in the PSM. The analysis of *Axin2*, the bona fide Wnt-target cyclic gene, is more complicated and inconclusive because of its very high basal expression level in the mutant embryo. One possibility is that these presumed Wnt-signaling targets are in fact not exclusive Wnt-signaling targets, but that their regulation receives a dynamic input from other signaling pathways. Alternatively, and not in contradiction to the previous possibility, our results could indicate that additional levels of Wnt signaling pathway regulation exists

downstream of β-catenin and thus, the level of nuclear β-catenin is not the only determinant of pathway activity. This is in contrast to the simplified textbook view of canonical Wnt signaling, which reads as follows: "Stabilized free β-catenin enters the nucleus where it forms a complex with the transcription factor TCF and activates expression of target genes…" ((Wolpert et al., 2003), page 75). In this view, the signaling activity is determined solely by the amount of free β-catenin. Our data indicate that the situation in the embryo is more complex. It appears that although cells contain a high amount of free, even nuclear β-catenin, the resulting activation of target genes can still be regulated and modulated downstream of β-catenin.

To summarize, we propose that PSM maturation is determined and instructed via the β-catenin gradient and, thus, protein levels. In contrast, the dynamic output of Wnt signaling appears to be regulated and modulated downstream of β-catenin. This regulation could be achieved by the dynamic recruitment of nuclear co-factors as a prerequisite to activate cyclic target genes. Such a possibility is suggested by *in vitro* experiments, in which the recruitment of β-catenin to the enhancer region of target genes was shown to depend on co-factors such as *adenomatous polyposis coli (APC)* (Sierra et al., 2006; Wang and Jones, 2006; Willert and Jones, 2006). Finally, our results suggest that the core segmentation clock does not rely on a negative feedback mechanism that targets β-catenin. The identification of the precise regulation mechanism allowing Wnt signaling to be gated dynamically constitutes a major current challenge and will allow evaluation of the relation of Wnt-signaling oscillations to the core segmentation clock mechanism.

4.3 The importance of experimental design

Interestingly, previous Wnt-signaling gain-of-function experiments resulted in a very different phenotypic outcome – both morphologically as well as molecularly – in respect to segmentation clock activity. For instance, when Wnt-signaling inhibitors secreted frizzled-related protein 1 (SFRP1), 2 and 5 were disrupted in compound mutants, presumably leading to a hyperactivation of Wnt signaling, the resulting mutant embryos did exhibit truncated and shortened PSMs (Satoh et al., 2006; Satoh et al., 2008). In addition, these SFRP-compound mutant embryos were reported as not showing indications of segmentation clock activity. This is in direct contrast to our study in which activation of Wnt signaling leads to a pronounced expansion of the PSM with persisting segmentation clock activity.

How can this apparent paradox be explained? One possibility is that it is essential how and at which level Wnt signaling is experimentally activated. This could reflect the physiological role of the described feedback component of Wnt signaling – that the activation of signaling activity leads to the production of its own inhibitors, creating a level of autoregulation. In our study, we introduced a stabilized form of β-catenin, one that is resistant to this autoregulation via feedback inhibition. The studies mentioned above activated the pathway by deleting extracellular Wnt-ligand inhibitors and in that experimental set up, the autoregulation via negative feedback remained presumably intact. Thus, although this has not been directly tested, these different routes of Wnt-signaling activation in gain-of-function experiments could explain the very different outcome – both in terms of phenotype, as well as in respect to the effect on the segmentation clock. If this assumption is true, it could be concluded that only by

disruption of the autoregulation via negative feedback is it possible to dramatically change PSM maturation and to extend the posterior PSM fate into the anterior PSM. In this scenario, activating Wnt signaling at the ligand level will be compensated by the overexpression of inhibitors, possibly affecting the phenotypic outcome. Nevertheless, it is astonishing that the introduction of a stabilized form of β-catenin in our experiments is somewhat less disruptive than the deletion of several peripheral inhibitors, and the reason for this is still unclear. In any case, it implies that it is not the activation of Wnt-signaling activity *per se* that disrupts segmentation clock activity as concluded from previous experiments (Satoh et al., 2006; Satoh et al., 2008). Another possibility is that SFRP1, 2 and 5 play additional roles within the Wnt-signaling transduction machinery, which could explain why their disruption causes a distinct phenotype. In this regard, it is interesting to note that a role for SFRP proteins downstream of β-catenin in regulating Wnt-signaling activity has been proposed based on *in vitro* studies (Suzuki et al., 2004). Finally, one should also note that while our experiments were designed by conditionally targeting the mesoderm during late-stage gastrulation, the deletion of SFRP1, 2 and 5 was done constitutively, which could affect the outcome, particularly in respect to the axial truncation phenotype.

4.4. About gradients without positional information

The question of directionality of somite formation is directly related to the mechanism of how cells in the PSM are endowed with positional information. In this context, we consider positional information to provide the coordinates that place a PSM cell in relation to its surrounding neighbors, and for the sake of this discussion, we ignore

the information required to instruct a cell about its axial position in relation to total body length (e.g., cervical versus thoracic). Put in other words: how does a cell sense that it is anterior of its posterior neighbor in the PSM? Maybe the more appropriate initial question should actually be: does a cell sense its relative position in the PSM at all? Multiple experimental evidence exists which indicates that cells possess this positional information. For instance, if a small piece of PSM is inverted cranio-caudally, the resulting somites will form in a posterior-to-anterior manner, thus, matching their original orientation. Accordingly, not only are these cells positioned relative to each other, but in addition, this information is determined as soon as cells enter the PSM (Christ et al., 1974). A second example is cell behavior in the anterior PSM, where a defined group of cells changes the developmental program synchronously. This is best exemplified at the onset of the transcription factor Mesp2, which becomes activated segmentally in the anterior PSM. Thus, these cells are all committed to being incorporated into one somite; whereas, more posterior cells are excluded from this developmental change at this time point. In order to define this unit of cells that undergoes synchronously a developmental switch and to exclude cells that are located more posteriorly, cells in the PSM must be informed about their relative position to each other.

Finally, the detailed observation of mRNA expression patterns of cyclic genes indicates that the wave of transcriptional activity slows down during its kinematic passage through the PSM. Two arguments can be used here. First, in all vertebrate species in which cyclic genes have been identified, it has been observed that the width of the traveling wave is changing, e.g., decreasing during the passage through the PSM. Thus, while the dimension of the wave is rather wide in the posterior PSM, it narrows to

a somite-wide domain in the anterior PSM. This refinement could reflect that the speed of activation (Va) does not equal the speed of inactivation (Vi) of the transcription of the cyclic gene, e.g., the wavefront of activation sweeps the PSM at a slower speed than the wavefront of inactivation (wavefront is used here to describe the anterior and posterior borders of the wave). This reflects a change in the ratio between "on" and "off" phases of expression activity along the PSM. Importantly, evidence exists that in addition, Va and Vi decrease along the PSM. This has been indicated by carefully plotting the expression patterns of a large cohort of embryos (Maroto et al., 2005; Niwa et al., 2007). More direct evidence for the slowing down of the kineamtic wavefront can be derived in situations in which several consecutive waves of transcriptional activity can be observed simultaneously, as is the case in zebrafish or snake embryos (Giudicelli et al., 2007; Gomez et al., 2008). Here, the decrease in distance between consecutive waves as a function of PSM position indicates that the kineamtic wave slows down during its passage through the PSM (Giudicelli et al., 2007; Gomez et al., 2008).

Importantly, the real-time imaging of segmentation clock activity allows us now to measure directly the speed of the kinematic wave and clearly shows that indeed the wave of transcriptional activity slows down during its passage through the PSM (Figures 7, 8, 9). The slowing down of the wave is caused by the gradual increase of the oscillation period of PSM cells. It follows that these values provide a means to define a relative PSM position. For example, in order to determine which of two randomly picked PSM cells is located more anteriorly, one could make use of their oscillation period value − the longer the period, the more anterior a cell is positioned in the PSM.

All of these observations (e.g., the intrinsic directionality of somite formation, the definition of a segment forming unit and the increase of the oscillation period along the PSM) indicate that the PSM is not a homogenous mass of cells, but rather, that cells have unique properties corresponding to their relative PSM position and thus, they posses intrinsic positional information. The question remains, what mechanism is responsible in setting up this information in the first place?

The common view is that this information is provided via the graded activity of several signaling pathways (section 3.1; Dubrulle et al., 2001; Dubrulle and Pourquie, 2004; Sawada et al., 2001; Diez del Corral et al., 2003; Delfini et al., 2005; Maruhashi et al., 2005). The graded values, e.g., the slopes, of these multiple gradients are excellent candidates to encode positional information in the PSM.

Thus, while a demonstration that the graded values of Wnt, Fgf and retinoic acid (RA) control the slowing down of the kinematic wavefront is missing, good evidence does exist that these gradients control the coordinated change in developmental potential in the anterior PSM and the definition of a segmental unit (section 3.1; Dubrulle et al., 2001; Dubrulle and Pourquie, 2004; Sawada et al., 2001; Diez del Corral et al., 2003; Delfini et al., 2005; Maruhashi et al., 2005).

These results support the existence of a gradient value threshold in the anterior PSM, called the wavefront in analogy to the "Clock and Wavefront" model by Cooke and Zeeman (Cooke and Zeeman, 1976), at which cells become competent to respond to the clock signal. The segmental unit is then determined by the domain that the wavefront traverses during its regression during one clock cycle (Dubrulle et al., 2001). Thus, both the positioning of the wavefront and the clock period are crucial determinants for

segment size. In turn, the precise positioning of a wavefront could result via the antagonistic interaction of Fgf and RA signaling and the creation of a window of coexistence of two stable states in respect to RA and FGF signaling (Goldbeter et al., 2007). This model of Bistability can explain how sharp thresholds can emerge from the graded distribution of multiple, antagonistic signaling pathways (Goldbeter et al., 2007). Thus, the current view is that the graded distribution of multiple signaling pathways is critical in defining a cell's PSM position.

However, our genetic experiments testing the significance of the Wnt/β-catenin signaling gradient in mouse embryos, surprisingly, suggest otherwise – namely that the slope *per se,* at least of the Wnt/β-catenin signaling gradient, is not the essential element encoding positional information in the PSM.

The arguments are based on the findings that several signs for positional information, namely the striped expression of *Mesp2,* the spatial refinement and the slowing down of of the kinematic wave of *Lfng*, are still present in β-catenin$^{\Delta ex3}$ mutant embryos in which the Wnt/β-catenin-signaling gradient appears to be abolished.

4.4.1 *Mesp2* is segmentally expressed in the absence of the Wnt-signaling gradient

The genetic stabilization of β-catenin protein abolishes the Wnt/β-catenin-signaling gradient, while Wnt-signaling activity is elevated.in the PSM. However, a well-defined stripe of *Mesp2* becomes activated, although its position is shifted to the anterior part of the expanded PSM. This appears contradictory given the results that the expanded PSM expresses all posterior PSM markers and the view, that *Mesp2* expression indicates the successful developmental switch from the posterior-to-anterior PSM. In addition, the

mosaic overexpression of Fgf8 in chick embryos through electroporation abolished MESP2 expression entirely (Delfini et al., 2005). While we can only speculate about the reason for our result, it contains very valuable information. The presence of a well-defined stripe of expression could indicate that despite the absence of a Wnt/β-catenin gradient, and thus slope, cells are still defined as a unit of about the same size as in wild-type embryos, indicative of the presence of positional information. Otherwise, it is inconceivable how the anterior and posterior borders of this group of cells could be defined so precisely and symmetrically on both sides of the neural tube. Thus, it appears that the graded aspect of Wnt signaling is not required to define the somite-forming unit.

At this point, one should be reminded that one possible reason why somites do not form, despite the fact that this unit is defined, was found to be the inability to activate downstream targets of *Mesp2*. Thus, while *Mesp2* is present, its downstream targets, such as *cerberus 1* homolog (*Cer1*) and Eph receptor A4 (*EphA4*), which mark the anterior half of the somite, are not expressed in β-catenin$^{\Delta ex3}$ mutant embryos. Likewise, *Uncx4.1*, a marker for the posterior compartment, is strongly downregulated in β-catenin$^{\Delta ex3}$ mutant embryos. Together, this suggests that the striped activation of *Mesp2* represents an intermediate state of differentiation, but that additional steps are required to fully activate the segment-forming machinery. Persistent high levels of β-catenin$^{\Delta ex3}$ inhibit these steps.

4.4.2 Oscillations still slow down along the PSM in the absence of the Wnt-signaling gradient

One of the most astonishing results presented here is the fact that segmentation clock oscillations not only occur in mutant embryos which express a stabilized form of β-catenin, but also, these oscillations still change their characteristics in relation to the relative PSM position. Thus, the multiple, traveling waves of *Lfng* present in β-catenin$^{\Delta ex3}$ mutants show both a spatial refinement and a decreasing wave-to-wave distance along the expanded PSM. Strikingly, this suggests that oscillations still slow down in these mutant embryos. Previously, it was thought that one possible source of information controlling this change in traveling speed of the kinematic wave could be found in the gradient, the slope, of Wnt and/or Fgf signaling. However, since the Wnt-signaling pathways appear to be no longer graded in the PSM of β-catenin$^{\Delta ex3}$ mutants, the slope of the β-catenin gradient *per se* is unlikely to control this change in oscillatory behavior.

It is important to consider that although the Wnt/β-catenin gradient is abolished, the graded activities of other signaling pathways, first of all Fgf8 signaling, could still persist in β-catenin$^{\Delta ex3}$ mutant embryos and hereby provide positional information. While this possibility can not be excluded here, several pieces of evidence argue against this. First, while Fgf8 mRNA appears upregulated in the extended PSM of β-catenin$^{\Delta ex3}$ and even appears graded in some β-catenin$^{\Delta ex3}$ embryos, the analysis of Fgf downstream targets *Pea3* and *Dusp4* does not indicate a graded signaling activity as is the case in wild-type embryos. Second and importantly, the phenotype is not entirely dependent on the presence of Fgf signaling *per se*, since a striped expression pattern of *Mesp2* and

multiple stripes of *Lfng* expression are found in embryos harboring a stabilized form of β-catenin in combination with a deletion of the Fgf-receptor1 (Wahl et al., 2007), in which Fgf signaling is impaired in the PSM (see Figure 4 in section 3.3). Finally, the interpretation that neither the slope of Wnt nor Fgf signaling carries the critical information for positional information is supported by preliminary findings not shown in this work. In these experiments, the conditional stabilization of β-catenin is achieved using a different Cre-driver mouse line in which Cre is active only in the anterior half of the PSM (Msd-Cre). While β-catenin protein levels decrease from the posterior to the middle of the PSM (as in wild-type embryos, since Cre is inactive in the posterior PSM), the protein levels increase from the middle to the anterior PSM. Importantly, the same applies to FGF signaling, since both Fgf8 as well as Fgf-signaling targets show a (re)activation in the middle and anterior PSM. Thus, a V-shaped Wnt/β-catenin gradient (and Fgf-signaling gradient) results. Such a gradient does not have the potential to carry positional information, since multiple (e.g., two) positions in the PSM show the same gradient value. With the exception that these embryos do not show an axial truncation phenotype (since the posterior part of the embryo is wild type) these mutants phenocopy the β-catenin$^{\Delta ex3}$ mutants described in section 3.3. Strikingly, although Wnt/β-catenin and Fgf signaling are increasing in the anterior PSM, all mentioned signs for positional information are present in these mutant embryos. This includes the striped *Mesp*2 expression, the refinement of (multiple) *Lfng* waves and the slowing down of oscillations as indicated by a decrease of wave-to-wave distance in the expanded anterior PSM.. This argues against the possibility that positional information is encoded by the slope *per se* of

either the Wnt or the Fgf gradient. It also prompts a search for different explanations for the change of oscillatory behavior along the PSM.

One possibility, therefore, is that the change in oscillatory behavior, e.g., the increase in oscillation period, is a direct function of the oscillations themselves. In other words: the gradient has the function of creating a permissive environment for oscillations to occur; however, once they occur, the oscillations themselves have an impact on subsequent oscillations causing, somewhat intrinsically, a change in oscillation behavior and an increase in oscillation period along the axis. In essence, this corresponds to an oscillation-counting mechanism. With each oscillation that a PSM cell has undergone, its oscillation behavior will change accordingly.

What then could be the function of the Wnt/β-catenin gradient? The slope of the gradient might function to ascertain whether a certain threshold is reached at a rather precise point in the anterior PSM. While in this view the slope itself has no instructive function, the slope influences the position at which the threshold is reached. Thus, while permissive in respect to the oscillations, the gradient is instructive in respect to PSM maturation. Importantly, however, this instruction is a bimodal one; thus, either the cells are above or below the threshold. Again, it follows that the information is not encoded via the slope of the β-catenin gradient.

4.5 An iconoclastic proposal: the clock is not the clock

Our current model predicts that the periodicity of somite formation is encoded by the network of oscillating cyclic gene activity. Here, I argue, based on our presented experimental data, that the observed oscillating gene activities do not control periodicity as commonly thought.

It is generally believed that the oscillatory mRNA expression of cyclic genes in the PSM reflects the activity of the segmentation clock, which in turn, provides the information for gating somite formation into a periodic event. One has to note, however, that there is no functional evidence that the observed oscillations of mRNA expression do indeed provide the temporal information for sequential somite formation. This interpretation is entirely based on the observation that the cycle period of mRNA expression patterns and the time required to form a somite are very similar. Consequently, cyclic genes were attributed a function in a hypothetical segmentation clock.

However, a key argument against this view exists − how can a cyclic gene network encode the temporal control of somite formation if one considers that the *de facto* oscillation period of cyclic genes constantly changes within the PSM and ultimately does not match the segmentation period?

As outlined in this work, the measured oscillation period in the anterior PSM is in the order of 170 minutes, while somites form at a different rate, namely every 135 minutes. The oscillation period is a single-cell perspective and describes the frequency at which mRNA transcription is activated in one cell. Thus, if cells in the anterior PSM possess a cyclic gene network whose period is considerably longer than the somite

formation period, how can these two phenomena be functionally, and more precisely, temporally linked? A similar discrepancy between the oscillation period and the segmentation period was proposed to occur in zebrafish embryos. In an elegant approach, spatial information in the form of mRNA expression patterns was used to model the oscillation period along the PSM (Giudicelli et al., 2007). The predictions were that the oscillation period clearly increases toward the anterior PSM. This must have as a consequence that the oscillation period does not match somite formation frequency.

The important, but admittedly, confusing distinction is the one made between the oscillation period and the cycle period. This is a distinction currently missing in the literature. While the former describes the period of a real biological process in a cell, the latter describes the repetition of mRNA expression patterns. Crucially, these expression patterns are generated by a constantly changing cell population. Therefore, the process in a single PSM cell is decoupled from the observation of repeated expression patterns and consequently, the oscillation period does not equal the cycle period.

In this work, we provide experimental data that underscore this notion. As illustrated in Figure 8, the oscillation period in a fixed group of cells progressively increases and, therefore, the oscillation period does not match the somite formation period in most of the PSM. In turn, this change in the oscillation period is caused by a gradual decrease of the wave traveling speed along the PSM, which is finally a result of the change in phase delay between cells while in the PSM.

If the frequency of mRNA oscillations does not match the frequency of somite formation, do we still have the segmentation clock in hand? All previous models are based on the assumption that the oscillator works at the same pace as the biological

phenomenon that it is supposed to underlie. If this logic is followed, it could be concluded that the striking mRNA oscillations are not the underlying segmentation clock, at least not in the form previously envisioned, namely, that the oscillation frequency sets the pace of somite formation. What then controls the periodicity of somite formation and what function do the striking oscillations in the PSM serve? In an attempt to provide an alternative explanation to this question, a novel model that assigns a different role to the observed oscillations, termed the Appendix model, is proposed.

4.6 The Appendix model

As pointed out previously, it appears that the progressive change in oscillatory behavior in PSM cells could be a direct consequence of the oscillations themselves, since no graded distribution of Wnt or Fgf signaling appears necessary to instruct this change. Thus, if the oscillations themselves serve a function in influencing their oscillatory behavior, then this would equal a counting mechanism for measuring time. With each oscillation, the time required to reactivate the transcription of a given cyclic gene increases, resulting in an increased phase delay between cells and an increased oscillation period. In this sense, the oscillation characteristics are defining the relative PSM position and as these oscillation characteristics are themselves a direct consequence of previous oscillations, the oscillations are part of the mechanism that provides positional information to PSM cells. Such a mechanism cannot, however, be regarded as simply counting to a pre-set number of oscillations. This is because, as our results indicate, cells can continue to oscillate well beyond their scheduled time if exposed to elevated levels of β-catenin, indicating that the total number of oscillations is not fixed. Thus, we propose

that an oscillation-counting mechanism exists that cooperates with the permissive gradient system in the following way – once the counting mechanism reaches a value that in relation to the gradient value exceeds a threshold, this gradient value is no longer permissive and a developmental switch is activated. At this time, oscillations will halt and the segmentation program then will be initiated. In this view, developmental change in the anterior PSM is determined both by an oscillation-dependent counting mechanism and by the permissive gradient of Wnt signaling. In other words, there is no absolute gradient value threshold and there is no absolute oscillation number that determines the axial position at which developmental change occurs. Rather, a relative threshold exists, one that is determined by the gradient value in relation to the number of undergone oscillations. In this model, positional information in the PSM is provided by the oscillation-counting mechanism, not by the slope of the Wnt/β-catenin-gradient, but developmental change only occurs once the gradient value is integrated.

The nature of the proposed counting mechanism is unknown. Logically, it could be proposed that with each oscillation cycle, some factors are accumulating and these factors are responsible for the change in oscillatory behavior. Thus, the oscillation-counting mechanism itself would generate a graded distribution of factors in the PSM, with the peak concentration toward the anterior PSM, and essentially, it is this gradient that provides positional information.

Such a model can also explain the findings that even when β-catenin accumulates and the Wnt-signaling gradient is elevated, at some point in the anterior, extended PSM, a developmental switch still occurs and *Mesp2* is activated. This could be explained by

proposing that relative to the elevated permissive Wnt-gradient value (which is no longer graded), the adequate number of oscillations now has occurred.

Since it is the relation between undergone oscillations and the permissive gradient value that determines when a developmental change occurs, it follows that the number of oscillations that will occur before a cell will form a somite is not a constant number, neither within one species nor between different species. By changing the value of the permissive gradient or by modifying the oscillation-counting mechanism, the total number of oscillations can be modified.

Thus far, the model explains how positional information is provided via an oscillation-counting mechanism and therefore, it could explain the directionality of somitogenesis. However, how does periodicity of somite formation emerge in this model? Here, we refer to the ingenious model presented in the appendix of the clock and wavefront model (Cooke and Zeeman, 1976). The model that is described in the appendix A (Cooke and Zeeman, 1976) is remarkable, since here periodicity emerges without invoking the presence of an oscillator. In contrast, periodicity emerges by the interaction of two gradients. It is shown that a periodic switch-like process can emerge if one assumes that one gradient is cell-autonomous; whereas, the second gradient is non-cell-autonomous once cells become coupled. Without going into detail of how cells become coupled (since here our model differs and, therefore, this would only complicate further this discussion), our model is directly based on this assumption that periodicity can be generated by the interaction of two gradients. To reflect the origin of our model, we call our model the Appendix model.

The first gradient is constituted by the known Wnt and Fgf gradients, and at least for the Wnt gradient, we have good evidence that this gradient functions cell-autonomously (these data will be presented elsewhere). We will refer to this gradient as gradient A (autonomous). The second gradient is generated via the oscillation-counting mechanism as outlined previously (Gradient O; oscillation counting). While the nature of this gradient O is unknown, we assume that this gradient can be of non-cell-autonomous character once cells become coupled or grouped. It appears that this assumption is not totally unjustified, since gradient O is a direct consequence of the mRNA oscillations, which in turn, have been shown to critically depend on cell-to-cell communication (Horikawa et al., 2006) and are proposed to be synchronized via the Notch-signaling pathway (Jiang et al., 2000; Ozbudak and Lewis, 2008). We further assume, that the value of gradient O is shared between cells that are coupled. The coupling, on the other hand, is determined by the oscillation phase. Thus, if cells are in the same oscillation phase, they are proposed to be coupled, and the gradient value locally equilibrates in this group of cells (This is a direct analogy to the model presented by Cooke and Zeeman, with our modification that the origin of the coupling is the phase characteristic of the cells). While in the posterior PSM the wave has spatially a large dimension and travels fast, this wave is spatially refined considerably once it reaches the anterior PSM. It follows that the cohort of phase-grouped cells narrows toward the anterior PSM.

As cells in the anterior PSM are recruited into the kinematic wave, the shared value of this phase-grouped cell population that constitutes the wave is constantly increasing. This is because cells at the anterior PSM have the highest gradient O value,

and their inclusion into the phase-group cohort raises the joint value of this cell population.

Thus, during its passage through the PSM, the kinematic wave is progressively refined spatially and within this phase-grouped cell population, the joint gradient O value increases the more anteriorly the wave is located. It follows, that at some time point and at some location, the shared gradient O value of this group of coupled cells will pass a threshold. This threshold, as discussed previously, is not an absolute one but has to be considered in relation to the cell-autonomous, permissive gradient. Once this relative threshold (for instance, A-O) is reached, this phase-grouped cohort of cells undergoes synchronously a developmental switch. Noteworthy in this model, the slope of the permissive, cell-autonomous gradient A is not essential and can actually be even absent (e.g., flat). Still, A-O will reach a threshold because of the steadily increasing shared gradient O value. This is in agreement with our experimental findings in β-catenin$^{\Delta ex3}$ mutant embryos.

In this model, a periodic switch is initiated once a relative threshold (A-O) is reached. Consequently, both variables, A and O, can influence the periodic outcome. Thus, in a way, the oscillations still contribute to periodicity since oscillations underlie the oscillation-counting mechanism which generates gradient O. This is very different from the way that periodicity is explained in current models, in which periodicity is a direct reflection of the oscillation period. Rather, in the Appendix model, periodicity emerges from the interaction between a cell-autonomous, permissive gradient with the shared, non-cell-autonomous gradient value of phase-grouped cells. Since these phase-grouped cells constitute the mRNA expression patterns that we observe in the PSM,

periodicity is now reflecting the cycle period. The cycle period does match somite formation period, just as the mRNA expression patterns always occur in synchrony with somite formation. Thus, the appendix model releases the contradiction that the somite formation period and the oscillation period do not match. It connects periodicity and mRNA oscillations only indirectly, via the oscillation counting mechanism and the grouping of cells according to their phase similarity.

A key feature of our Appendix model is that the oscillation behavior itself (the phase grouping and the phase delay between PSM cells) is considered a crucial and instructive property. Thus, this model takes into account that the observed oscillations of mRNA expression are not just a simple oscillator shared by all PSM cells (as proposed, for instance, by the 'clock and wavefront" model and the Meinhardt model). The peculiar oscillation behavior encountered in the PSM involves highly synchronized oscillations, which are, however, phase delayed between cells and constantly changing in respect to the oscillation period. Our Appendix model incorporates these observations and findings, and actually ascribes them a central, instructive function.

To summarize, our Appendix model changes the orthodox assignment of spatial and temporal information: while the temporal information is encoded by two interacting gradient systems (of which one is a direct consequence of the oscillation phenomenon), the spatial information that defines the segment-forming unit is encoded by the oscillation characteristics in the form of a phase grouping of cells in the anterior PSM.

This model contains several new assumptions, notably the existence of an oscillation-counting mechanism that generates gradient O, the coupling between phase-

grouped cells and the existence of a relative threshold A-O. These assumptions are intended as conceptual framework that must be challenged by future discoveries.

4.7 Outlook

The discussion indicates the challenges that we are facing. Perhaps most urgently, we need to discover the origin of oscillations and define the roles that the oscillating gene transcription network plays. To this end, it will be essential to find experimental conditions that can alter the oscillatory behavior (e.g., accelerating or slowing down the oscillations). Central to this goal is the development of refined and more sophisticated reporter systems that include the visualization of oscillating Wnt-signaling activity in living mouse embryos in real time. This is because we aim to have a reporter system that is as close as possible to the underlying pacing mechanism and not only a peripheral readout.

Another challenge refers to the identification of the proposed oscillation-counting mechanism. Here, candidate proteins are currently analyzed for their abundance in the PSM in order to uncover a relationship between abundance and oscillation number. In addition, to learn more about the oscillatory behavior of PSM cells, we strive to achieve a single-cell resolution of mRNA oscillations using the real-time imaging technology. In combination with transplantation studies, this will allow us to determine in more detail the oscillatory characteristics of PSM cells.

Finally, it appears essential to approach the question of how somitogenesis is coordinated with other embryological processes, since any temporal control of somite formation only makes sense if this control is of a global nature and capable of integrating the rate of overall development.

5. References

Aulehla, A., and Johnson, R.L. (1999). Dynamic expression of lunatic fringe suggests a link between notch signaling and an autonomous cellular oscillator driving somite segmentation. Dev Biol *207*, 49-61.

Bessho, Y., Hirata, H., Masamizu, Y., and Kageyama, R. (2003). Periodic repression by the bHLH factor Hes7 is an essential mechanism for the somite segmentation clock. Genes Dev *17*, 1451-1456.

Bessho, Y., Sakata, R., Komatsu, S., Shiota, K., Yamada, S., and Kageyama, R. (2001). Dynamic expression and essential functions of Hes7 in somite segmentation. Genes Dev *15*, 2642-2647.

Borycki, A., Brown, A.M., and Emerson, C.P. (2000). Shh and Wnt signaling pathways converge to control Gli gene activation in avian somites. Development *127*, 2075-2087.

Borycki, A.G., Mendham, L., and Emerson, C. (1998). Control of somite patterning by Sonic hedgehog and its downstream signal response genes. Development *125*, 777-790.

Brand-Saberi, B., Ebensperger, C., Wilting, J., Balling, R., and Christ, B. (1993). The ventralizing effect of the notochord on somite differentiation in chick embryos. AnatEmbryol(Berl) *188*, 239-245.

Bronner-Fraser, M. (1986). Analysis of the early stages of trunk neural crest migration in avian embryos using monoclonal antibody HNK-1. Dev Biol *115*, 44-55.

Burgess, R., Rawls, A., Brown, D., Bradley, A., and Olson, E.N. (1996). Requirement of the paraxis gene for somite formation and musculoskeletal patterning. Nature *384*, 570-573.

Christ, B., Huang, R., and Scaal, M. (2007). Amniote somite derivatives. Dev Dyn *236*, 2382-2396.

Christ, B., Jacob, H.J., and Jacob, M. (1974). Somitogenesis in the chick embryo. Determination of the segmentation direction. VerhAnatGes *68*, 573-579.

Christ, B., and Ordahl, C.P. (1995). Early stages of chick somite development. AnatEmbryol(Berl) *191*, 381-396.

Christ, B., Schmidt, C., Huang, R., Wilting, J., and Brand-Saberi, B. (1998). Segmentation of the vertebrate body. AnatEmbryol(Berl) *197*, 1-8.

Cockroft, D.L. (1997). A comparative and historical review of culture methods for vertebrates. Int J Dev Biol *41*, 127-137.

Cole, S.E., Levorse, J.M., Tilghman, S.M., and Vogt, T.F. (2002). Clock Regulatory Elements Control Cyclic Expression of Lunatic fringe during Somitogenesis. Dev Cell *3*, 75-84.

Cooke, J. (1975). Control of somite number during morphogenesis of a vertebrate, Xenopus laevis. Nature *254*, 196-199.

Cooke, J. (1981). The problem of periodic patterns in embryos. PhilosTransRSocLondBBiolSci *295*, 509-524.

Cooke, J., and Zeeman, E.C. (1976). A clock and wavefront model for control of the number of repeated structures during animal morphogenesis. J Theor Biol *58*, 455-476.

Correia, K.M., and Conlon, R.A. (2000). Surface ectoderm is necessary for the morphogenesis of somites. Mech Dev *91*, 19-30.

Dale, J.K., Malapert, P., Chal, J., Vilhais-Neto, G., Maroto, M., Johnson, T., Jayasinghe, S., Trainor, P., Herrmann, B., and Pourquie, O. (2006). Oscillations of the snail genes in the presomitic mesoderm coordinate segmental patterning and morphogenesis in vertebrate somitogenesis. Dev Cell *10*, 355-366.

Delfini, M.C., Dubrulle, J., Malapert, P., Chal, J., and Pourquie, O. (2005). Control of the segmentation process by graded MAPK/ERK activation in the chick embryo. Proc Natl Acad Sci U S A *102*, 11343-11348.

Denk, W., and Svoboda, K. (1997). Photon upmanship: why multiphoton imaging is more than a gimmick. Neuron *18*, 351-357.

Dequeant, M.L., Glynn, E., Gaudenz, K., Wahl, M., Chen, J., Mushegian, A., and Pourquie, O. (2006). A complex oscillating network of signaling genes underlies the mouse segmentation clock. Science *314*, 1595-1598.

Diez del Corral, R., Olivera-Martinez, I., Goriely, A., Gale, E., Maden, M., and Storey, K. (2003). Opposing FGF and retinoid pathways control ventral neural pattern, neuronal differentiation, and segmentation during body axis extension. Neuron *40*, 65-79.

Dubrulle, J., McGrew, M.J., and Pourquie, O. (2001). FGF signaling controls somite boundary position and regulates segmentation clock control of spatiotemporal Hox gene activation. Cell *106*, 219-232.

Dubrulle, J., and Pourquie, O. (2004). fgf8 mRNA decay establishes a gradient that couples axial elongation to patterning in the vertebrate embryo. Nature *427*, 419-422.

Evrard, Y.A., Lun, Y., Aulehla, A., Gan, L., and Johnson, R.L. (1998). lunatic fringe is an essential mediator of somite segmentation and patterning Nature *394*, 377-381.

Feller, J., Schneider, A., Schuster-Gossler, K., and Gossler, A. (2008). Noncyclic Notch activity in the presomitic mesoderm demonstrates uncoupling of somite compartmentalization and boundary formation. Genes Dev *22*, 2166-2171.

Forsberg, H., Crozet, F., and Brown, N.A. (1998). Waves of mouse Lunatic fringe expression, in four-hour cycles at two-hour intervals, precede somite boundary formation. CurrBiol *8*, 1027-1030.

Gajewski, M., Sieger, D., Alt, B., Leve, C., Hans, S., Wolff, C., Rohr, K.B., and Tautz, D. (2003). Anterior and posterior waves of cyclic her1 gene expression are differentially regulated in the presomitic mesoderm of zebrafish. Development *130*, 4269-4278.

Giudicelli, F., Ozbudak, E.M., Wright, G.J., and Lewis, J. (2007). Setting the Tempo in Development: An Investigation of the Zebrafish Somite Clock Mechanism. PLoS Biol *5*, e150.

Goldbeter, A., Gonze, D., and Pourquie, O. (2007). Sharp developmental thresholds defined through bistability by antagonistic gradients of retinoic acid and FGF signaling. Dev Dyn *236*, 1495-1508.

Gomez, C., Ozbudak, E.M., Wunderlich, J., Baumann, D., Lewis, J., and Pourquie, O. (2008). Control of segment number in vertebrate embryos. Nature.

Hilgers, V., Pourquie, O., and Dubrulle, J. (2005). In vivo analysis of mRNA stability using the Tet-Off system in the chicken embryo. Dev Biol *284*, 292-300.

Hirata, H., Bessho, Y., Kokubu, H., Masamizu, Y., Yamada, S., Lewis, J., and Kageyama, R. (2004). Instability of Hes7 protein is crucial for the somite segmentation clock. Nat Genet *36*, 750-754.

Holley, S.A., Geisler, R., and Nusslein-Volhard, C. (2000). Control of her1 expression during zebrafish somitogenesis by a delta-dependent oscillator and an independent wave-front activity. Genes Dev *14*, 1678-1690.

Holley, S.A., Julich, D., Rauch, G.J., Geisler, R., and Nusslein-Volhard, C. (2002). her1 and the notch pathway function within the oscillator mechanism that regulates zebrafish somitogenesis. Development *129*, 1175-1183.

Horikawa, K., Ishimatsu, K., Yoshimoto, E., Kondo, S., and Takeda, H. (2006). Noise-resistant and synchronized oscillation of the segmentation clock. Nature *441*, 719-723.

Huang, R., Zhi, Q., Neubüser, A., Müller, T.S., Brand-Saberi, B., Christ, B., and Wilting, J. (1996). Function of somite and somitocoele cells in the formation of the vertebral motion segment in avian embryos. Acta Anat(Basel) *155*, 231-241.

Ishikawa, A., Kitajima, S., Takahashi, Y., Kokubo, H., Kanno, J., Inoue, T., and Saga, Y. (2004). Mouse Nkd1, a Wnt antagonist, exhibits oscillatory gene expression in the PSM under the control of Notch signaling. Mech Dev *121*, 1443-1453.

Jacob, M., Christ, B., and Jacob, H.J. (1975). Regional determination of the paraxial mesoderm in young chick embryos. VerhAnatGes *69*, 263-269.

Jiang, Y.J., Aerne, B.L., Smithers, L., Haddon, C., Ish-Horowicz, D., and Lewis, J. (2000). Notch signalling and the synchronization of the somite segmentation clock. Nature *408*, 475-479.

Jones, E.A., Crotty, D., Kulesa, P.M., Waters, C.W., Baron, M.H., Fraser, S.E., and Dickinson, M.E. (2002). Dynamic in vivo imaging of postimplantation mammalian embryos using whole embryo culture. Genesis *34*, 228-235.

Jouve, C., Palmeirim, I., Henrique, D., Beckers, J., Gossler, A., Ish-Horowicz, D., and Pourquie, O. (2000). Notch signalling is required for cyclic expression of the hairy-like gene HES1 in the presomitic mesoderm. Development *127*, 1421-1429.

Julich, D., Hwee Lim, C., Round, J., Nicolaije, C., Schroeder, J., Davies, A., Geisler, R., Lewis, J., Jiang, Y.J., and Holley, S.A. (2005). beamter/deltaC and the role of Notch ligands in the zebrafish somite segmentation, hindbrain neurogenesis and hypochord differentiation. Dev Biol *286*, 391-404.

Keynes, R.J., and Stern, C.D. (1984). Segmentation in the vertebrate nervous system. Nature *310*, 786-789.

Keynes, R.J., and Stern, C.D. (1988). Mechanisms of vertebrate segmentation. Development *103*, 413-429.

Kieny, M., Mauger, A., and Sengel, P. (1972). Early regionalization of somitic mesoderm as studied by the development of axial skeleton of the chick embryo. Dev Biol *28*, 142-161.

Kmita, M., and Duboule, D. (2003). Organizing axes in time and space; 25 years of colinear tinkering. Science *301*, 331-333.

Leitges, M., Neidhardt, L., Haenig, B., Herrmann, B.G., and Kispert, A. (2000). The paired homeobox gene uncx4.1 specifies pedicles, transverse processes and proximal ribs of the vertebral column [In Process Citation]. Development *127*, 2259-2267.

Li, X., Zhao, X., Fang, Y., Jiang, X., Duong, T., Fan, C., Huang, C.C., and Kain, S.R. (1998). Generation of destabilized green fluorescent protein as a transcription reporter. J Biol Chem *273*, 34970-34975.

Li, Y., Fenger, U., Niehrs, C., and Pollet, N. (2003). Cyclic expression of esr9 gene in Xenopus presomitic mesoderm. Differentiation *71*, 83-89.

Maroto, M., Dale, J.K., Dequeant, M.L., Petit, A.C., and Pourquie, O. (2005). Synchronised cycling gene oscillations in presomitic mesoderm cells require cell-cell contact. Int J Dev Biol *49*, 309-315.

Maruhashi, M., Van De Putte, T., Huylebroeck, D., Kondoh, H., and Higashi, Y. (2005). Involvement of SIP1 in positioning of somite boundaries in the mouse embryo. Dev Dyn *234*, 332-338.

Masamizu, Y., Ohtsuka, T., Takashima, Y., Nagahara, H., Takenaka, Y., Yoshikawa, K., Okamura, H., and Kageyama, R. (2006). Real-time imaging of the somite segmentation clock: revelation of unstable oscillators in the individual presomitic mesoderm cells. Proc Natl Acad Sci U S A *103*, 1313-1318.

McGrew, M.J., Dale, J.K., Fraboulet, S., and Pourquie, O. (1998). The lunatic fringe gene is a target of the molecular clock linked to somite segmentation in avian embryos. Curr Biol *8*, 979-982.

McIntyre, D.C., Rakshit, S., Yallowitz, A.R., Loken, L., Jeannotte, L., Capecchi, M.R., and Wellik, D.M. (2007). Hox patterning of the vertebrate rib cage. Development *134*, 2981-2989.

Meinhardt, H. (1982). Models of biological pattern formation (London, Academic Press).
Meinhardt, H. (1986). Models of segmentation. In Somites in Developing Embryos, B. R, E. DA, and L. JW, eds. (New York and London, Plenum press), pp. 179-191.

Menkes, B., Sandor, S., and Elias, S. (1968). Researches on the formation of axial organs of the chick embryo. IV. Rev Roum Embryol Cytol *5*, 131-137.

Morales, A.V., Yasuda, Y., and Ish-Horowicz, D. (2002). Periodic Lunatic fringe Expression Is Controlled during Segmentation by a Cyclic Transcriptional Enhancer Responsive to Notch Signaling. Dev Cell *3*, 63-74.

Morimoto, M., Takahashi, Y., Endo, M., and Saga, Y. (2005). The Mesp2 transcription factor establishes segmental borders by suppressing Notch activity. Nature *435*, 354-359.

Nagai, T., Ibata, K., Park, E.S., Kubota, M., Mikoshiba, K., and Miyawaki, A. (2002). A variant of yellow fluorescent protein with fast and efficient maturation for cell-biological applications. Nat Biotechnol *20*, 87-90.

Nakaya, M.A., Biris, K., Tsukiyama, T., Jaime, S., Rawls, J.A., and Yamaguchi, T.P. (2005). Wnt3alinks left-right determination with segmentation and anteroposterior axis elongation. Development *132*, 5425-5436.

New, D.A. (1966). Development of rat embryos cultured in blood sera. Journal of reproduction and fertility *12*, 509-524.

New, D.A., Coppola, P.T., and Cockroft, D.L. (1976a). Comparison of growth in vitro and in vivo of post-implantation rat embryos. J Embryol Exp Morphol *36*, 133-144.

New, D.A., Coppola, P.T., and Cockroft, D.L. (1976b). Improved developement of head-fold rat embryos in culture resulting from low oxygen and modifications of the culture serum. Journal of reproduction and fertility *48*, 219-222.

Niwa, Y., Masamizu, Y., Liu, T., Nakayama, R., Deng, C.X., and Kageyama, R. (2007). The initiation and propagation of Hes7 oscillation are cooperatively regulated by Fgf and notch signaling in the somite segmentation clock. Dev Cell *13*, 298-304.

Oates, A.C., and Ho, R.K. (2002). Hairy/E(spl)-related (Her) genes are central components of the segmentation oscillator and display redundancy with the Delta/Notch signaling pathway in the formation of anterior segmental boundaries in the zebrafish. Development *129*, 2929-2946.

Ordahl, C.P. (1993). Myogenic lineages within the developing somite. In Molecular Basis of Morphogenesis, M. Bernfield, ed. (New-York, John Wiley and Sons), pp. 165-176.

Ozbudak, E.M., and Lewis, J. (2008). Notch signalling synchronizes the zebrafish segmentation clock but is not needed to create somite boundaries. PLoS genetics *4*, e15.

Packard, D.S.J. (1978). Chick somite determination: the role of factors in young somites and the segmental plate. JExpZool *203*, 295-306.

Palmeirim, I., Dubrulle, J., Henrique, D., Ish-Horowicz, D., and Pourquié, O. (1998). Uncoupling segmentation and somitogenesis in the chick presomitic mesoderm. Dev Genet *23*, 77-85.

Palmeirim, I., Henrique, D., Ish-Horowicz, D., and Pourquié, O. (1997). Avian hairy gene expression identifies a molecular clock linked to vertebrate segmentation and somitogenesis. Cell *91*, 639-648.

Pourquie, O. (2001). The vertebrate segmentation clock. J Anat *199*, 169-175.

Pourquie, O., Coltey, M., Breant, C., and Le Douarin, N.M. (1995). Control of somite patterning by signals from the lateral plate. Proc Natl Acad Sci U S A *92*, 3219-3223.

Pourquie, O., Coltey, M., Teillet, M.A., Ordahl, C., and Le Douarin, N.M. (1993). Control of dorsoventral patterning of somitic derivatives by notochord and floor plate. Proc Natl Acad Sci U S A *90*, 5242-5246.

Pourquie, O., Fan, C.M., Coltey, M., Hirsinger, E., Watanabe, Y., Breant, C., Francis-West, P., Brickell, P., Tessier-Lavigne, M., and Le Douarin, N.M. (1996). Lateral and axial signals involved in avian somite patterning: a role for BMP4. Cell *84*, 461-471.

Pourquie, O., and Tam, P.P. (2001). A nomenclature for prospective somites and phases of cyclic gene expression in the presomitic mesoderm. Dev Cell *1*, 619-620.

Remak, R. (1850). Untersuchungen über die entwicklung der Wirbeltiere (Berlin, Reimer).

Rickmann, M., Fawcett, J.W., and Keynes, R.J. (1985). The migration of neural crest cells and the growth of motor axons through the rostral half of the chick somite. JEmbryolExpMorphol *90*, 437-455.

Rifes, P., Carvalho, L., Lopes, C., Andrade, R.P., Rodrigues, G., Palmeirim, I., and Thorsteinsdottir, S. (2007). Redefining the role of ectoderm in somitogenesis: a player in the formation of the fibronectin matrix of presomitic mesoderm. Development *134*, 3155-3165.

Saga, Y., and Takeda, H. (2001). The making of the somite: molecular events in vertebrate segmentation. Nat Rev Genet *2*, 835-845.

Satoh, W., Gotoh, T., Tsunematsu, Y., Aizawa, S., and Shimono, A. (2006). Sfrp1 and Sfrp2 regulate anteroposterior axis elongation and somite segmentation during mouse embryogenesis. Development *133*, 989-999.

Satoh, W., Matsuyama, M., Takemura, H., Aizawa, S., and Shimono, A. (2008). Sfrp1, Sfrp2, and Sfrp5 regulate the Wnt/beta-catenin and the planar cell polarity pathways during early trunk formation in mouse. Genesis *46*, 92-103.

Sawada, A., Shinya, M., Jiang, Y.J., Kawakami, A., Kuroiwa, A., and Takeda, H. (2001). Fgf/MAPK signalling is a crucial positional cue in somite boundary formation. Development *128*, 4873-4880.

Schmidt, C., Stoeckelhuber, M., McKinnell, I., Putz, R., Christ, B., and Patel, K. (2004). Wnt 6 regulates the epithelialisation process of the segmental plate mesoderm leading to somite formation. Dev Biol *271*, 198-209.

Shepard, T.H., Tanimura, T., and Park, H.W. (1997). Glucose absorption and utilization by rat embryos. Int J Dev Biol *41*, 307-314.

Shifley, E.T., Vanhorn, K.M., Perez-Balaguer, A., Franklin, J.D., Weinstein, M., and Cole, S.E. (2008). Oscillatory lunatic fringe activity is crucial for segmentation of the anterior but not posterior skeleton. Development *135*, 899-908.

Sieger, D., Tautz, D., and Gajewski, M. (2004). her11 is involved in the somitogenesis clock in zebrafish. Dev Genes Evol *214*, 393-406.

Sierra, J., Yoshida, T., Joazeiro, C.A., and Jones, K.A. (2006). The APC tumor suppressor counteracts beta-catenin activation and H3K4 methylation at Wnt target genes. Genes Dev *20*, 586-600.

Squirrell, J.M., Wokosin, D.L., White, J.G., and Bavister, B.D. (1999). Long-term two-photon fluorescence imaging of mammalian embryos without compromising viability. Nat Biotechnol *17*, 763-767.

Suriben, R., Fisher, D.A., and Cheyette, B.N. (2006). Dact1 presomitic mesoderm expression oscillates in phase with Axin2 in the somitogenesis clock of mice. Dev Dyn *235*, 3177-3183.

Suzuki, H., Watkins, D.N., Jair, K.W., Schuebel, K.E., Markowitz, S.D., Chen, W.D., Pretlow, T.P., Yang, B., Akiyama, Y., Van Engeland, M., *et al.* (2004). Epigenetic inactivation of SFRP genes allows constitutive WNT signaling in colorectal cancer. Nat Genet *36*, 417-422.

Takahashi, Y., Inoue, T., Gossler, A., and Saga, Y. (2003). Feedback loops comprising Dll1, Dll3 and Mesp2, and differential involvement of Psen1 are essential for rostrocaudal patterning of somites. Development *130*, 4259-4268.

Takahashi, Y., Yasuhiko, Y., Kitajima, S., Kanno, J., and Saga, Y. (2007). Appropriate suppression of Notch signaling by Mesp factors is essential for stripe pattern formation leading to segment boundary formation. Dev Biol *304*, 593-603.

Tam, P.P. (1981). The control of somitogenesis in mouse embryos. JEmbryolExpMorphol *65 Suppl*, 103-128.

Tam, P.P., and Tan, S.S. (1992). The somitogenetic potential of cells in the primitive streak and the tail bud of the organogenesis-stage mouse embryo. Development *115*, 703-715.

Turing, A.M. (1952). The chemical basis of morphogenesis. Philosophical Transactions of the Royal Society of London *B 237*, 37-72.

Von Ebner, V. (1888). Urwirbel und Neugliederung der WirbelSäule. SitzungsberAkadWissWien *III/97*, 194-206.

Wahl, M.B., Deng, C., Lewandoski, M., and Pourquie, O. (2007). FGF signaling acts upstream of the NOTCH and WNT signaling pathways to control segmentation clock oscillations in mouse somitogenesis. Development *134*, 4033-4041.

Wang, S., and Jones, K.A. (2006). CK2 controls the recruitment of Wnt regulators to target genes in vivo. Curr Biol *16*, 2239-2244.

Wellik, D.M., and Capecchi, M.R. (2003). Hox10 and Hox11 genes are required to globally pattern the mammalian skeleton. Science *301*, 363-367.

Willert, K., and Jones, K.A. (2006). Wnt signaling: is the party in the nucleus? Genes Dev *20*, 1394-1404.

Wolpert, L., Beddington, R., Jessell, T., Lawrence, P., Meyerowitz, E., and Smith, J. (2003). Principles of Development, 2nd edn (Oxford University).

Yasuhiko, Y., Haraguchi, S., Kitajima, S., Takahashi, Y., Kanno, J., and Saga, Y. (2006). Tbx6-mediated Notch signaling controls somite-specific Mesp2 expression. Proc Natl Acad Sci U S A *103*, 3651-3656.

Zhang, N., and Gridley, T. (1998). Defects in somite formation in lunatic fringe-deficient mice Nature *394*, 374-377.

Zubiaga, A.M., Belasco, J.G., and Greenberg, M.E. (1995). The nonamer UUAUUUAUU is the key AU-rich sequence motif that mediates mRNA degradation. Mol Cell Biol *15*, 2219-2230.